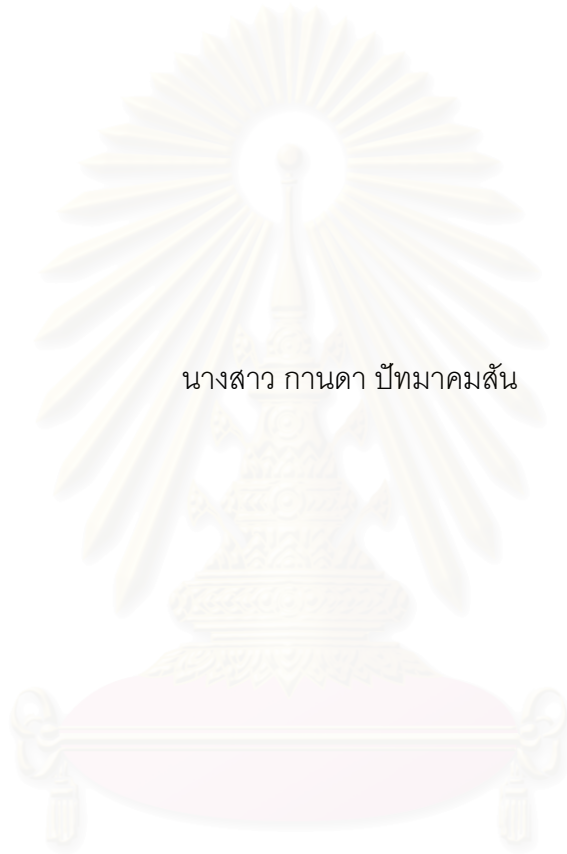ปฏิกิริยาไฮโดรจิเนชันในวัฏภาคของเหลวของ 1-เฮกซีนบนตัวเร่งปฏิกิริยาแพลเลเดียม
บนตัวรองรับซิลิกาชนิดต่างๆ

นางสาว กานดา ปัทมาคมสัน
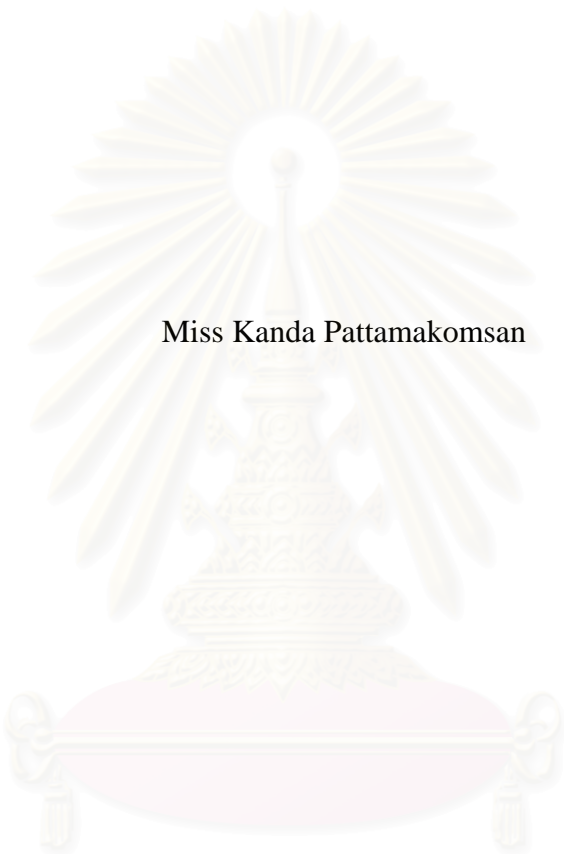
LIQUID-PHASE HYDROGENATION OF 1-HEXENE ON
DIFFERENT SILICA-SUPPORTED PALLADIUM CATALYSTS

Miss Kanda Pattamakomsan

A Thesis Submitted in Partial Fulfillment of the Requirements

for the Degree of Master of Engineering in Chemical Engineering

Department of Chemical Engineering

Faculty of Engineering

Chulalongkorn University

Academic Year 2003

ISBN: 974-17-4422-6

Thesis Title	LIQUID-PHASE HYDROGENATION OF 1-HEXENE ON DIFFERENT SILICA-SUPPORTED PALLADIUM CATALYSTS
By	Miss Kanda Pattamakomsan
Field of Study	Chemical Engineering
Thesis Advisor	Joongjai Panpranot, Ph.D.
Thesis Co-advisor	Professor Piyasan Praserthdam, Dr.Ing

Accepted by the Faculty of Engineering, Chulalongkorn University in Partial Fulfillment of the Requirements for the Master's Degree

…….……..……………. Dean of the Faculty of Engineering

(Professor Direk Lavansiri, Ph.D.)

THESIS COMMITTEE

………………………………… Chairman

(Associate Professor Suttichai Assabumrungrat, Ph.D.)

…………………………………. Thesis Advisor

(Joongjai Panpranot, Ph.D.)

…………………………………. Thesis Co-advisor

(Professor Piyasan Praserthdam, Dr.Ing)

…………………………………. Member

(Muenduen Phisalaphong, Ph.D.)

…………………………………. Member

(Bunjerd Jungsomjit, Ph.D.)

กานดา ปัทมาคมสัน: ปฏิกิริยาไฮโดรจิเนชันในวัฏภาคของเหลวของ 1-เฮกซีนบนตัวเร่งปฏิกิริยาแพลเลเดียมบนตัวรองรับซิลิกาชนิดต่างๆ (LIQUID-PHASE HYDROGENATION OF 1-HEXENE ON DIFFERENT SILICASUPPORTED PALLADIUM CATALYSTS) อ. ที่ปรึกษา: ดร. จูงใจ ปั้นประณต, อ. ที่ปรึกษา (ร่วม): ศาสตราจารย์ ดร.ปิยะสาร ประเสริฐธรรม 98 หน้า. ISBN: 974-17-4422-6

วิทยานิพนธ์นี้ศึกษาเปรียบเทียบลักษณะเฉพาะและคุณสมบัติการเร่งปฏิกิริยาของตัวเร่งปฏิกิริยาแพลเลเดียมบนตัวรองรับซิลิกาชนิดต่างๆในเทอมของการกระจายตัวของโลหะแพลเลเดียม ความว่องไวของปฏิกิริยาสำหรับปฏิกิริยาไฮโดรจิเนชันในวัฏภาคของเหลวของ1-เฮกซีน และการเสื่อมสภาพของตัวเร่งปฏิกิริยา ตัวเร่งปฏิกิริยาถูกแสดงลักษณะเฉพาะโดยวิธีการวัดการดูดซับของอะตอม การดูดซับโดยใช้ไนโตรเจน การกระเจิงรังสีเอ็กซ์ การส่องผ่านด้วยกล้องจุลทรรศน์อิเลคตรอน การวัดการดูดซับด้วยก๊าซคาร์บอนมอนออกไซด์และการทดสอบความสามารถการสลายตัวของแพลเลเดียมออกไซด์โดยการเพิ่มอุณหภูมิเป็นลำดับ แพลเลเดียมมีการกระจายตัวสูงถูกพบบนตัวเร่งปฏิกิริยาแพลเลเดียมบนตัวรองรับMCM-41รูพรุนขนาดใหญ่ขณะที่ตัวเร่งปฏิกิริยาแพลเลเดียมบนตัวรองรับอื่นๆแสดงการกระจายตัวต่ำเนื่องมาจากแพลเลเดียมจำนวนมากอยู่นอกรูพรุนของตัวรองรับ ผลการทดสอบปฏิกิริยาและการแสดงลักษณะเฉพาะพบว่า(1) การถ่ายโอนมวลมีผลกระทบระหว่างการเกิดปฏิกิริยาอาจเกิดขึ้นเนื่องจากตัวเร่งปฏิกิริยาบนตัวรองรับที่มีรูพรุนขนาดใหญ่ว่องไวมากกว่าตัวรองรับรูพรุนขนาดเล็กและ (2) โครงสร้างของMCM-41มีอิทธิพลต่อมวลและพื้นผิวของโลหะแพลเลเดียมจากหลักฐานที่MCM-41มีความว่องไวในการเกิดปฏิกิริยาที่สูงกว่า การชะล้างของแพลเลเดียมในการเกิดปฏิกิริยาเกิดขึ้นในทุกกรณีอย่างไรก็ตาม ตำแหน่งที่ว่องไวในการเร่งปฏิกิริยามีความต้านทานการตกชะล้างของแพลเลเดียมมากกว่าตำแหน่งที่ไม่ว่องไวเนื่องจากจำนวนของตำแหน่งที่ว่องไวถูกวัดโดยการดูดซับด้วยก๊าซคาร์บอนมอนออกไซด์ยังคงเท่าเดิมหลังจากผ่านการเกิดปฏิกิริยามาแล้ว2ครั้ง ขณะที่เปอร์เซ็นต์ทั้งหมดของแพลเลเดียมลดลงอย่างมากหลังการเกิดปฏิกิริยา การมีอนุภาคแพลเลเดียมขนาดเล็กอยู่ในรูพรุนขนาดกลางของMCM-41ก่อให้เกิดการชะล้างของแพลเลเดียมจำนวนน้อยที่สุด

ภาควิชา......วิศวกรรมเคมี.............	ลายมือชื่อนิสิต..	
สาขาวิชา......วิศวกรรมเคมี.............	ลายมือชื่ออาจารย์ที่ปรึกษา....................................	
ปีการศึกษา.........2546................	ลายมือชื่ออาจารย์ที่ปรึกษาร่วม............................	

4570214021 : MAJOR CHEMICAL ENGINEERING

KEYWORDS: LIQUID PHASE HYDROGENATION/ MCM-41/ SILICA SUPPORTED PALLADIUM CATALYST/ 1-HEXENE

KANDA PATTAMAKOMSAN: LIQUID-PHASE HYDROGENATION OF 1-HEXENE ON DIFFERENT SILICA-SUPPORTED PALLADIUM CATALYSTS THESIS ADVISOR: JOONGJAI PANPRANOT Ph.D., THESIS CO-ADVISOR: PIYASAN PRASERTHDAM, Dr.Ing. 98 pp. ISBN: 974-17-4422-6

The characteristics and catalytic properties of different silica supported palladium catalysts were investigated and compared in terms of Pd dispersion, catalytic activities for liquid-phase hydrogenation of 1-hexene, and deactivation of the catalysts. The catalysts were characterized by atomic adsorption (AA), N_2 physisorption, X-ray diffraction (XRD), transmission electron microscopy (TEM), CO pulse chemisorption, and temperature program reduction (TPR). High Pd dispersion was observed on Pd/MCM-41-large pore catalyst while the other catalysts showed relatively low Pd dispersion due to significant amount of Pd being located out of the pores of the supports. The reaction and characterization results suggest that (1) mass transport effects during reaction may occur since larger pore supported catalysts were more active than smaller pore supported ones and (2) MCM-41 structure has an influence on bulk and surface properties of the Pd metal as evidenced by higher activity of Pd/MCM-41. Leaching of palladium into the reaction media occurred in all cases, however, the catalytically active metal sites were probably more resistant to leaching than the non-catalytically active ones since the number of active sites as measured by CO chemisorption remained constant after two cycles of reaction while the total wt% of Pd dramatically decreased after reaction. Having smaller Pd particle sizes located in the mesopores of MCM-41 resulted in the lowest amount of metal leaching.

Department …..Chemical Engineering…..   Student's signature …………………….

Field of Study ..Chemical Engineering……   Advisor's signature …………………….

Academic year ………2003……………   Co-advisor's signature…………………

ACKNOWLEDGEMENTS

TABLE OF CONTENTS

TABLE OF CONTENTS (Cont.)

TABLE OF CONTENTS (Cont.)

LIST OF TABLES

LIST OF FIGURES

LIST OF FIGURES

CHAPTER I

INTRODUCTION

Hydrogenation is one of the most useful, versatile, and environmentally acceptable reaction routes available for organic synthesis (Farrauto and Bartholomew, 1997). It also represents an essential part of hydrotreatment of crude in the oil industry, which eliminates aromatics and unsaturated hydrocarbons during diesel and aero fuel production. The increase in oil consumption between the years 2000 to 2010 is to forecast to be around 17% and by the year 2010 the relation petro-diesel is expected to change in favor diesel (Dominguez-Quintero, 2003). These facts reveal the importance of the development of new catalytic materials with substantially increment activities and selectivities that could imply costs reductions, especially in hydrogenation process (Krylov, 2001).

The types of hydrogenation catalysts finding commercial application include noble metals, group VIII transition metals, organometallic complexes, and activated alloy catalysts that are either unsupported or supported. The major advantages of noble metal catalysts are their relatively high activity, mild process conditions, easy separation, and better handling properties. The most commonly used noble metals are Pt, Pd, Rh, and Ru. Generally Pd is more active than Rh or Pt for many hydrogenation reactions on the same carbon carrier (Rylander, 1985a, b).

Generally, the active phase in hydrogenation reaction is metallic phase. Therefore, having the metal highly dispersed and reduced is required for a catalyst to have high activity. The metal surface areas can be increased by dispersing the palladium precursor on high surface area supports. The supports that have been used are carbon, silica, alumina, polymer and zeolite in order to obtain high selectivity and activity supported Pd catalysts.

Many important organic transformations a carried out in liquid phase, using batch type slurry processes and a supported precious metal catalyst. Several factors

affecting the performance of noble metal catalysts in liquid phase hydrogenation have been extensively investigated. Typically, the factors can be classified into (i) the role of the liquid phase composition (substrate structure, solvent effects, etc.), (ii) the effect of catalysts (active sites composition and morphology, support effects, SMSI, modifiers, etc.), and (iii) the effect of reaction conditions (temperature, pressure, etc.) on reaction kinetics. There have also been several attempts to generalize structural effect in such system (Kacer and Cerveny, 2002).

A new class of mesoporous molecular sieve materials designated as MCM-41 was first synthesized in 1992 by the researchers of the Mobil Oil Corporation, USA (Kresge *et al.*, 1992). The structure of MCM-41 consists of uniform cylindrical pores arranged in a hexagonal array. The pore dimensions can be tailored in the range of 1.5-10 nm depending on synthesis chemicals and conditions. The BET surface area is usually greater than 1000 m^2/g with high sorption capacities of 0.7 ml/g. It can also be synthesized in a large range of framework Si/Al ratio; therefore, can develop acid sites of different strengths. MCM-41 has been studied as a catalyst, a catalyst support, and a sorbent (Xiu S. Zhao *et al.*, 1996).

In this study, the characteristics and catalytic properties of Pd/MCM-41 with 2 different pore sizes (3 and 7 nm) and Pd/SiO$_2$ (narrow and large pore) were compared. The effects of silica-structure and pore size of the silica supports were investigated in terms of metal dispersion, metal location on the supports, catalytic activity in liquid-phase hydrogenation, and deactivation due to metal leaching. These results supply useful information on the role of support porosity and type of silica used in supported Pd catalysts for liquid phase hydrogenation reactions.

CHAPTER II
THEORY

The basic knowledge of hydrogenation reaction and hydrogenation of alkene was explained in the first part (section 2.1) and second part (section 2.2). Then, the third part (section 2.3) describes about hydrogenation catalyst. Finally, the synthesis of MCM-41 and applications were present in the last part (section 2.4).

2.1 Hydrogenation Reaction

One of the oldest and most diverse catalytic processes is the selective hydrogenation of functional groups contained in organic molecules to produce (1) fine chemicals, (2) intermediates used in the pharmaceutical industry, (3) monomers for the production of various polymers, and (4) fats and oils for producing edible and nonedible products. Indeed, there are more hydrogenation catalysts available commercially than any other type, and for good reason, because hydrogenation is one one of the most useful, versatile, and environmentally acceptable reaction routes available for organic synthesis. With the exception of a few large scales, continuous hydrogenation processes in petroleum refining, hydrogenation products are often made on a small scale in batch reactors. Batch processes are usually most cost effective since the equipment need not to be dedicated to a single reaction. Generally, large stirred autoclave is capable of H_2 pressure up to 140 atm. The catalyst is generally powdered and slurried with reactants; a solvent is usually present to influence product selectivity and to absorb the reaction heat liberated by the reation. Since most hydrogenations are highly exothermic, careful temperature control is required to achieve the desired selectivity and to prevent temperature runaway (Farrauto and Bartholomew, 1997).

2.2 Hydrogenation of Alkenes

The carbon-carbon double bond is in general among the functional groups that are most readily hydrogenated, unless highly substituted and/or strongly hindered. Although the discovery of Sabatier and Senderens in 1897 that ethylene reacted with hydrogen over reduced nickel oxide to give ethane was made at a high temperature in the vapor phase, a large number of alkenes have later been hydrogenated successfully in the liquid phase, frequently under mild conditions using platinum, palladium, and active nickel catalysts such as Raney Ni. However, application of elevated temperatures and/or pressures is preferred in larger-scale hydrogenations to complete the reaction within a reasonable time using relatively small amounts of catalyst.

The hydrogenation of mono- and disubstituted double bonds is usually rather rapid over most catalysts even under mild conditions. The heat of hydrogenation is also greater for mono- and disubstituted ethylenes than for tri- and tetrasubstitutted ones. Accordingly, care must be taken to prevent the reaction from proceeding too violently with less hindered olefins this can be achieved by adjustion the reaction temperature and the amount of catalyst (Nishimura, 2001).

The generally accepted mechanism for the hydrogenation of double bonds over heterogeneous catalysts was first proposed by Horiuti and Polanyi and was later supported by results of deuteration experiments. It assumes that both hydrogen and alkene are bound to the catalyst surface. The hydrogen molecule undergoes dissociative adsorption [Eq.1], while the alkene adsorbs associative [Eq. 2]. Addition of hydrogen to the double bond occurs in a stepwise manner [Eq. 3 and 4].

While the last step [Eq. 4] is virtually irreversible under hydrogenation conditions, both the adsorption of alkene [Eq. 2] and the formation of alkyl intermediate (half-hydrogenated state) [Eq. 3] are reversible. The reversibility of these steps accounts for the isomerization of alkenes accompanying hydrogenation (Sheldon *et al.*, 2001).

$$H_2 + 2M \rightleftharpoons H-M \qquad (1)$$

$$\underset{/}{\overset{\backslash}{C}}=\underset{\backslash}{\overset{/}{C}} + 2M \rightleftharpoons -\underset{M}{\overset{|}{C}}-\underset{M}{\overset{|}{C}}- \qquad (2)$$

$$-\underset{M}{\overset{|}{C}}-\underset{M}{\overset{|}{C}}- + H-M \xrightleftharpoons{-2M} -\underset{M}{\overset{|}{C}}-\underset{H}{\overset{|}{C}}- \qquad (3)$$

$$-\underset{M}{\overset{|}{C}}-\underset{H}{\overset{|}{C}}- + H-M \xrightleftharpoons{-2M} -\underset{H}{\overset{|}{C}}-\underset{H}{\overset{|}{C}}- \qquad (4)$$
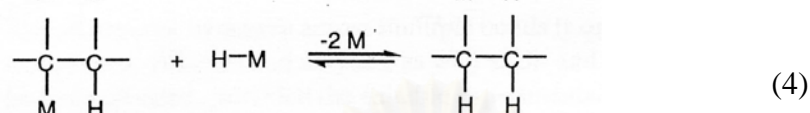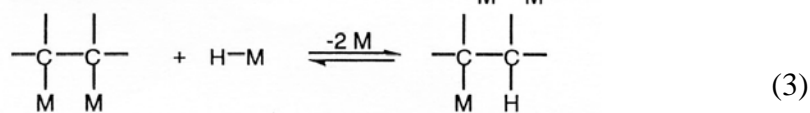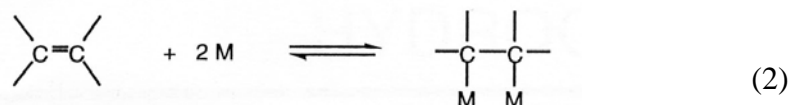
2.3 Hydrogenation Catalysts

The types of hydrogenation catalysts finding commercial applications include noble metals, group VIII transition metals, organometallic complexes, and activated alloy catalysts that are either unsupported or supported. The major advantages of noble metal catalysts are their relatively high activity, mild process conditions, easy separation, and better handling properties. The most commonly used noble metals are Pt, Pd, Rh, and Ru. Generally Pd is more active than Rh or Pt for many hydrogenation reactions on the same carbon carrier (Rylander, 1985a, b). In general, use of a support allows the active component to have a larger exposed surface area, which is particularly important in those cases where a high temperature is required to activate the active component. The supports may be as different as carbon (Rylander, 1979, March, 1985 and Chou, and Vannice, 1987), silica (Frolov *et al.,* 1984 and Cherkashin *et al.,* 1985), alumina (Mathew and Srinivasan, 1995, Weyrich and Holderich, 1997, Kresge *et al.*, 1992 and Beck *et al.*, 1992) and polymer (Corma *et al.*, 1997) in order to obtain higher selectivity and activity. Supported catalysts may be prepared by a variety of methods, depending on the nature of active components as well as the characteristics of carriers for examples, decomposition, impregnation, precipitation, coprecipitation, adsorption, or ion exchange. Both low and high surface area materials are employed as carriers (Nishimura, 2001).

2.4 Order Mesoporous Materials

According to the definition of IUPAC, mesoporous materials are those that have pore diameters between 20 and 500 Å. Examples of mesoporous solids include silica gel (Iler, 1979) and modified layered materials (Landis and Aufdembrink, 1991), but the pores in these materials are irregularly spaced and usually have a wide distribution of pore sizes. A considerable synthetic effort has been devoted to developing highly uniform frameworks with pore diameters within the mesoporous range. The structure of this mesoporous silicate and aluminosilicate family that has received the most attention is referred to as MCM-41, which consists of uniform cylindrical pores arranged in a hexagonal array. The pore dimensions can be tailored in the range of 1.5-10 nm depending on synthesis chemicals and conditions. The BET surface area is usually greater than 1000 m^2/g with high sorption capacities of 0.7 ml/g.

The MCM-41 mesoporous structure formation of silica is base upon biomineralization and biomimetic chemistry in which organic and inorganic species interact and self-assemble into nanosize structures. A typical synthesis starts from preparation of an aqueous surfactant solution. A silica source, combined with an acid or base liquid catalyst to aid in the polymerization of the silica, is then added to the aqueous surfactant solution, and the slurry is stirred. This room temperature mixing of the reactants allows the hydrophilic heads of the surfactant to interact with the silica in solution by electrostatically attracting silica molecules to the micelle surface. The solution is then heated under autogeneous pressure at temperatures of 100-200 °C for 24 to 48 hours. At these elevated temperatures, the silica extensively polymerizes and condensed around the micelles. The interaction of the inorganic and organic phases is believed to align the micelles via a self-assembly mechanism to form the as-synthesized mesostructured composite. Subsequent removal of the organic surfactant by calcination in air or by solvent extraction creates the highly ordered mesoporous structure. Beck *et al.* proposed two possible mechanistic pathways for MCM-41 formation: (1) a liquid crystal templating mechanism, where the MCM-41 structure is formed around micelles existing as single cylindrical aggregates; (2) a mechanism where the addition of the silicate results in the ordering of the subsequent silicate-encaged surfactant micelles. A schematic of this formation mechanism is shown in Figure 2.1.

The synthesis of these mesoporous materials has been found to be a strong function of several variables in the system (Corma, 1997; Kruk *et al.*, 1999; Carrott *et al.*, 1999; Chen *et al.*, 1997; Liepold *et al.*, 1996; Kruk *et al.*, 2000). The surfactant-to-silica ratio in the synthesis mixture has been identified as capable of determining the type of mesoporous structrue formed. Typically, this molar ratio is less than or equal to 0.5 for MCM-41 formation. At values greater than 0.5, other mesostructures i.e., cubic symmetry MCM-48 and Lamellar symmetry MCM-50, have been reported. The basicity, temperature, and time also determine the rate of polymerization of the silica precursor.
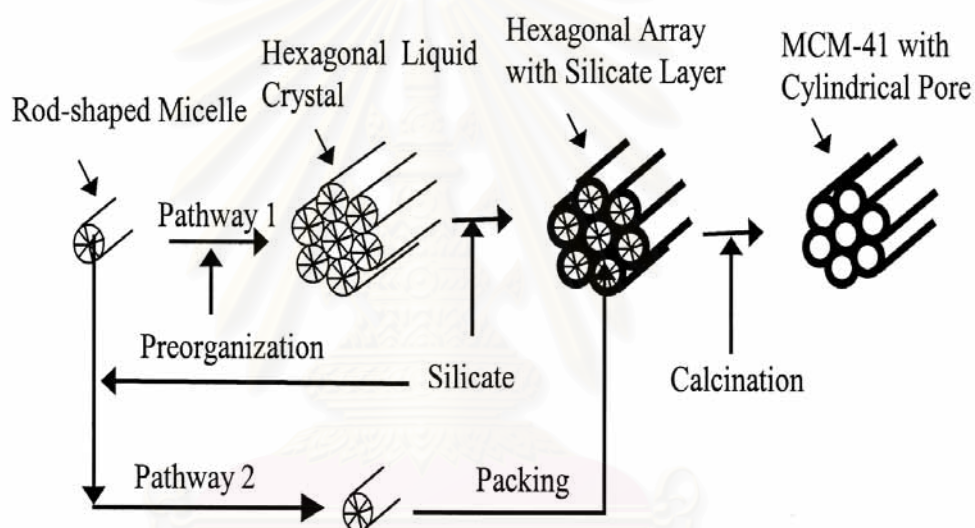
Figure 2.1 Possible mechanistic pathways for the formation of MCM-41: (1) liquid-crystal initiate and (2) silicate anion initiate

CHAPTER III

LITERATURE REVIEWS

This chapter reviews the previous studies about liquid phase hydrogenation reaction which can be divided into four parts. The first part (section 3.1) is about supported Pd catalyst in various liquid phase hydrogenations. The second part (section 3.2) and third part (section 3.3) involved the details about synthesis and application of MCM-41. The catalysts deactivation such as sintering and leaching of palladium were reported in the fourth part (section 3.4).

3.1 Supported Pd Catalyst in Liquid Phase Hydrogenation

Catalytic liquid-phase hydrogenation is widely used in many important organic transformations such as hydrogenation of acetylenes, olefins carbonyls in aromatic aldehydes and ketones, aromatic and aliphatic nitro compounds, reductive alkylation, hydrogenolysis, and hydrodehalogenation reactions.

The development of new catalytic materials with high activities and selectivities is very important because it could imply cost reductions, especially in hydrogenation reaction. The most commonly catalysts using in hydrogenation are noble metal such as Pd, Pt, Rh, and Ru. Pd is more active than Rh or Pt for many hydrogenations. Supported metal particles are commonly used heterogeneous catalysts. Studying of different supported Pd catalysts for the various liquid phase hydrogenations have been reported more than ten years.

M. Schneider *et al.* (1994) synthesized mesoporous to macroporous palladium-titania aerogels with high surface by the sol-gel-aerogel route. Both the palladium particles and the titania matrix possess a remarkable structural stability up to 773 K. By varying the Pd precursor solution, different palladium particle size distributions can be obtained. The catalytic studies showed that the activities were much higher for the hydrogenation of trans-stilbene than those for the benzophenone.

The hightest dispersed palladium-titania aerogels, derived from $Pd(OAc)_2$, showed superior activity and selectivity for 4-methylbenzaldehyde hydrogenation compared to impregnated titania-supported Pd catalyst.

Dario Duca *et al.* (1995) studied the liquid phase, selective hydrogenation of phenylacetylene on pumice-supported palladium catalysts for a large range of metallic dispersions ($14\% \leq D_x \leq 62\%$). The powder used as support for their catalysts was a waste product from the production of Pumex Spa-Lipari, with a particle size smaller than 45 μm. Activity and selectivity data were reported and compared with other supported palladium catalysts. They suggested that Pd/pumice catalysts could be interesting for industrial application because of their high activity and selectivity at high metal dispersions.

Istvan Palinko (1995) studied hydrogenation of 1-hexene and cyclohexene over silica-supported Pt, Pd and Rh catalysts in the liquid phase, in the presence of quinoline or carbon tetrachloride at room temperature. The catalysts were prepared using either impregnation or ion-exchange methods. They reported that the hydrogenation was a zero-order reaction. and carbon tetrachloride strongly influences the hydrogenation of 1-hexene over Rh/SiO_2 and Pd/SiO_2 catalysts. Deactivation of 1-hexene hydrogenation upon the adsorption of either additive seemed to be structure sensitive over Pd/SiO_2 catalysts. But this was not the case for hydrogenation of cyclohexene.

S. David Jackson and Lindsay A. Shaw (1996) studied the hydrogenation of phenyl acetylene and styrene over a palladium/carbon catalyst. They found that the order in phenyl acetylene changed from zero order to first order at approximately 60% conversion. This behavior was ascribed to catalyst surface being unable to saturate with the hydrocarbon due to low concentration in solution.

M.A. Armendia *et al.* (1997) studied the hydrogenation of citral with Pd catalysts supported on mixed 80:20 $SiO_2/AlPO_4$ and sepiolite from Vallecas (Madrid, Spain). They investigated the influence of reaction variables such as temperature, hydrogen pressure and the type of solvent in order to optimize the reduction process. .

The solvent has a marked effect on the reduction rate; thus, nonpolar solvents lead to greater reduction rates. They found that the presence of additives of Lewis acid type such as $FeCl_2$ increases the selectivity towards geraniol and nerol.

Z.M. Michalska *et al.* (1998) studied the catalytic behavior of palladium supported on polyamides having a pyridine moiety in the liquid phase hydrogenation of alkadienes and alkynes at 25 °C and 1 atm pressure. The polymer supported palladium catalyst demonstrated high activity for alkyne hydrogenation. Such a different in selectivity was ascribed to the strong metal-support interaction that exists between palladium and the polymer functionalities. The results indicated that the rate of hydrogenation was affected more by the solvent polarity than by the solubility of hydrogen in the solvent. The stability and very good recycling efficiency of these catalysts made them useful for prolonged use.

Z. Dobrovolna *et al.* (1998) studied competitive hydrogenation of alkene, alkyne and diene substrates (C_6- C_8) over palladium and platinum catalysts at 20 °C and atmospheric pressure. They found that hydrogenation of alkynic and dienic substrates were preferred in alkyne-alkene and diene-alkene systems, respectively. In these systems, palladium catalyst selectivity was higher than that of the platinum catalyst due to higher relative adsorption coefficients for corresponding substrate couple on the palladium catalyst.

S. David Jackson *et al.* (1999) studied the hydrogenation of cyclopentene, cyclohexene, cycloheptene, and cis-cyclooctene over Pd/alumina, Pd/carbon, Pd/silica, and Pd/zirconia catalysts. The hydrogenation reaction and the carbon deposition reaction both showed evidence for particle size sensitivity and the trend in activity with particle size was not the same for all the cycloalkenes, with cycloheptene hydrogenation increasing with particle size. This behaviour can principally be related to the strength and mode of adsorption of the cycloalkene, although the adsorbed state of hydrogen may also influence reactivity.

A. Mastalir *et al.* (2000) prepared palladium particles incorporated into organophilic montmorillonite. TEM measurements indicated that the diameters of the Pd particles observed were in the range 1.5-6 nm. They investigated two samples (Pd-

M1 and Pd-M2), with metal contents of 0.1% and 0.46%, respectively. The catalytic activity of the Pd-montmorillonite formed was tested in the liquid-phase hydrogenation of 1-phenyl-1-butyne. For the production of the cis-alkene stereoisomer, Pd-M2 proved to be less active but more stereoselective than Pd-M1. The stereoselectivities obtained for Pd-M2 in n-hexane (86%-88%) were nearly as high as those experienced for the Lindlar catalyst.

M. Gruttadauria *et al.* (2001) studied the semihydrogenation of C-C triple bonds using palladium on pumice with a metal loading of 0.5, 1.5, 3% wt as catalyst. They investigated the parameters such as metal loading, hydrogen flow, molar ratio substrate/Pd, stirring rate, nitrogen base. They found that the Pd/pumice with the highest metal content (3%) showed a very low dispersion as a consequence of the low specific surface area of pumice. The growth of large metal particle produced a few neighboring catalytic sites. For the effect of solvent, they found that the reaction carried out in tetrahydrofuran showing slower activity than in ethanol.

T. Nozoe *et al.* (2001) investigated the non-solvent hydrogenation of solid alkynes and alkenes using supported palladium catalysts. *trans*-Stilbene and carboxylic acids with α,β-C=C bonds were employed as the alkene-type substrates for the non-solvent hydrogenation. Their hydrogenation proceeded over a Pd/SiO$_2$ catalyst at room temperature in a hydrogen stream. The hydrogenation rate of the trans-stilbene under the non-solvent conditions was lower than the hydrogenation in tetrahydrofuran (THF). The non-solvent hydrogenation of the C=C bond in diphenylacetylene or phenylpropiolic acid proceeded over a Pd/C catalyst more smoothly than their hydrogenation in THF.

U. K. Singh and M. Vannice (2001) studied liquid-phase citral hydrogenation over SiO$_2$-supported Group VIII metals at 300 K and 1 atm. The catalysts were prepared using an incipient wetness technique. The initial TOF (turnover frequency) for citral hydrogenation varied by three orders of magnitude and exhibited the following trend: Pd>Pt>Ir>Os>Ru>Rh>Ni>Co>>Fe (no activity was detected over FeSiO$_2$). With the exception of Ni/SiO$_2$, all catalysts exhibited substantial deactivation due to citral and/or unsaturated alcohol decomposition to yield adsorbed CO that poisoned active sites responsible for hydrogenation.

A. Mastalir *et al.* (2001) investigated the catalytic performance in liquid-phase hydrogenation of 1-phenyl-1-pentyne on low-loaded, organophilic Pd-montmorillonites (Pd-M1 and Pd-M2, with Pd contents of 0.1 and 0.46%, respectively) preparing in a micellar system. The organophilic character of the catalysts was utilized to study solvent effect. They found that both THF and toluene may be considered to be appropriate solvents for the above reaction, since they tend to increase the amount of active Pd atoms available for the reactants through swelling and disaggregation of the clay host. Accordingly, the Pd-Ms may find further applications as possible alternatives of the Lindlar catalyst for the stereoselective hydrogenation of different alkyne derivatives.

H. Blaser *et al.* (2001) reviewed the application of heterogeneous Pd catalysts for the manufacture of fine chemicals with special emphasis of their organic synthetic potiential. Two types of catalysts were used: heterogeneous catalysts where metallic Pd is supported on carrier and homogeneous catalysts consisting of mononuclear Pd (ligand) complexes. The application of heterogeneous Pd catalysts for oxidation and C-C coupling reactions is far less developed and in many cases homogeneous Pd catalysts are more effective and more versatile. In many cases, leached Pd has been detected in solution, and generally the nature of the catalytic species (surface or dissolved) is under discussion for transformation in absence of hydrogen.

S. Tanaka *et al.* (2002) prepared Pd/SiO_2 catalysts by a complexing agent-assisted sol-gel method and impregnation methods using an organic complexing agent (imp-org) or water (imp-w) as the impregnation solvent. The Pd/SiO_2 were characterized by TG-DTA, FT-IRs, C NMR, XRD, TEM, XPS, and CO adsorption, and the difference between the preparation methods was discussed. They found that the palladium particles in the sol-gel catalysts were much smaller and more uniform in size than those in the corresponding impregnation catalysts. The CO adsorptions for both impregnation catalysts decrease with the activation temperature after showing the maxima.

R.A.W. Johnstone *et al.* (2003) studied hydrogenation of alkenes over palladium and platinum metals supported on a variety of metal (IV) phosphates.

Platinum and palladium catalysts were prepared by first exchanging the acidic protons followed by their reduction to metal. They found that rate of hydrogenation of 1-octene and 4-methylcyclohexene over a series of platinized and palladized metal (IV) phosphates, some of which were more effective than standard Pd/C catalyst. The variation may correlate with surface topography but does not appear to correlate within the electronegativity of the metal in the metal phosphate.

T.A. Nijhuis *et al.* (2003) studied the selective liquid phase hydrogenation of alkynes to alkenes on different silica-supported palladium catalysts. The results showed that for the catalysts supported on Davisil, both the activity and selectivity increase with a decreasing particle size, indicating internal mass-transfer limitations. On the kinetics study, the alkyne is hydrogenated up to nearly full conversions following zero order kinetics when the concentration of the alkyne is sufficiently low, the hydrogenation of alkene is observed. The selectivity of the palladium catalysts was successfully improved by modifying the catalyst with copper.

O. Dominguez-Quintero *et al.* (2003) investigated palladium nanoparticle in the hydrogenation catalysis of different substrates (1-hexene, cyclohexene, benzene, 2-hexanone and benzonitrile). Palladium nanoparticles (1.9 nm.) stabilized was obtained from the reduction of organometallic precursor (palladium (II) bis-dibencylidene acetone) with hydrogen. The highest hydrogenation rate was found with 1-hexene with a TOF of 38,250 mole of product/ (mole of metal/h) at 25°C and 30 psi pressure. They presented that the catalytic potential of the Pd/SiO$_2$ systhesized by an organometallic route renders an extremely active nanomaterial which shows little aggregation after catalytic reactions even at 145 °C.

M. Lashdaf *et al.* (2003) studied the catalytic activity and selectivity of alumina and silica supported palladium and ruthenium catalysts in cinnamaldehyde hydrogenation. Palladium and ruthenium were introduced onto alumina and silica supports by atomic layer epitaxy and by impregnation technique. Palladium catalysts were more active than ruthenium catalysts. ALE-prepared palladium catalysts showed the highest initial activity because of the small metal particle size. However, the reactivity of surface palladium atoms was highest in the large metal particles.

3.2 Synthesis of MCM-41

A new class of mesoporous molecular sieve materials designated as MCM-41 was first reported in 1992 by the researchers of the Mobil Oil Corporation, USA. After the discovery of MCM-41, the researcher interest focused on the following main subjects: (1) characterization; (2) the mechanism of formation; (3) the synthesis of new materials based on the MCM-41 synthesis concept; (4) morphology control; and (5) the technical applications of MCM-41 and related mesoporous materials.

C. T. Kresge *et al.* (1992) studied a new synthetic composition of ultra-large pore crystalline material and use thereof as sorbent and in catalytic conversion of organic and inorganic compounds. The new crystalline material exhibits unusually large sorption capacity demonstrated by its benzene adsorption capacity of greater than about 15 grams benzene/100 grams at 50 torr and 25°C, a hexagonal electron diffraction pattern that can be indexed with a d_{100} value greater than about 18 Å and a hexagonal arrangement of uniformly sized pores with a maximum perpendicular cross section of at least about 13 Å.

J. S. Beck *et al.* (1992) have synthesized a new synthetic composition of ultra-large pore crystalline material. This material is called M41S family. Different mesostructures have been named as MCM-41 (hexagonal), MCM-48 (cubic), and MCM-50 (lamellar).

. S. Zhao *et al.* (1996) presented a comprehensive overview of recent advances in the field of MCM-41. Beginning with the chemistry of surfactant/silicate solutions, progresses made in design and synthesis, characterization, and physicochemical property evaluation of MCM-41 are enumerated. Proposed formation mechanisms are presented, discussed, and identified. Potential applications are reviewed and projected.

A. Corma (1997) studied the synthesis procedures and synthesis mechanisms, heteroatom insertion, characterization, adsorption, and catalytic properties, rapidly

occurs. It would be highly desirable to produce high thermal and hydrothermal stablility materials. The importance of the adsorption and diffusion of reactants and products in micro- and mesoporous catalysts on their activity and decay, especially when working in liquid phase have been reported. He suggested that it is of much interest in catalysis to prepare good mesoporous with different pore size, since in this case a high dispersion of Pt, Pd, Pt-Re, and Ni-Mo could be achieved and this could generate such new and highly active hydrogenation, re-forming, and HDS catalysts.

3.3 MCM-41 Supported Pd Catalyst

C.A. Koh *et al.* (1997) studied the structure of MCM-41 material during heat treatment (calcination) and determined catalytic performance of a series of Pd/MCM-41 catalysts, prepared by an incipient wetness technique, for selective hydrogenation of 1-hexene and benzene. Their temperature-programmed reduction (TPR) measurements for the calcined Pd catalyst series showed that about 70% of the PdO contained in the catalysts were reduced at sub-ambient temperature and the other 30% of PdO were reduced within 298-323 K (G.C. Bond, private communication), while the pure MCM-41 showed no reduction up to 873 K. TEM results showed that the Pd metal particles in the reduced Pd/MCM-41 catalysts were located in the pores of MCM-41 with good distribution.

B.M. Choudary *et al.* (1999) compared Pd catalysts supported on mesoporous materials, Pd/Si-K10 and Pd/MCM-41, with a microporous Pd/Y-zeolite. Catalysts were prepared by ion exchange method and their catalytic properties for the hydrogenation of alkenes, alkynes and semi-hydrogenation of alkynes were investigated. Pd/MCM-41 was about two times more active than Pd/Si-K10. Pd is not well dispersed on any of the three supports when the catalyst was prepared in organic media. It is known that selectivity decreases for semi-hydrogenation when dispersion increases, so that this poor dispersion is acceptable. All catalysts were active in the hydrogenation of alkynes giving high yields of alkenes but Pd/MCM-41 showed highest activity. In conclusion, mesoporous supports give satisfactory results for the semi-hydrogenation of acetylenic compound in fine chemistry.

S. Shimazu *et al.* (2002) studied the synthesis and the characterization of the palladium complexes grafted on MCM-41 mesopore surface via silane coupling ligands (AEAPSi) and their catalytic behavior for the hydrogenation of dienes with/within a hydroxyl group. The MCM-41 supported catalyst had a large amount of the unmodified-OH groups in th mesopore as well as the AEAPSi functional group. The MCM-41 supported catalyst exhibited high activity and high regioselectivity in the hydrogenation of dienes with -OH group.

S. Albertazzi *et al.* (2003) studied the behavior of different catalysts containing 1 wt. % of noble-metal inside a Mesoporous MCM-41 in the hydrogenation of naphthalene. Only the Rh- and Pd-containing catalysts were active in the test performed at atmospheric pressure. Performing the tests under pressure (6.0 MPa) the catalytic activity grew significantly, evidencing the following scale of activity for the noble-metals investigated: Pt>Rh>>Pd>>>>Ru≈Ir, with the latter two catalysts that deactivated in the 1 h of time on steam.

3.4 Catalyst Deactivation in Liquid Phase Reaction

Study of catalyst deactivation in liquid phase reaction studies is somewhat difficult because of the high number of factors potentially involved such as sintering and leaching of active components, poisoning of active sites by heteroatom-containing molecules, inactive metal or metal oxide deposition, impurities in solvents and reagents, and oligomeric or polymeric by-products. Because of many factors involved in activity and selectivity decay and non-identical catalysts for different lots, there is a high probability of irreproducible results (Michele Besson and Pierre Gallaezot, 2003). In this work, the main causes of deactivation in liquid phase reaction such as sintering of metal and leaching of catalysts were focused.

Fengyu Zhao *et al.* (2000) studied the details of this mass transfer between solvent and support by using homogeneous or heterogeneous catalysts in the absence or presence of additional palladium-free support materials. The results showed that Pd exists in solution, on the support, and in the form of free colloidal particles during

and after the Heck reaction and the transfer of Pd between these phases depends on the surface nature of the supports and reaction conditions used.

Peter Albers *et al.* (2001) studied the major causes for deactivation such as particle growth for, coke deposition, and leaching. They found that the leaching of precious metal can be minimized by either improving the availability of hydrogen in the liquid reaction medium or by optimizing the "catalyst side" of the process. In term of modifying the "catalyst side" of the process two approaches are proposed (1) to use of smaller quantities of catalyst for reaction and or (2) decrease the precious metal loading of the catalyst. Unfavorable and undesired effect about sintering and agglomeration may be suppressed by means of adequate impregnation agents and procedures, controlled temperature, and use of suitable support materials (R.J. Card, *et al.*, 1983)

Roland G. Heidenreich *et al.* (2002) studied parameter that influence the palladium leaching during and after Heck reactions of aryl bromides with olefins catalyzed by heterogeoeous Pd on activated carbon systems. The results showed that the Pd concentration in solution correlated with the nature of the starting materials and products, the temperature, the solvent, the base and the atmosphere (argon or air). Lower temperatures, higher concentrations and stronger interactions of the bromoarenes with Pd^0 clearly increase Pd leaching.

Michele Besson and Pierre Gallezot (2003) reviewed the factors contributing to the deactivation of metal catalysts employed in liquid phase reactions for the synthesis of fine or intermediate chemicals. The main causes of catalyst deactivation are particle sintering, metal and support leaching, deposition of inactive metal layers or polymeric species, and poisoning by strongly adsorbed species. Leaching of metal atoms depends upon the reaction medium (pH, oxidation potential, chelating properties of molecules) and upon bulk and surface metal properties.

CHAPTER IV
EXPERIMENTAL

The experimental in this chapter is divided into three major parts: (1) catalyst preparation, (2) reaction study in liquid phase hydrogenation, and (3) catalyst characterization. The first part (section 4.1) presents preparation of catalyst including synthesis of MCM-41 support and palladium loading. The second part (section 4.2) illustrates the reaction study in liquid phase hydrogenation. And the third part (section 4.3) explains the detail of characterization techniques such as AA, BET, XRD, TPR, CO-pulse chemisorption, SEM, and TEM.

4.1 Catalyst Preparation.

4.1.1 Synthesis of MCM-41 small pore

Pure silica MCM-41 with 3 nm pore diameter was prepared in the same manner as that of Cho et al. (D.H.Cho *et al.*) using the gel composition of CTABr: 0.3 NH$_3$: 4 SiO$_2$: Na$_2$O: 200 H$_2$O, where CTABr denotes cetyltrimethyl ammonium bromide. Briefly, 20.03 g of colloidal silica Ludox AS 40% (Aldrich) was mixed with 22.67 g of 11.78% sodium hydroxide solution. Another mixture comprised of 12.15 g of CTABr (Aldrich) in 36.45 g of deionized water, and 0.4 g of an aqueous solution of 25% NH$_3$. Both of these mixtures were transferred into a Teflon lined autoclave, stirred for 30 min, then heated statically at 100°C for 5 days, the pH of the gel was adjusted to 10.2 using 30% acetic acid every 24 h. The obtained solid material was filtered, washed with water until no base and dried at 100°C. The sample was then calcined in flowing nitrogen up to 550°C (1-2 ^{o}C/min), then in air at the same temperature for 5 hours, and is referred to in this work as small pore MCM-41. The chemicals used in synthesis of MCM-41 small pore are shown in Table 4.1

4.1.2 Synthesis of MCM-41 large pore

The larger pore MCM-41 with 7 nm pore diameter was prepared by treating the MCM-41-small pore (before calcination) in an emulsion containing *N,N*-dimethyldecylamine (0.625 g in 37.5 g of water for each gram of MCM-41) for 3 days at 120°C. This was washed thoroughly, dried, and calcined in flowing nitrogen up to 550°C (1-2 $^\circ$C/min), then in air at the same temperature for 5 hours.

4.1.3 Preparation of Silica-small pore

Silica support was obtained by commercial silica gel (SiO_2) granulars 100-200 mesh.

4.1.4 Preparation of Silica-large pore

Silica support was obtained by grinding Grade 57 silica gel (SiO_2) granulars and collecting particles in the 40-60 range. The silica support particles were calcined at 550°C for 8 h. in a furnace to eliminate adsorbed water and other impurities. The temperature of furnace was increased from ambient temperature to 550°C at the heating rate 2°C/min. The calcined silica was removed from the furnace, cooled down to room temperature and stored in a desiccator.

Table 4.1 Chemicals used in the synthesis of MCM-41 small pore

Chemical	Supplier
cetyltrimethyl ammonium bromide	Aldrich
colloidal silica Ludox AS 40%	Aldrich
aqueous solution of 25% NH_3	BDH
30% acetic acid	Carlo Erba

4.1.4 Palladium Loading

The palladium loading procedures are as follows:

1.   The previously calcined different silica supports were impregnated with an aqueous solution of palladium by the incipient wetness technique. The type of silica supports are shown in Table 4.2   Using the water capacity measurement obtained previously for the silica particles, a sufficient amount of the palladium salt (Pd nitrate dehydrate) was added to obtain a 0.5% by weight of palladium.

2.   After an impregnation, the catalysts were dried at 110°C for 16 h.

3.   The dried catalysts were calcined at 500°C for 2 hours in a furnace.

4.   Finally, the catalysts were cooled down and stored in desiccators.

Table 4.2 The types of silica support

Type of silica	Supplier
Silica small pore	Davison Chemical
Silica large pore	Strem Chemical
MCM-41 small pore	Synthesized in laboratory
MCM-41 small pore	Laval university, Canada

4.2 The Reaction Study in Liquid Phase Hydrogenation

4.2.1 Chemicals and Reagents

The chemicals and reagents used in the reactions are shown in Table.4.3

Table 4.3 The chemicals and reagents used in the reaction

The chemicals and reagents	Supplier
High purity grade Hydrogen (99.99vol. %)	Thai Industrial Gases Limited
High purity grade Nitrogen (99.99vol. %)	Thai Industrial Gases Limited
Absolute ethyl alcohol (99.99vol. %)	Mallinckrodt
1-Hexene purum (96vol. %)	Fluka

4.2.2 Instruments and Apparatus

The schematic diagram of the liquid phase hydrogenation reaction of 1-hexene is shown in Figure 4.1 The part of instruments and apparatus are illustrated and explained as follows:

1) The Autoclave reactor

The autoclave is made of stainless steel with a volume of 2000 ml and 10 cm inside diameter. It consists of four valves, which are used to feed or vent the reactant and a stirring core. This autoclave can be operated at moderate temperature (0-300°C) and pressure (0-300 psi) as shown in Figure4.2a and 4.2b.

2) The Automatic temperature controller

The automatic temperature controller consists of a magnetic switch connected to a variable voltage transfer and a RKC temperature controller, which is connected t a 1 mm. diameter thermocouple for temperature measurement of

the system. A dial setting establishes a set point at any temperature within the range 0 to 400°C

3) Electrical furnace

This supplies the required temperature to the autoclave for reaction. The autoclave can be operated from room temperature up to 300°C at voltage of 150 voltages.

4) Gas controlling system

Nitrogen cylinder is equipped with a pressure regulator (0-2000 psi). Hydrogen gas is allowed to flow into autoclave by using a pressure regulator (0-350 psi). A needle valve is used to release gas from the autoclave. A ball valve is used to feed reactant flow into autoclave.

5) Gas chromatograph

A gas chromatograph (Shimadzu GC-9A) equipped with a flame ionization detector (FID) was used to analyzed liquid feed and product. The operating conditions for GC and detector are shown in Table 4.4

Table 4.4 Operating conditions for the gas chromatograph

Gas Chromatograph	Shimadzu GC-14A
Detector	FID
Packed column	Chemical C 18 80/100 8ft
Carrier gas	Nitrogen (99.99vol. %)
Flow rate of carrier gas	25 cc/min
Column temperature	50°C
Detector temperature	200°C
Injector temperature	200°C
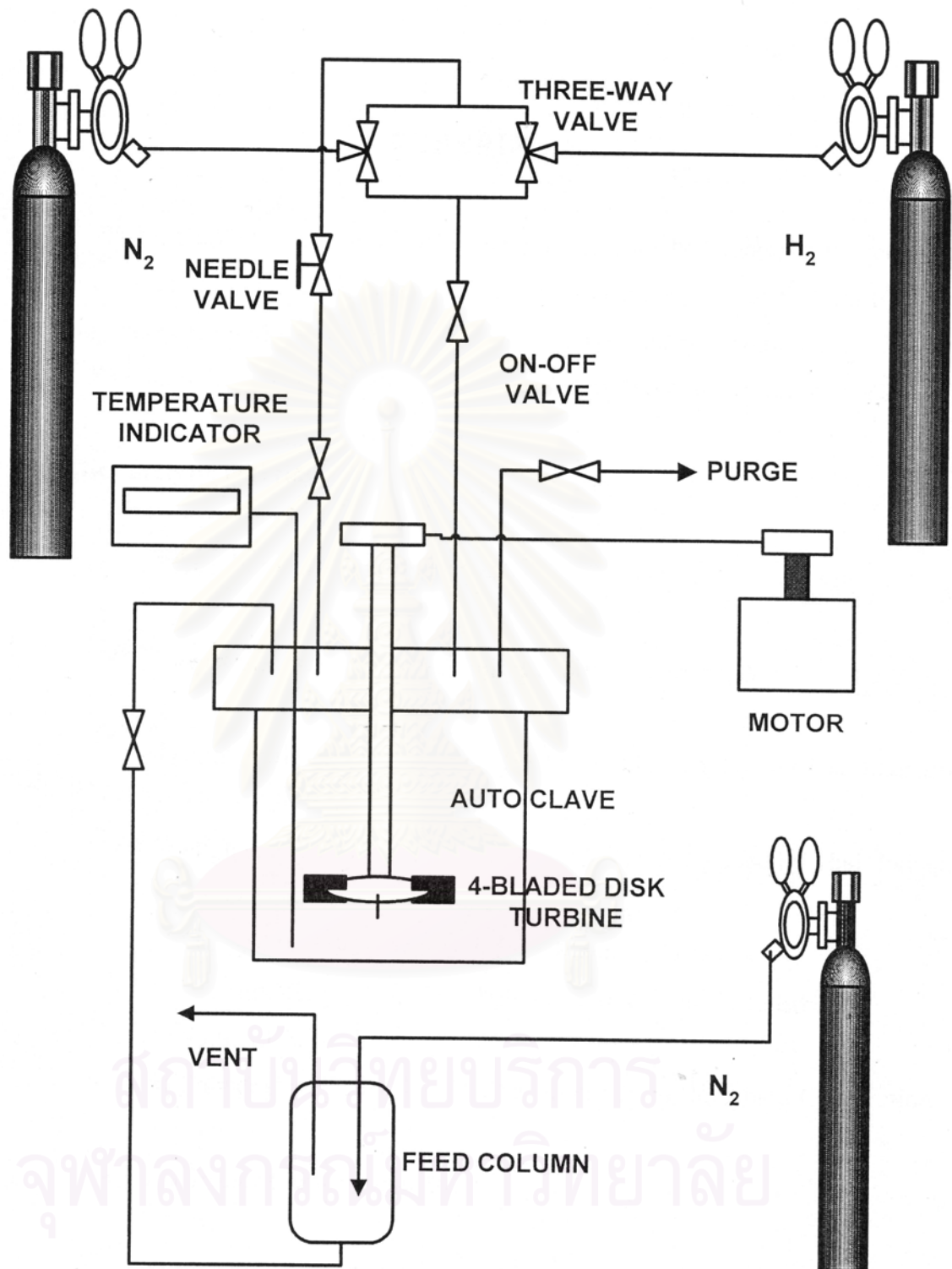
Figure 4.1 A schematic of liquid phase hydrogenation system
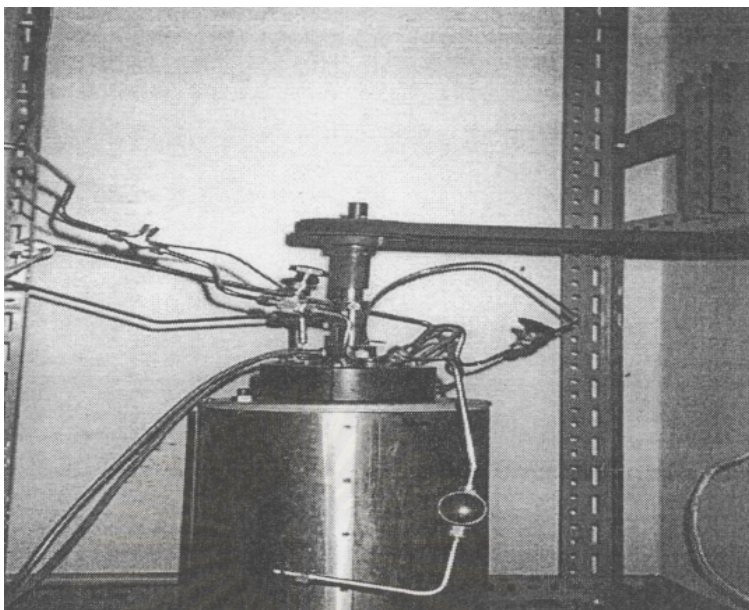
Figure 4.2 a   Autoclave and propeller
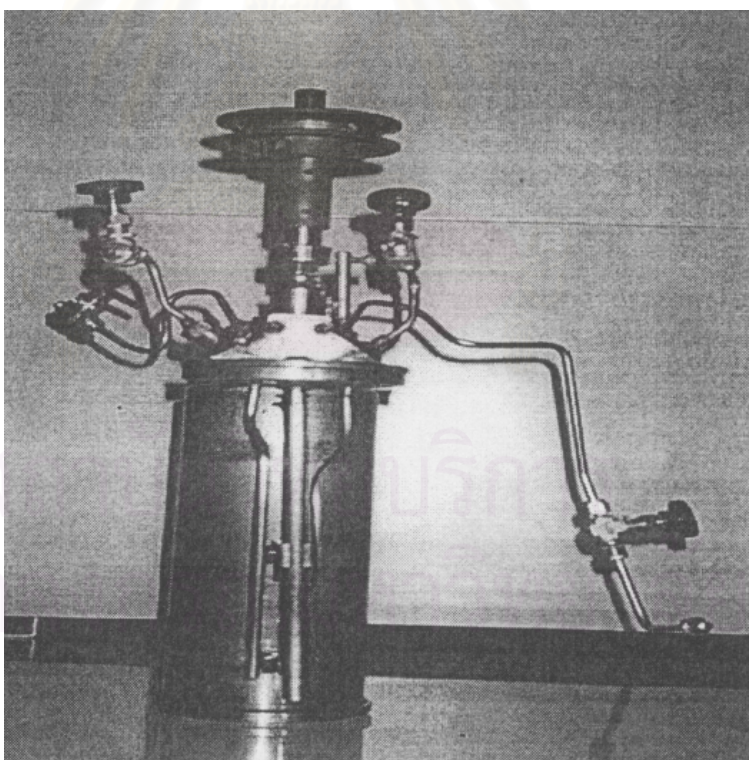
Figure 4.2 b   Autoclave and propeller
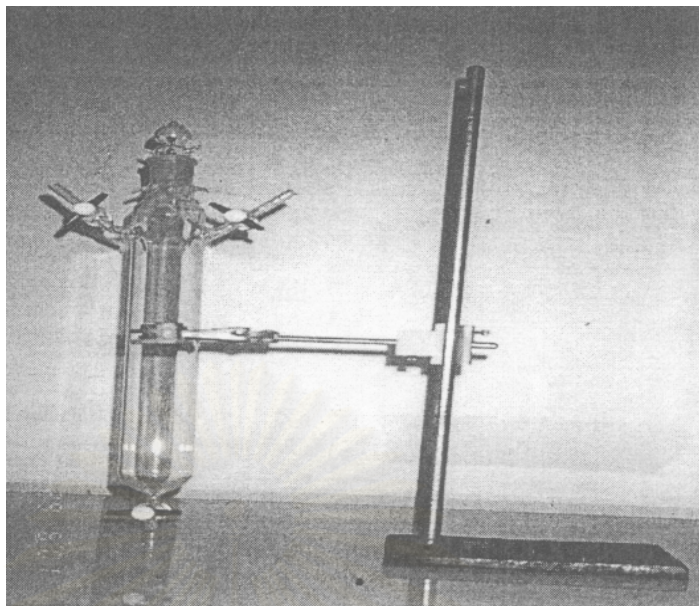
Figure 4.3   Feed column

4.2.3 Hydrogenation procedure

The hydrogenation procedures are explained in the details below that consist of 2 steps of reaction.

1) Reduction step

Approximately 1 gram of supported Pd catalyst was placed into the autoclave. The system was purged with nitrogen to remove remaining air. Next, hydrogen was switch at a volumetric flow rate of 100 ml/min to reduce supported Pd catalyst at room temperature for 2 h.

2) Reactant preparation and hydrogenation step

15 ml of 1-hexene and 400 ml of ethyl alcohol were mixed in a beaker, and then set in the 600 ml feed column (Figure 4.3). Next, the reaction mixture was introduced into the reactor with nitrogen. Afterwards, hydrogen was purged to remove remained nitrogen and keep for the reaction. The liquid phase hydrogenation reactions were carried out at room temperature and 1 atm and started the reaction with a stirring core. The content of hydrogen consumption was monitoring every ten minutes by noting the change in pressure of hydrogen for 4 h. The products were determined by a gas chromatograph.

4.3 Catalyst Characterization

4.3.1 Atomic adsorption spectroscopy

The bulk composition of palladium was determined using a Varian Spectra A800 atomic adsorption spectrometer at the Department of science service Ministry of science technology and environment. The calculation of the sample preparation is shown in Appendix A.

4.3.2 N_2 physisorption

The BET surface areas pore volumes, average pore diameters, and pore size distributions of the catalysts were determined by N_2 physisorption using a Micromeritics ASAP 2000 automated system. Each sample was degassed in the Micromeritics ASAP 2000 at 200^oC for 4 hours prior to N_2 physisorption.

4.3.3 X-ray diffraction (XRD)

The XRD spectra of the catalysts was measured using a SIEMENS D5000 X-ray diffractometer and Cu Kα radiation with a Ni filter in the 2-10° or 20-80° 2θ angular regions. The crystallite size was calculated from the Scherrer equation. The value of shape factor, K, was taken to be 0.9.

4.3.4 Scanning electron microscopy (SEM)

Catalyst granule morphology was obtained using a JEOL JSM-35CF scanning electron microscope operated at 20 kV at the Scientific and Technological Research Equipment Center, Chulalongkorn University (STREC).

4.3.5 Transmission electron microscopy (TEM)

Sample of catalysts for TEM are loaded into volatile liquid (ethanol) and then, a suspension in volatile liquid is prepared from the sample powder, often assisted by

Ultrasonic agitation for ten minutes. Next, this suspension is dropped on to thin Formvar supported on copper grids and dry. The palladium oxide particle size and distribution of palladium were observed using a JEOL-TEM 200CX transmission electron microscope operated at 100 kV at the Scientific and Technological Research Equipment Center, Chulalongkorn University (STREC)

4.3.6 CO-pulse chemisorption

Relative percentages of palladium dispersion were determined by pulsing carbon monoxide over the reduced catalyst. Approximately 0.2 g of catalyst was placed in a quartz tube, incorporated in a temperature-controlled oven and connected to a thermal conductivity detector (TCD). Prior to chemisorption, the catalyst was reduced in a flow of hydrogen (30cc/min) at room temperature for 2 h. Then the sample was purged with helium for 1 h. Carbon monoxide was pulsed at room temperature over the reduced catalyst until the TCD signal from the pulse was constant.

4.3.7 Temperature programmed reduction (TPR)

TPR will be used to determine the reducibility of catalysts. The catalyst sample of ca. 200 mg and temperature ramping from $35^{o}C$ to $300^{o}C$ at $10^{o}C/min$ were used in the operation. The carrier gas will be 5 %H_2 in argon. During reduction, a cold trap was placed before the detector in order to remove water produced. A thermal conductivity detector (TCD) was used to measure the amount of hydrogen consumption.

CHAPTER V

RESULTS

The different silica supported palladium catalysts prepared and evaluated in this study are consisted of Pd/SiO$_2$-small pore, Pd/SiO$_2$-large pore, Pd/MCM-41-small pore, and Pd/MCM-41-large pore. The results in this chapter present the catalytic activities of these catalysts for liquid phase hydrogenation of 1-hexene at 30°C and 1 atm and their charactistics before and after reaction. The catalysts before reaction are called fresh catalysts and the catalysts after reaction are called spent catalysts. The results are divided into three parts. The first part (section 5.1) shows kinetic study of liquid phase hydrogenation of 1-hexene over supported Pd catalysts. The second part (section 5.2) demonstrates the characteristic of the catalysts obtained from various analysis techniques such as N$_2$ physisorption, X-ray diffraction, scanning electron microscopy, transmission electron microscopy, atomic adsorption spectroscopy, CO-pulse chemisorption, and temperature programmed reduction. In the third part (section 5.3) catalyst durability and catalyst deactivation are reported.

Discussion in details about how silica type and silica support structure (SiO$_2$ and MCM-41) affected characteristics and catalytic activities of these catalysts is presented in the next chapter (chapter VI).

5.1 Liquid-Phase Hydrogenation Reaction

Liquid-phase hydrogenation of 1-hexene under mild conditions was carried out as a model reaction to compare the hydrogenation activity of all the catalysts. In terms of kinetics study, the effects of 1-hexene concentration, hydrogen pressure, and temperature were investigated. The reaction conditions for each measurement are shown in Table 5.1. In all cases the same amount of the catalysts of approximately 1 gram was used.

Reaction mechanism for 1-hexene hydrogenation on Pd catalyst is generally proposed as follows:

H_2 + $2Pd^*$ $\longleftrightarrow$ $2H\text{-}Pd^*$

$$C=C\text{-}C\text{-}C\text{-}C\text{-}C \quad + \quad 2Pd^* \longleftrightarrow \quad \overset{\displaystyle Pd^*Pd^*}{\underset{\displaystyle \text{-}C\text{-}C\text{-}C\text{-}C\text{-}C\text{-}C}{\big| \quad \big|}}$$

$$\overset{\displaystyle Pd^* \ Pd^*}{\underset{\displaystyle C\text{-}C\text{-}C\text{-}C\text{-}C\text{-}C}{\big| \quad \big|}} \quad + \quad H\text{-}Pd^* \longleftrightarrow \quad \overset{\displaystyle Pd^*H}{\underset{\displaystyle \text{-}C\text{-}C\text{-}C\text{-}C\text{-}C\text{-}C}{\big| \quad \big|}}$$

$$\overset{\displaystyle Pd^* \ H}{\underset{\displaystyle C\text{-}C\text{-}C\text{-}C\text{-}C\text{-}C}{\big| \quad \big|}} \quad + \quad H\text{-}Pd^* \longrightarrow \quad \overset{\displaystyle H \ H}{\underset{\displaystyle \text{-}C\text{-}C\text{-}C\text{-}C\text{-}C\text{-}C}{\big| \quad \big|}} + \ 2Pd^*$$
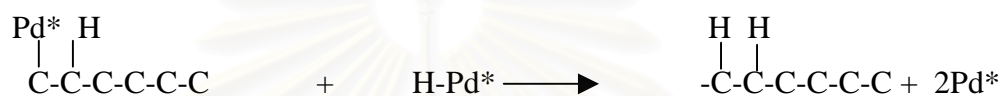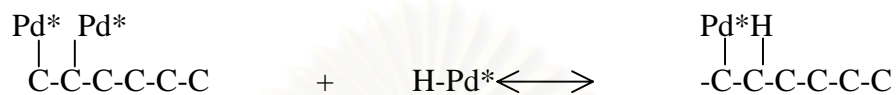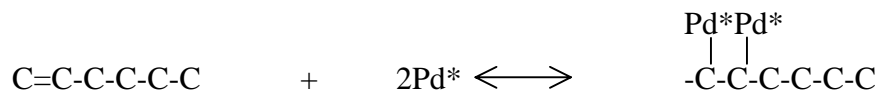
Table 5.1 The reaction conditions of liquid phase hydrogenation of 1-hexene

Effect	Catalyst	Temperature (°C)	Pressure (atm)	Ratio of hexene:ethanol
Ratio of hexene:ethanol	Pd/SiO$_2$-small pore	30	1	1:3 1:4 1:10 1:30
Hydrogen pressure	Pd/SiO$_2$-small pore	30	1 1.5 2	1:30
Temperature	Pd/SiO$_2$-small pore	30 35 40	1	1:30
Support	Pd/SiO$_2$-small pore Pd/SiO$_2$-large pore Pd/MCM-41-small pore Pd/MCM-41-large pore	30	1	1:30
Life cycle	Pd/MCM-41-small pore	30	1	1:30

5.1.1 Effect of 1-Hexene: Ethanol Ratio

The effect of 1-hexene: ethanol ratio on the rate of hydrogenation was studied. The reaction conditions are shown in Table 5.1. The kinetic of hydrogenation of 1-hexene can be followed by measuring the rate of consumption of hydrogen presented in Figure 5.1. It was observed that the linear decrease of volume of hydrogen consumed showed zero order as a function of time for initial period.
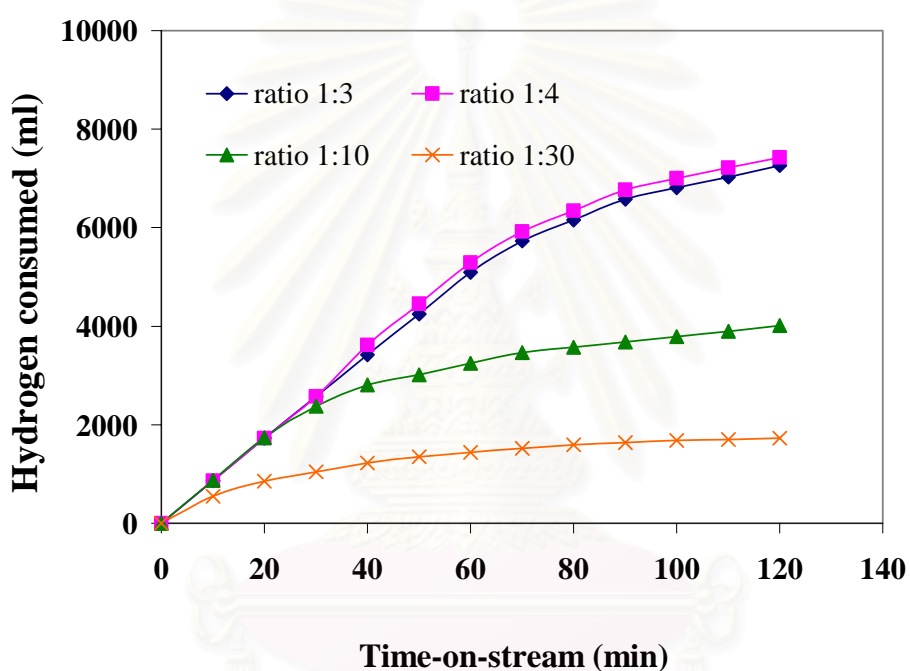
Figure 5.1 Effect of 1-hexene/ethanol ratio on the consumption of hydrogen as a function of time-on-stream during the hydrogenation of 1-hexene on SiO_2-small pore supported Pd catalysts

Figure 5.2 shows the plot of rate versus ratio of 1-hexene/ethanol. It was found that for 1-hexene/ethanol ratios of 1:3, 1:4, and 1:10, the initial rate of hydrogenation of 1-hexene was independent on the ratio of 1-hexene/ethanol.

For the ratio 1:30, the ratio of 1-hexene/ethanol had a little effect on the initial rate of hydrogenation of 1-hexene probably because the adsorption/desorption step of 1-hexene was slow due to very low concentration of 1-hexene. However, for strictly identical measurement conditions, the initial rate of 1-hexene/ethanol ratio of 1:30 can also yield a relative ranking of catalyst activity for studying of the other effects.

Figure 5.2 Plot of initial rate vs 1-hexene: ethanol ratio
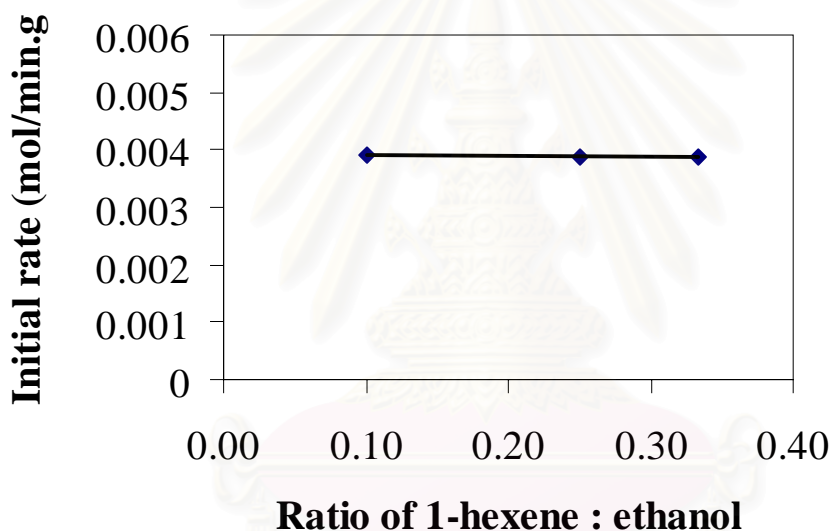
5.1.2 Effect of Hydrogen Pressure

The effect of hydrogen pressure on the initial rate of hydrogenation of 1-hexene was investigated in the range of 1 atm to 2 atm. The reaction conditions are shown in Table 5.1. The linear plot of initial rate versus hydrogen pressure is presented in Figure 5.3. The initial rate of hydrogenation of 1-hexene was found to be independent on hydrogen pressure.
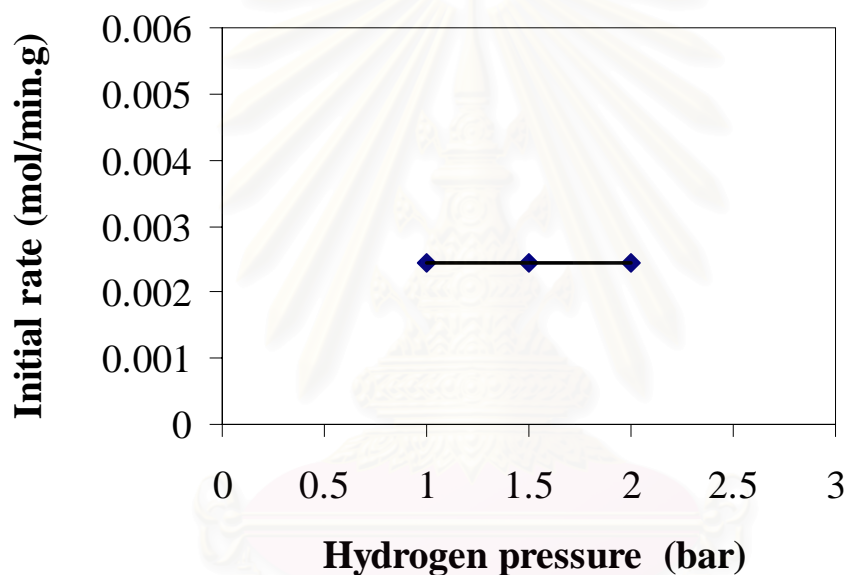
Figure 5.3 Plot of initial rate vs. hydrogen pressure

5.1.3 Effect of Temperatures

The kinetic of hydrogenation of 1-hexene was studied at various temperatures in the range of 30-40°C. The reaction conditions are also shown in Table 5.1. The initial rate of hydrogenation of 1-hexene was found to be dependent on temperature. The apparent activation energy calculated from the Arrhenius plot (Figure 5.4) was found to be 41 kJ/mol. It is quite typical for hydrogenation of 1-hexene as determined for other catalysts in the literature, the activation energy was in the range of 36-70 kJ/mol.
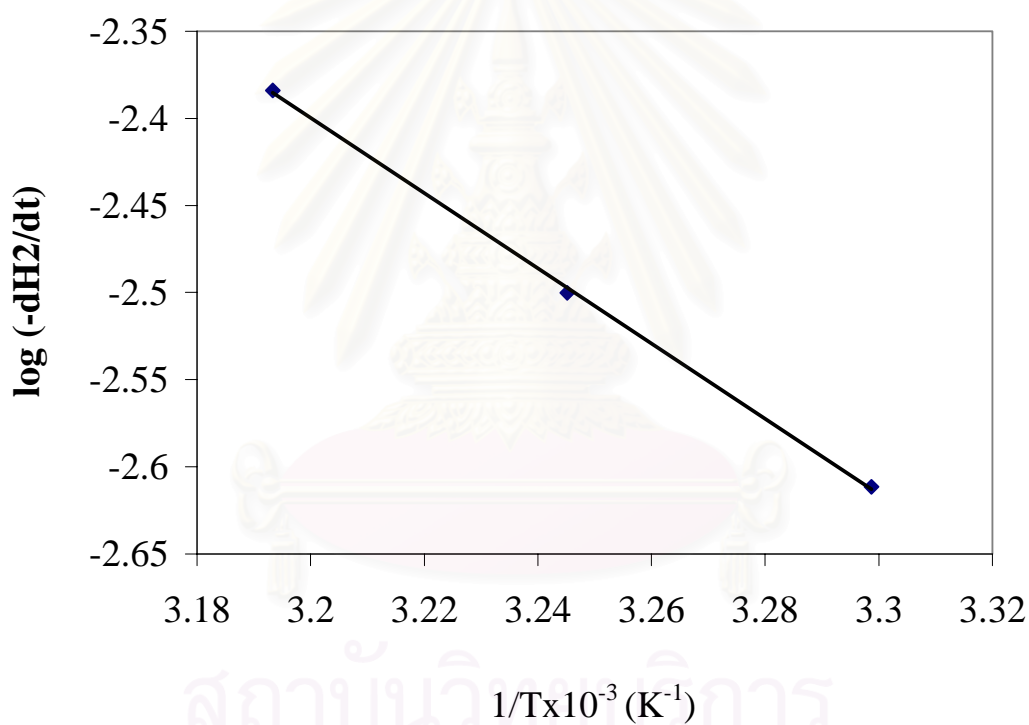
Figure 5.4 Arrhenius plot for SiO_2-small pore supported on Pd catalyst

5.1.4 Effect of Silica Support Structure

The reaction conditions for this study are shown in Table 5.1. The rates of hydrogen consumption versus time-on-stream for different silica-supported Pd catalysts are shown in Figure 5.5. Since the reaction is found to be zero order of both hydrogen and 1-hexene, the slope of the line at the beginning represent both initial rate and rate constant of the reaction. The rate constant of the different supported Pd catalysts in liquid phase hydrogenation of 1-hexene at $30^{o}C$ and the turnover frequencies are reported in Table 5.3. The activity of the catalysts were found to be in the order of Pd/MCM-41-large pore > Pd/MCM-41-small pore $\approx$ Pd/SiO_2-large pore > Pd/SiO_2-small pore. For a given silica type, the larger pore supported Pd catalysts were more active than the smaller pore supported ones, suggesting that the reaction was influenced by mass transport effect during reaction.

The turnover frequencies (TOF) were calculated using the active sites measured by pulse CO-chemisorption (discussion in section5.2.6)

$$TOF = \frac{rate}{(numbers\ of\ active\ site)}$$

$$= \frac{[mole\ H_2\ consumed]}{[g\ cat.]\ [min]} \left| \frac{[g\ cat.]}{[mol\ active\ site]} \right| \frac{[min]}{[s]}$$

$$= [s^{-1}]$$

For a similar pore size, Pd/MCM-41-small pore and Pd/SiO_2-small pore had a similar number of active sites as measured by CO chemisorption, but Pd/MCM-41-small pore showed higher activity than Pd/SiO_2-small pore suggesting that the structure of MCM-41 may promote the reaction.
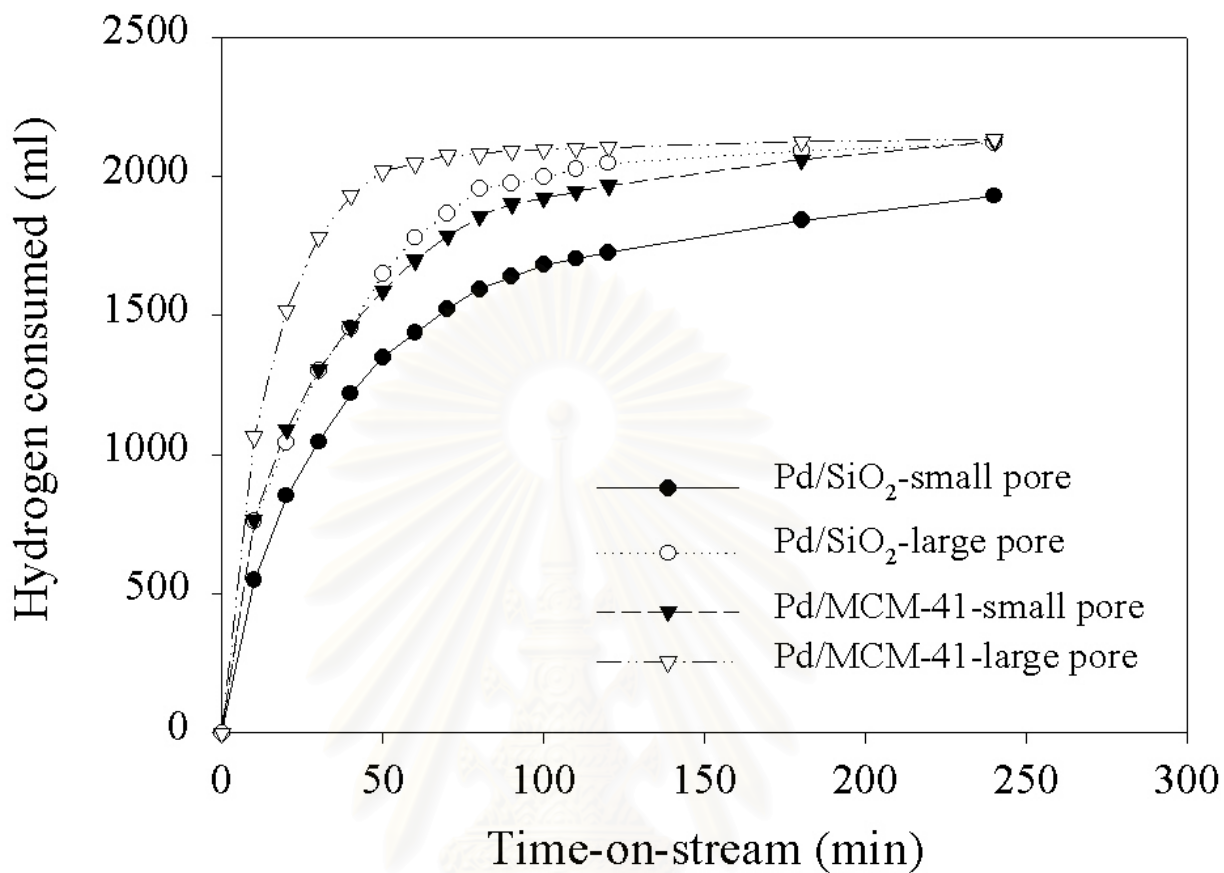
Figure 5.5 Consumption of hydrogen as a function of time for the hydrogenation of
1-hexene on different silica supported Pd catalysts.

Table 5.2 Catalytic activity of different supported Pd catalysts in liquid phase hydrogenation of 1-hexene

Catalysts	Rate Constant x10^3 (mol min^{-1}g^{-1}cat)	Turnover Frequencies (s^{-1})
Pd/SiO$_2$-small pore	2.45	19
Pd/SiO$_2$-large pore	3.40	29
Pd/MCM-41-smallpore	3.41	28
Pd/MCM-41-large pore	4.75	23

5.2 Catalyst Characterization Before and After Reaction

5.2.1 N_2 Physisorption

The most common procedure for determining the surface area of a solid and its pore size distribution is based on adsorption and condensation of N_2 at liquid N_2 temperature using static vacuum procedure. This method is also called BET (Brunauer Emmett Teller) method.

The BET surface areas, pore volumes, and average pore diameters of the original supports and the catalysts before and after reaction are given in Table 5.3. Except for the low surface area commercial large pore silica, SiO_2-small pore, MCM-41-small pore, and MCM-41-large pore possessed high BET surface areas of 716-921 m^2/g. After impregnation of palladium, the BET surface area and pore volume of the original supports decreased by approximately 6-20%, suggesting that palladium was deposited in some of the pores of the supports. The BET surface areas of the spent catalysts ranged between 191-546 m^2/g. The changes in BET surface areas after reaction indicated that there was probably pore blocking and/or destruction of support pore structure after reaction.

The pore size distribution of the four different silica supports used in this study and the supported catalysts are shown in Figure 5.6. A narrow pore size distribution was observed for all the catalyst supports except the commercial large pore silica. Palladium loading did not appreciably change the average pore diameter of the SiO_2- and small pore MCM-41-supported Pd catalysts. It did, however, significantly decrease that of the Pd large pore MCM-41.

Table 5.3 N_2 Physisorption results before and after reaction

	BET S.A.[a] m^2/g	Pore Volume cm^3/g	Avg. pore size (nm.)
Support			
SiO$_2$-small pore	716	0.39	2.2
SiO$_2$-large pore	277	1.14	16.4
MCM-41-small pore	921	0.87	3.8
MCM-41-large pore	901	1.59	7.0
Fresh catalysts			
Pd/ SiO$_2$-small pore	675	0.36	2.14
Pd/ SiO$_2$-large pore	201	0.92	18.2
Pd/ MCM-41-small pore	670	0.71	4.3
Pd/ MCM-41-large pore	726	0.62	3.4
Spent catalysts[b,c]			
Pd/ SiO$_2$-small pore	343	2.26	26.4
Pd/ SiO$_2$-large pore	191	1.93	40.5
Pd/ MCM-41-small pore	377	1.01	5.6
Pd/ MCM-41-large pore	546	0.52	3.8

[a] Error of measurement was $\pm$ 5%.

[b] After 4-h batch hydrogenation of 1-hexene at 30°C and 1 atm.

[c] Measurement at the institute of research and technology, the Petroleum Authority of Thailand (PTT)
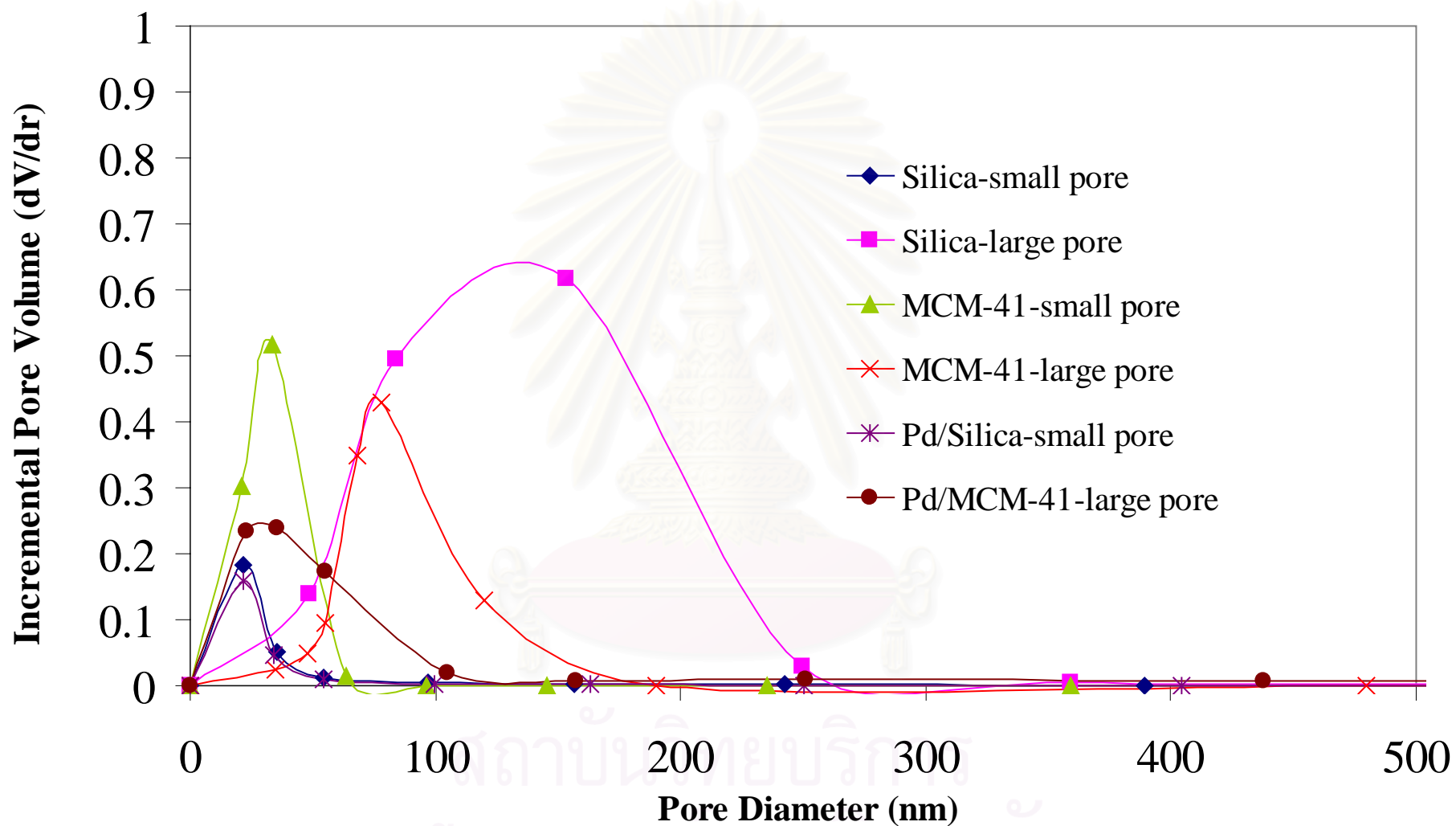
Figure 5.6 Pore size distribution of different silica supports and silica supported Pd catalysts.

5.2.2 X-Ray Diffraction (XRD)

Bulk crystal structure and chemical phase composition of a crystalline material having crystal domains of greater than 3-5 nm can be detected by diffraction of an X-ray beam as a function of the angle of the incident beam. Broadening of the diffraction peaks can be used to estimate crystallite diameter.

The X-ray diffraction patterns of the original MCM-41-small pore and the Pd/MCM-41-small pore catalysts (before and after reaction) are shown in Figure 5.17. The ordered structure of small pore MCM-41 gave XRD peaks at 2.40, 3.96, and $4.53^o2\theta$. After impregnation of palladium, the intensities of the XRD peaks for MCM-41 were decreased suggesting either the structure of MCM-41 became less ordered upon impregnation with palladium or that large Pd particles caused significant X-ray scattering. In any case, the structure of MCM-41 was not destroyed, although the long-range order of MCM-41 may have shrunk (Pasqua *et al.*, 2001).

The large pore MCM-41 appears to have been more amorphous than the small pore MCM-41 since it did not exhibit any XRD pattern at low 2θ. However; it still had a narrow pore size distribution with uniform pore diameters around 7 nm.

After reaction, the characteristic peaks of MCM-41-small pore decreased further, probably due to the instability of pure silica MCM-41 and/or the greater X-ray scattering ability of sintered metal particles (Marler *et al.*, 1996).

The XRD patterns at higher diffraction angles of the different silica supported on Pd catalysts are shown in Figure 5.8. In the calcined state, diffraction peaks for palladium oxide (PdO) were detectable at 33.8 and less so at 42.0, 54.8, 60.7, and $71.4^o2\theta$. After reaction the used catalysts were filtered out and dried at room temperature. XRD patterns of such catalysts were shown in Figure 5.17 After reduction and reaction, palladium metal (Pd^0) was in evidence with diffraction peaks at 40.1 and less so at $46.6^o2\theta$.

The recovered catalysts were then re-calcined in air at 500 ºC for 2 hours in order to compare the PdO particle sizes before and after reaction. The XRD patterns at higher diffraction angles of the silica supported on Pd catalysts in recalcined state are shown in Figure5.10

The PdO particle sizes were calculated from XRD line broadening of the peak at 33.8 ^{o} 2θ using Scherrer's equation (Klug and Alexander, 1974) and are reported in Table 5.4. In the fresh calcined catalysts, the PdO particles/clusters were found to be ca. 8-14 nm in the order of Pd/MCM-41-small pore > Pd/SiO$_2$-large pore > Pd/MCM-41-large pore ≈ Pd/SiO$_2$-small pore. After reduction, reaction and re-calcination, it was found that the PdO particle sizes for all catalyst samples became larger, indicating that palladium metal particles sintered after reaction and re-calcined. Sintering of metal particles after reduction and reaction has been reported earlier by Choudary *et al.*, 1999 and Dominguez-Quintero *et al.*, 2003. Use of large pore supports (both SiO$_2$ and MCM-41) resulted in the greatest amount of Pd sintering (almost 2 times larger).
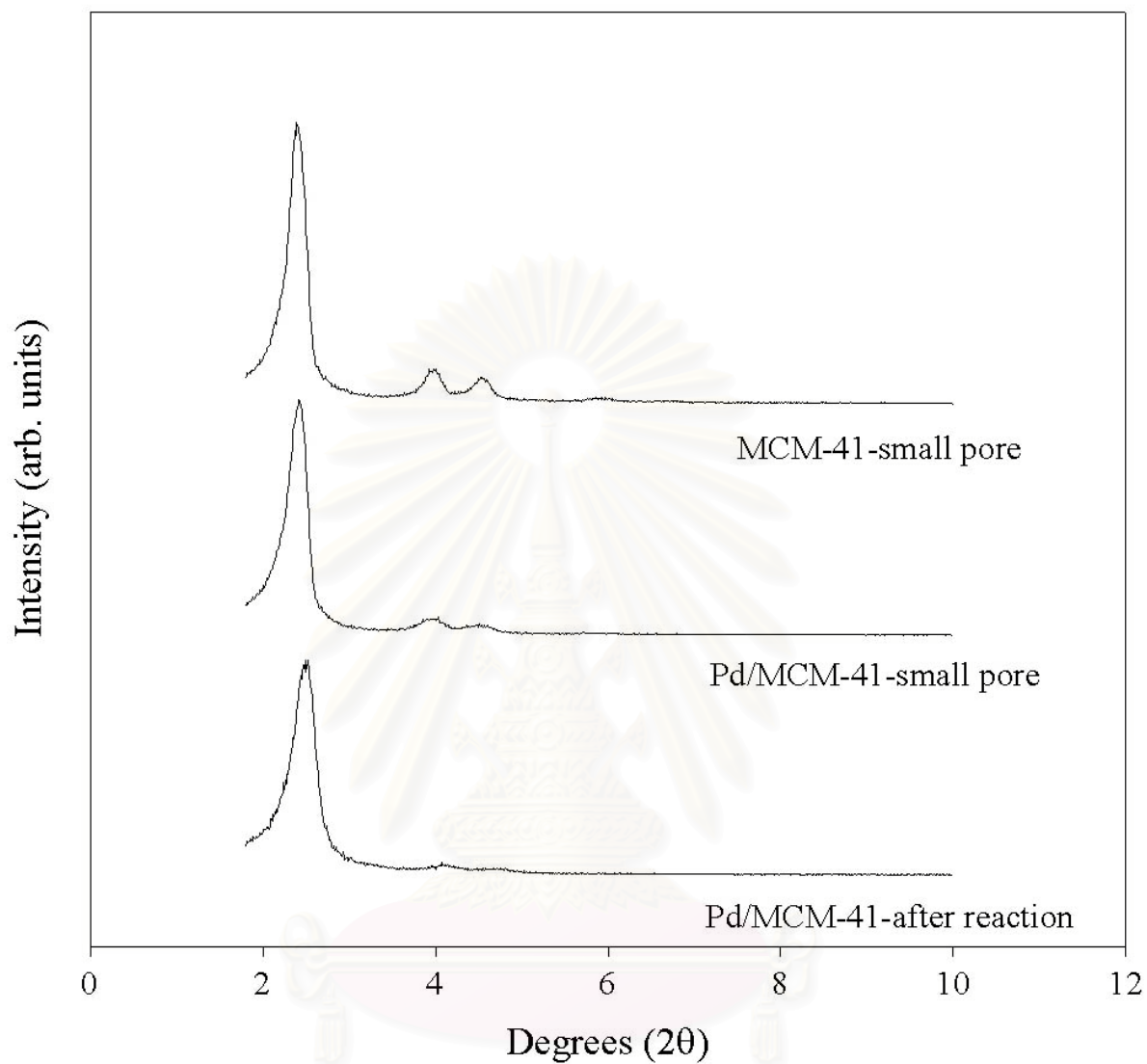
Figure 5.7 XRD patterns of MCM-41-small pore and Pd/MCM-41-small pore before and after reactions.
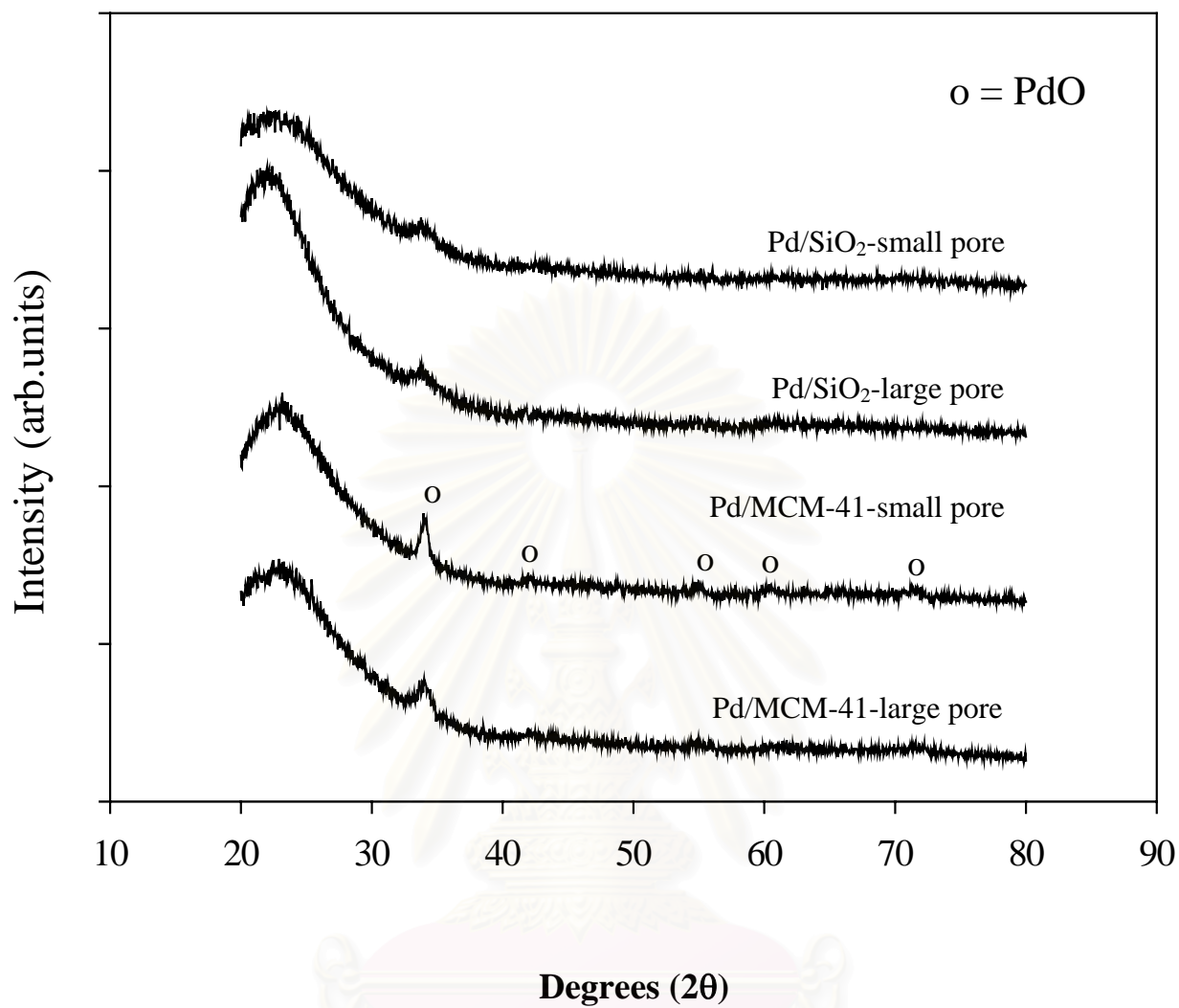
Figure5.8 XRD patterns of fresh catalyst at high degree 2θ
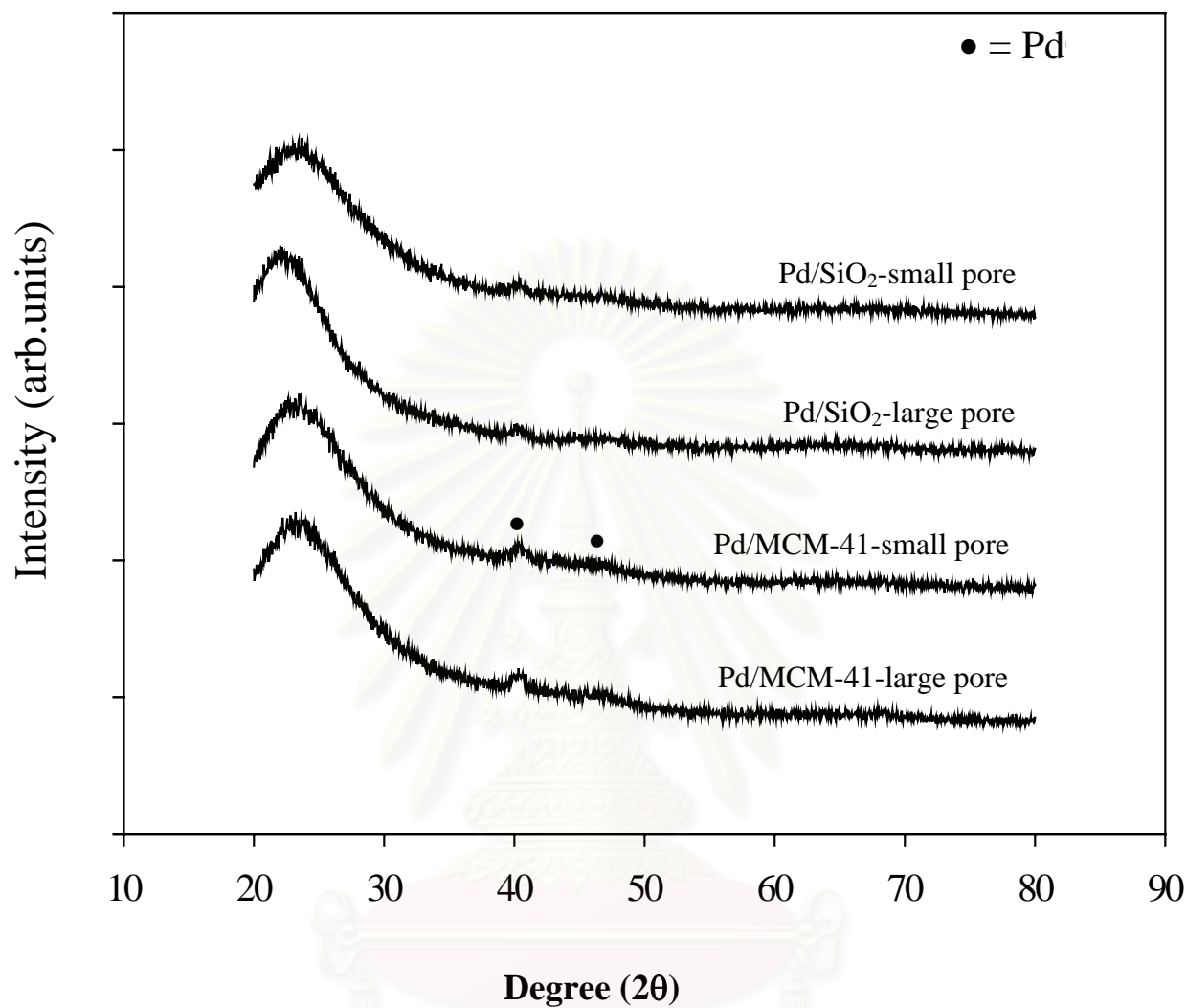
Figure 5.9 XRD patterns of spent catalyst at high degree (2θ)

o = PdO

Pd/SiO$_2$-small pore

Pd/SiO$_2$-large pore

Pd/MCM-41small pore

Pd/MCM-41-large pore

Intensity (arb.units)
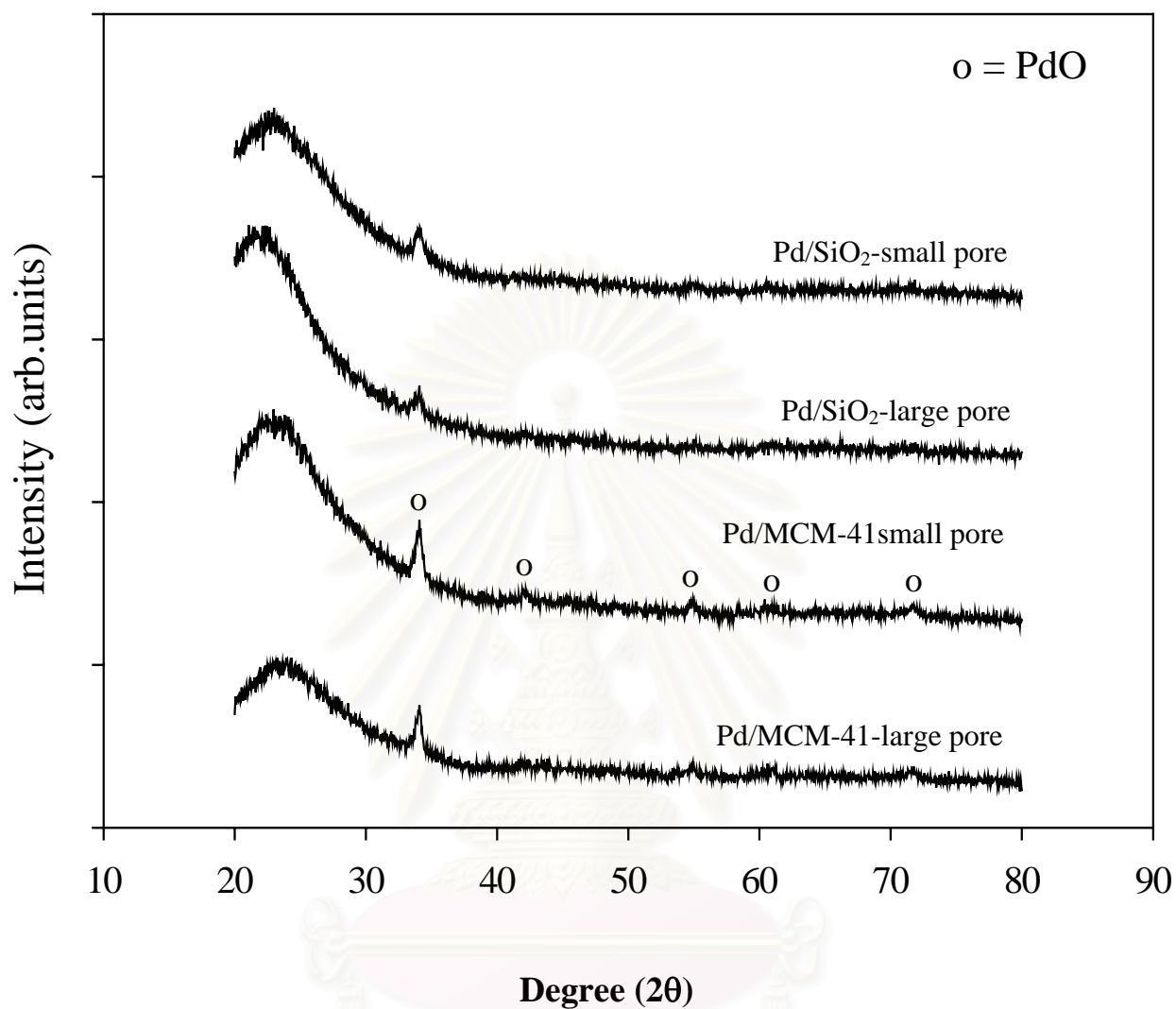
Degree (2θ)

Figure 5.10 XRD patterns of spent and re-calcined at 500℃ for 4 hours catalyst at high degree 2θ

5.2.3 Transmission Electron Microscopy (TEM)

TEM is a useful tool for determining crystallite size and size distribution of supported metals. It allows determination of the micro-texture and microstructure of electron transparent samples by transmission of a focused parallel electron beam to a fluorescent screen with a resolution presently better than 0.2 nm.

TEM micrographs of the fresh and spent supported Pd catalysts are shown in Figure 5.11-5.14. TEM micrographs were taken in order to physically measure the size of the palladium oxide particles and/or palladium clusters. Since the metal loading is low and the surface area of the sample is very high, in principle it is quite difficult to observe metal dispersion by TEM. However, a large number of pictures were collected from different portion of the samples in order to obtain further evidence about the dispersion of the palladium. The TEM images of the used catalysts were taken after all the carbon deposits have been removed. The particle size of PdO particles measured from TEM images (Table 5.4) before and after reaction was found to be in accordance with the results from XRD. The particle size of palladium on fresh catalyst were found to be in the order of Pd/MCM-41-small pore> Pd/SiO$_2$-large pore> Pd/MCM-41-large pore≈ Pd/SiO$_2$-small pore. For the spent catalysts, both silica and MCM-41 large pore resulted in larger palladium than small pore support. The differences in PdO particle sizes on different supports can be ascribed to differences induced by the support on the sintering of Pd during preparation and reaction (Choudary *et al.*, 1999)

Table 5.4 Average PdO particle sizes in the calcined catalysts before and after reaction

	PdO d_p (nm)			
	XRD		TEM	
	Fresh	Spent[a]	Fresh	Spent[a]
Pd/SiO$_2$-small pore	7.8	13.8	8.0	13.3
Pd/SiO$_2$-large pore	10.8	21.9	10.0	23.0
Pd/MCM-41-small pore	14.2	16.1	12.8	14.3
Pd/MCM-41-large pore	9.1	18.0	6.7	14.7

[a] After 4-h batch hydrogenation of 1-hexene at 30°C and 1 atm.

1mm. = 6.7 nm.

(a)

1mm. = 6.7 nm.
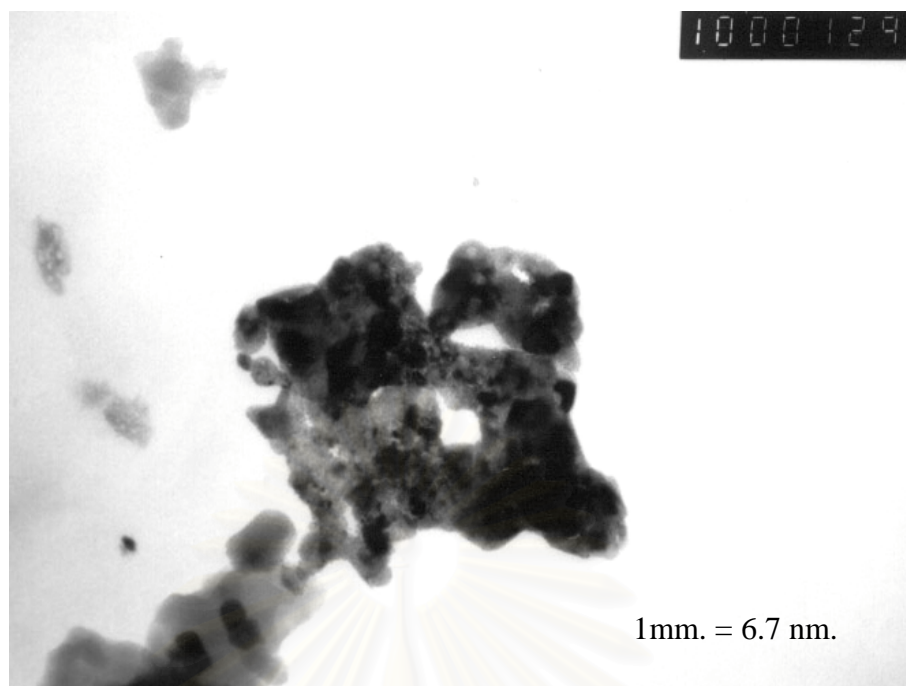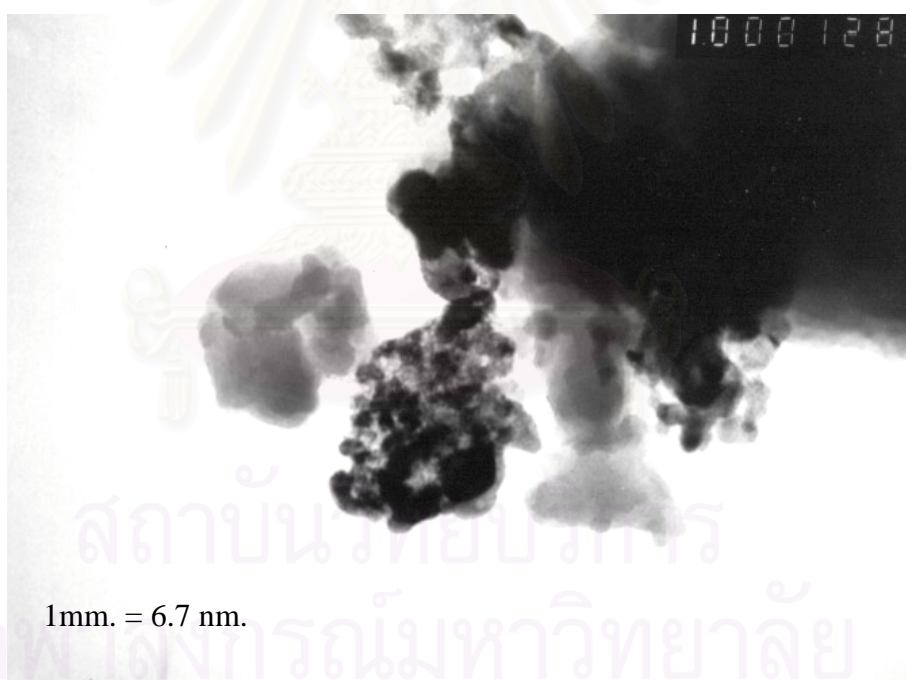
(b)

Figure 5.11 TEM Micrographs of (a) fresh and (b) spent SiO_2-small pore
supported Pd catalyst

1mm. = 6.7 nm.

(a)
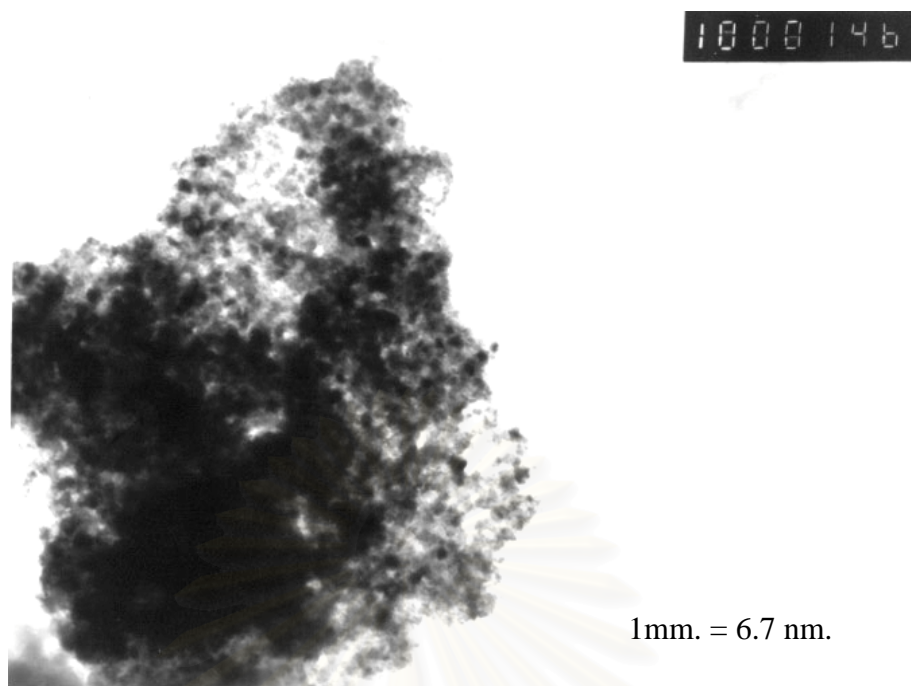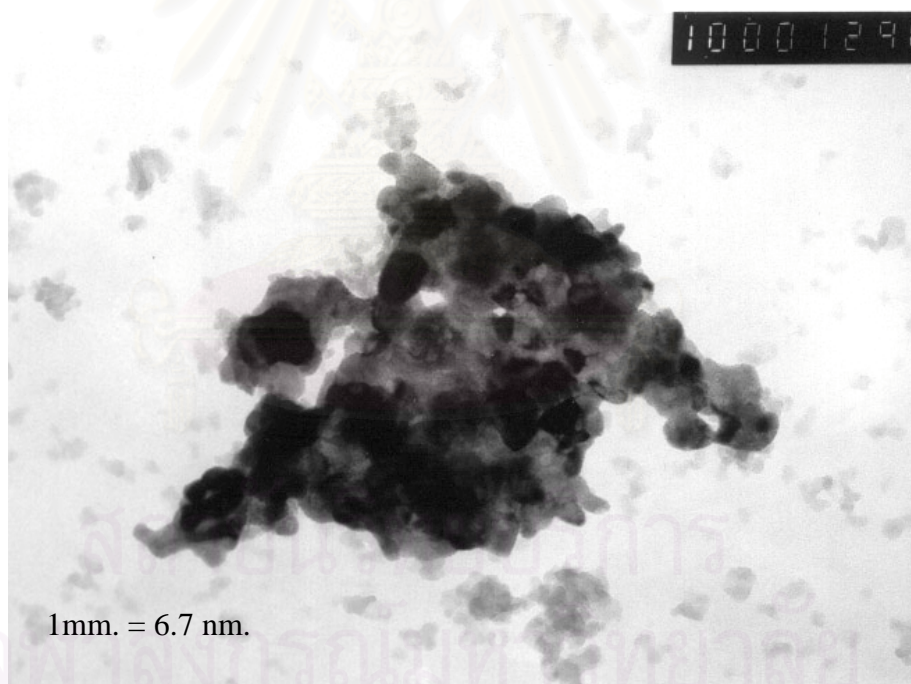
1mm. = 6.7 nm.

(b)

Figure 5.12 TEM Micrographs of (a) fresh and (b) spent SiO_2-large pore
supported Pd catalyst

1mm. = 6.7 nm.

(a)

1mm. = 6.7 nm.

(b)
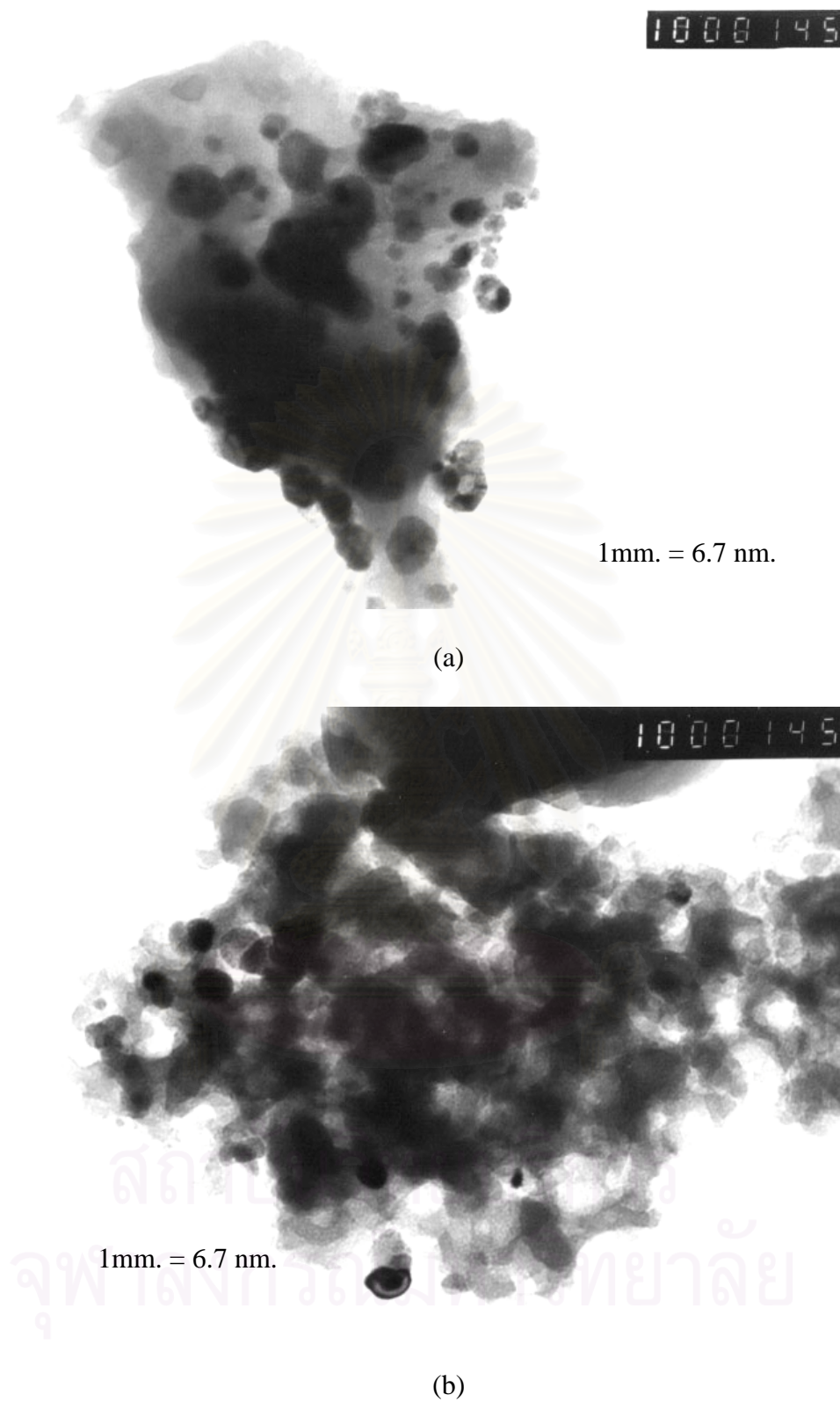
Figure 5.13 TEM Micrographs of (a) fresh and (b) spent MCM-41-small pore
supported Pd catalyst

1mm. = 6.7 nm.

(a)

1mm. = 6.7 nm.

(b)

Figure 5.14 TEM Micrographs of (a) fresh and (b) spent MCM-41-large pore
supported Pd catalyst

5.2.4 Scanning Electron Microscopy (SEM)

Scanning electron microscopy (SEM) is a powerful tool for observing directly surface texture, morphology and crystallite size of catalyst materials. In the scanning mode (SEM) the electron beam focused on the sample is scanned by a set of deflection coils. Backscattered electrons or secondary electrons emitted from the sample are detected.

Typical SEM micrographs of catalyst granules are shown in Figure5.15-5.18. The term "granule" here refers to a catalyst particle composed of palladium and silica. The SEM micrographs show different catalyst granule sizes. For both small pore and large pore MCM-41 supported catalysts, the granule sizes were approximately 20-30 μm, whereas granule sizes of the small and large pore SiO_2 were around 130-150 and 400-500 μm, respectively. It would appear that the size and shape of the catalyst granules were not affected during the 4-hour batch liquid-phase hydrogenation reaction suggesting that the different silica supports used in this study have reasonably high attrition resistances.

Figure 5.19-5.22 showed SEM micrograph of catalyst granules in the backscattering mode. In this mode, the white spots represent the dispersion of Pd on the catalyst granules. A signigicant amount of Pd lost after reaction was evidenced by SEM for Pd/SiO_2-small pore and Pd/SiO_2-large pore catalysts. However, for MCM-41 supported ones, it was not clearly seen such phenomena. The loss of Pd from the catalysts suggested that leaching of Pd occurred during liquid-phase hydrogenation of 1-hexene. The details about metal leaching were discussed in the next chapter (chapter VI).
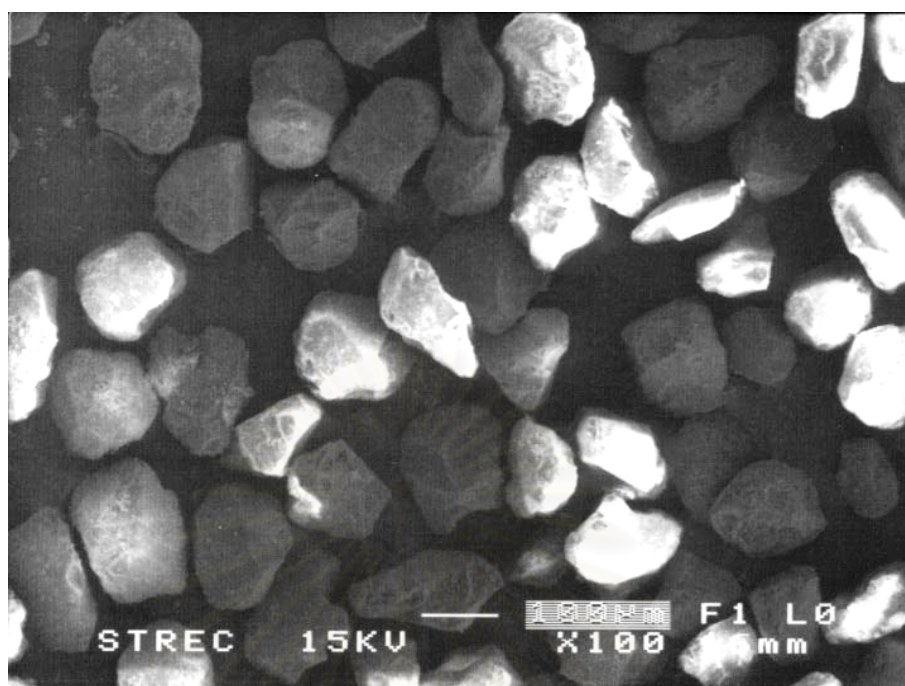
(a)
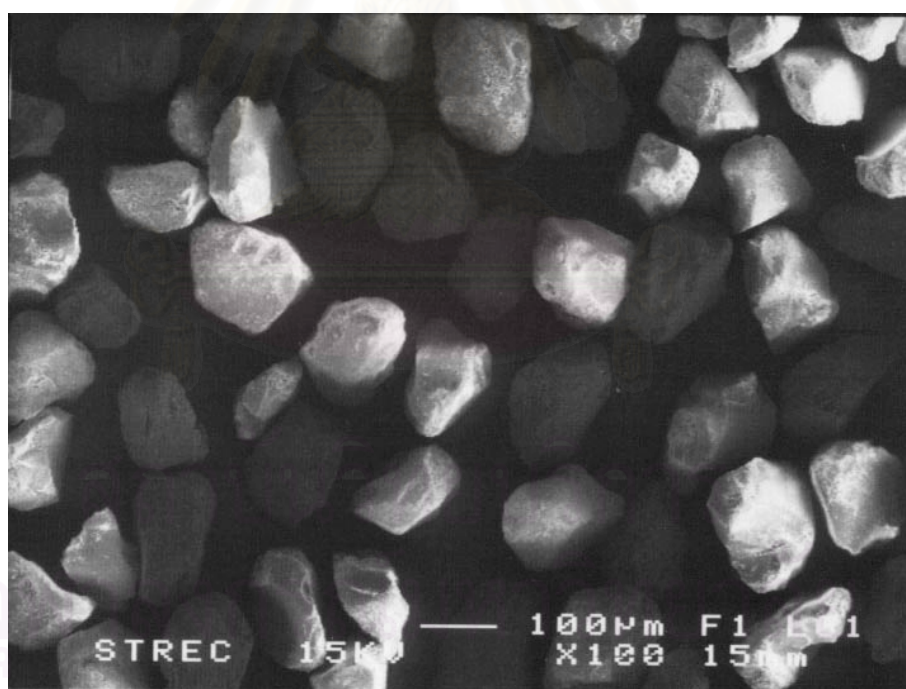
(b)

Figure 5.15 SEM Micrographs (scanning mode) of (a) fresh and (b) spent SiO_2-small
pore supported Pd catalyst
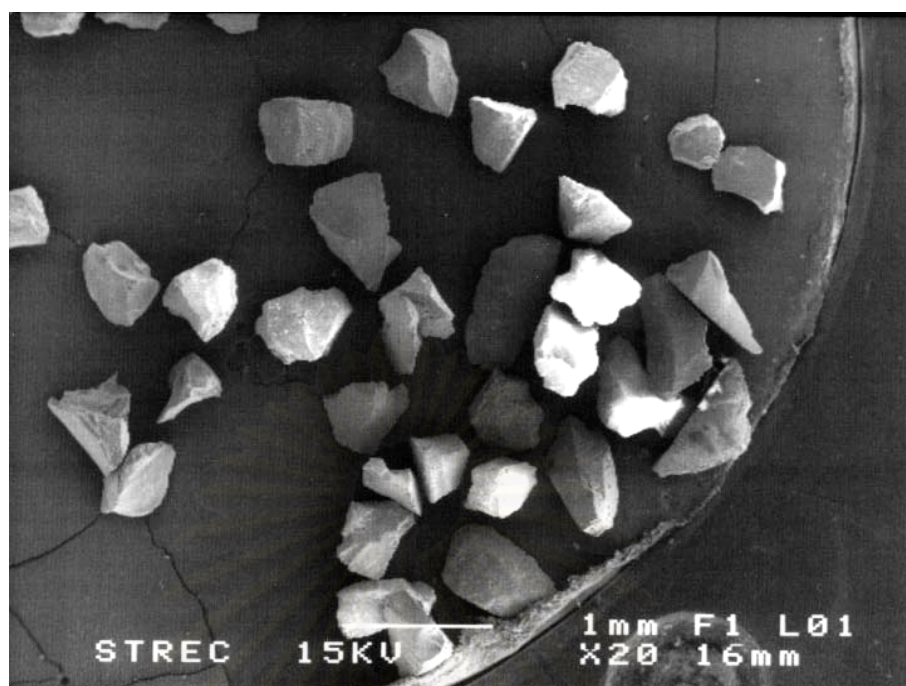
(a)
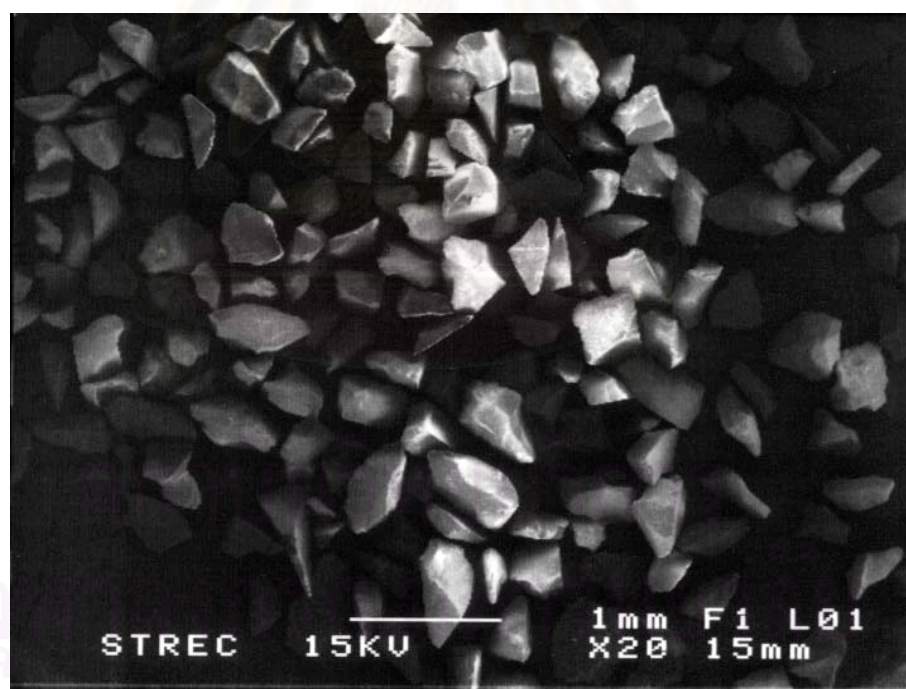
(b)

Figure 5.16 SEM Micrographs (scanning mode) of (a) fresh and (b) spent SiO_2-large
pore supported Pd catalyst
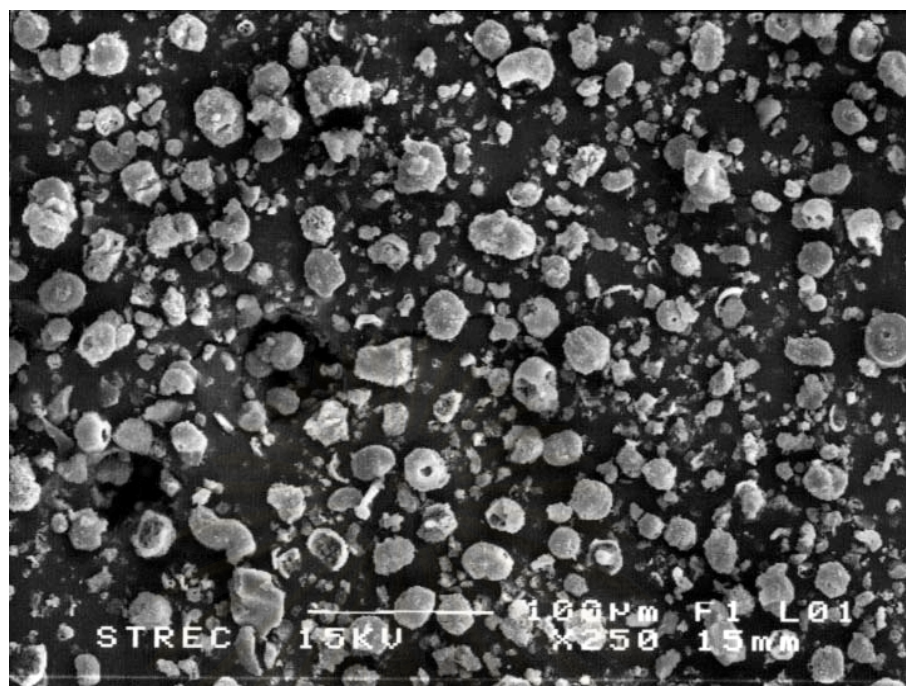
(a)
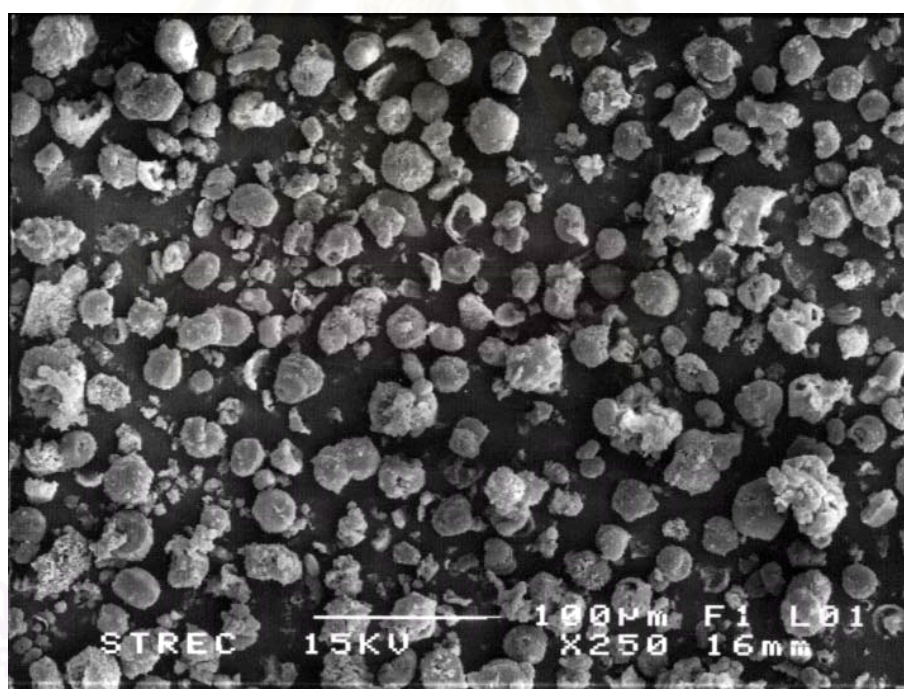
(b)

Figure 5.17 SEM Micrographs (scanning mode) of (a) fresh and (b) spent MCM-41-
small pore supported Pd catalyst
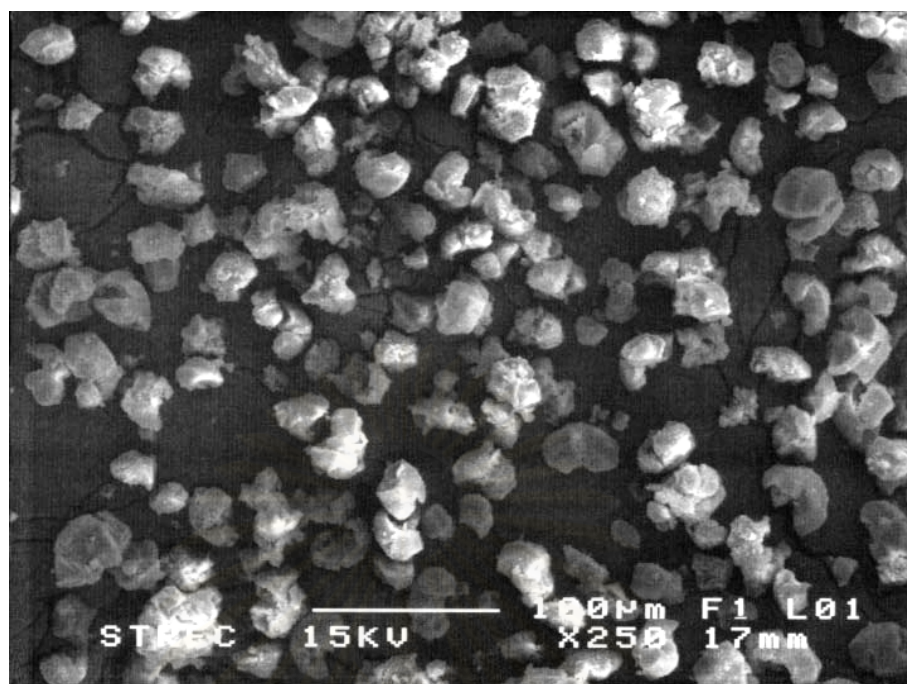
(a)
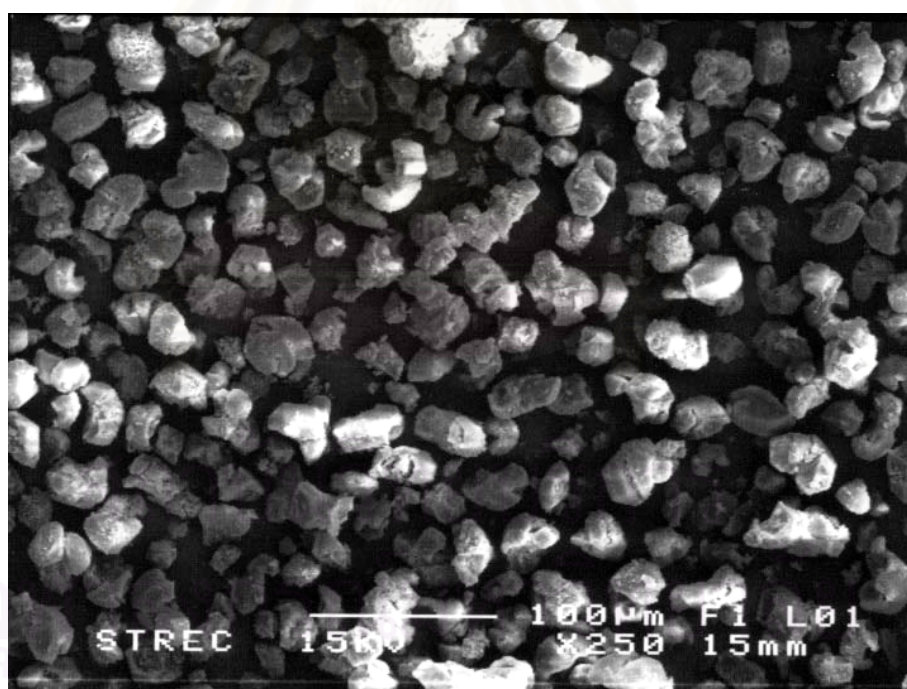
(b)

Figure 5.18 SEM Micrographs (scanning mode) of (a) fresh and (b) spent MCM-41-
large pore supported Pd catalyst
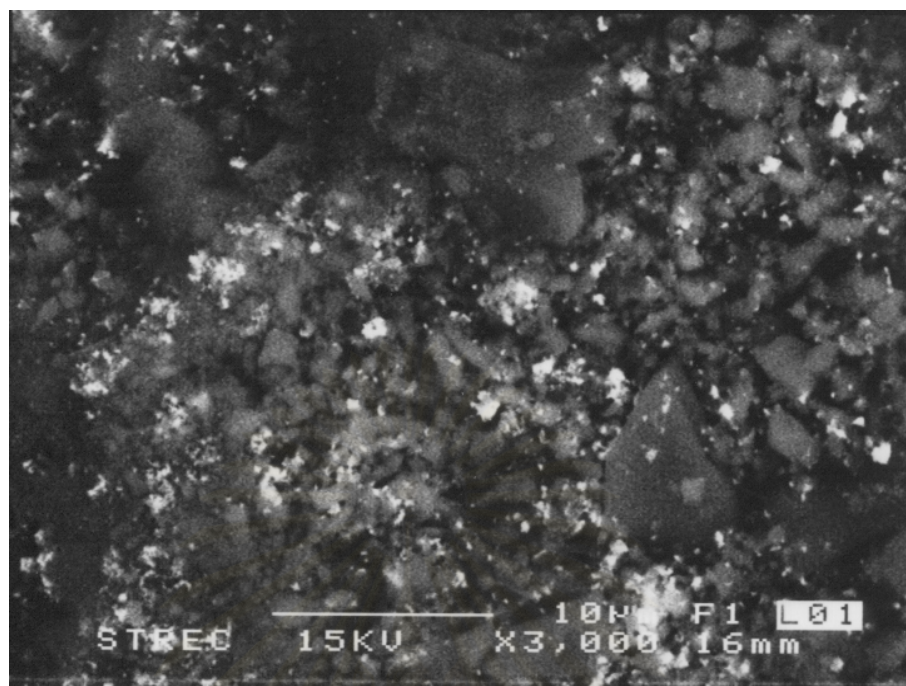
(a)
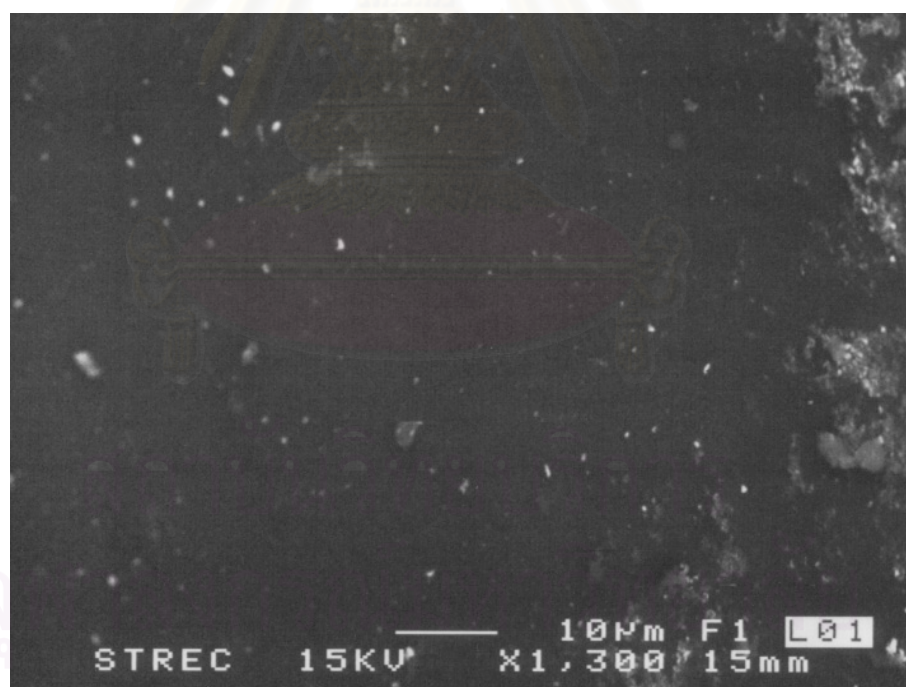
(b)

Figure 5.19 SEM Micrographs (BSE mode) of (a) fresh and (b) spent SiO_2-small pore
supported Pd catalyst
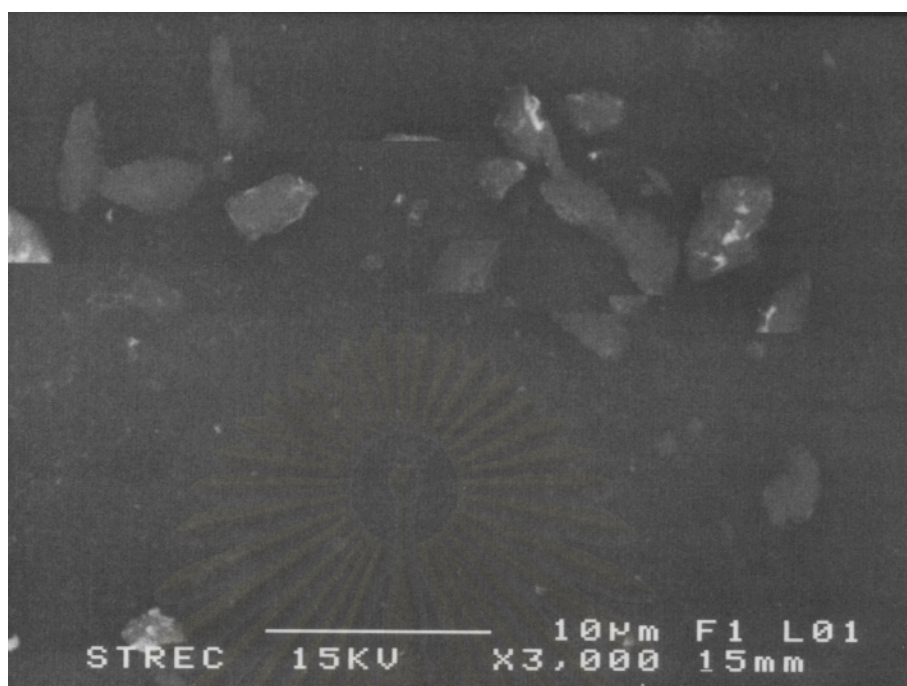
(a)
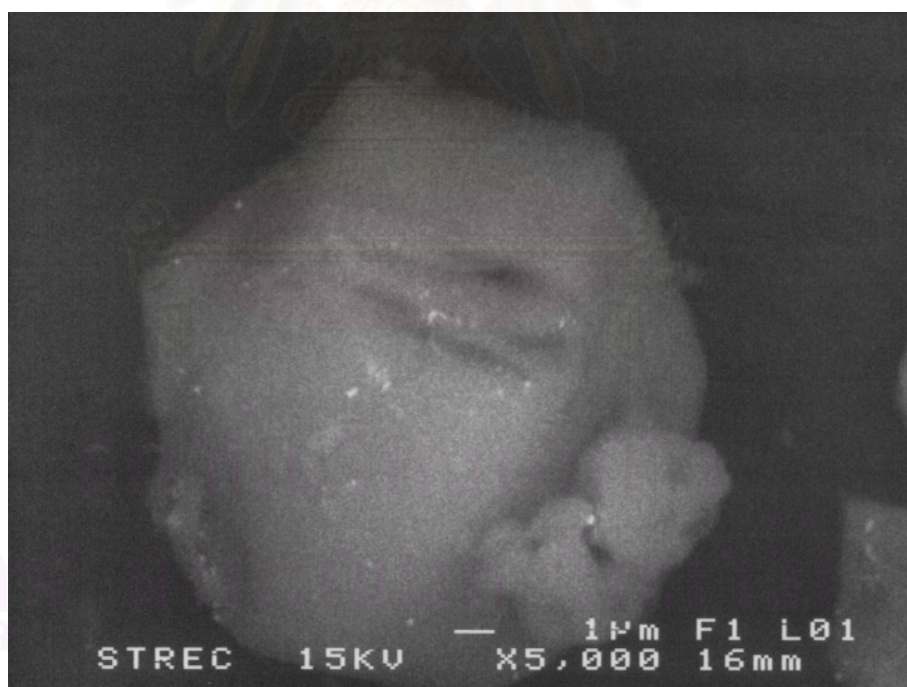
(b)

Figure 5.20 SEM Micrographs (BSE mode) of (a) fresh and (b) spent SiO$_2$-large pore
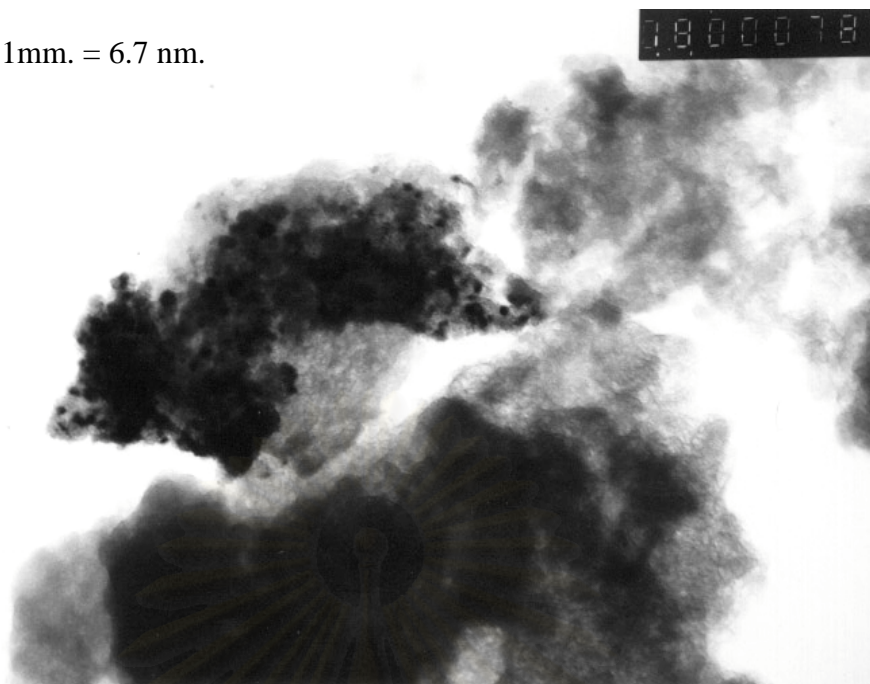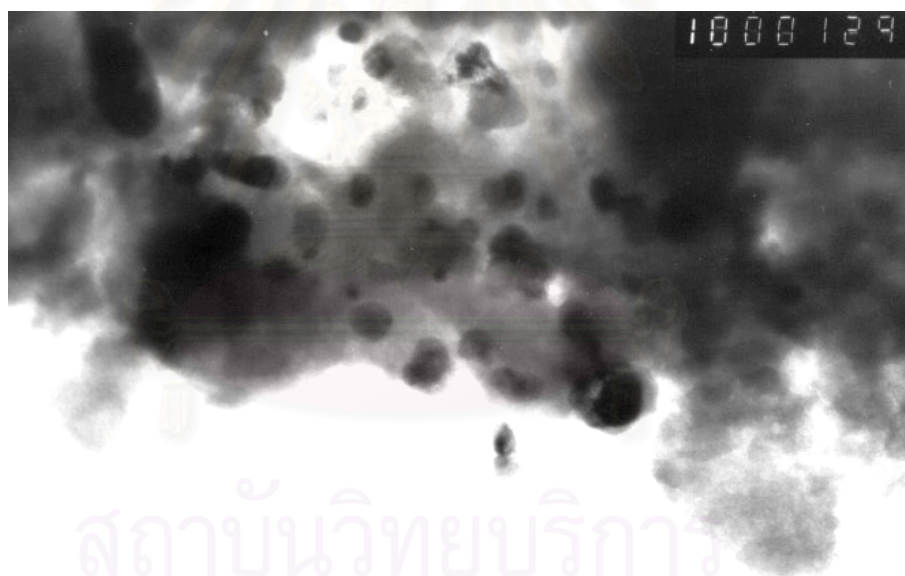supported Pd catalyst

(a)
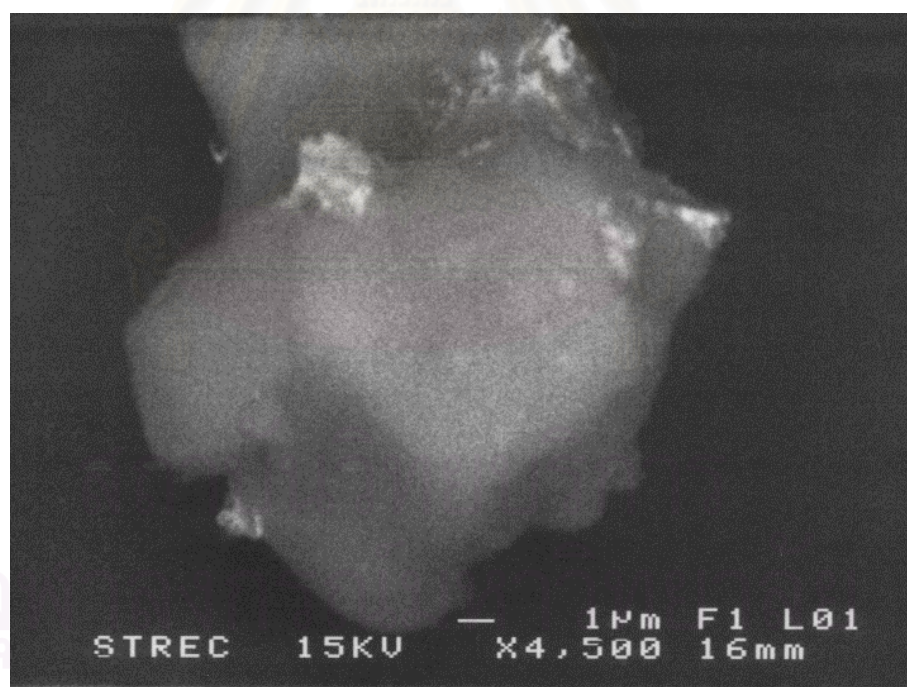
(b)

Figure 5.21 SEM Micrographs (BSE mode) of (a) fresh and (b) spent MCM-41-small
pore supported Pd catalyst
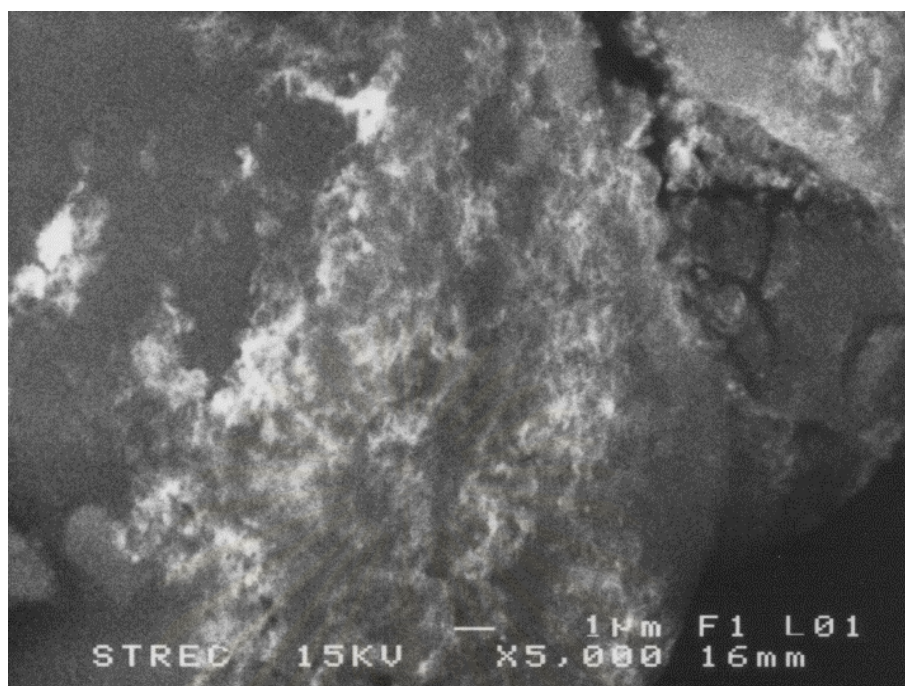
(a)
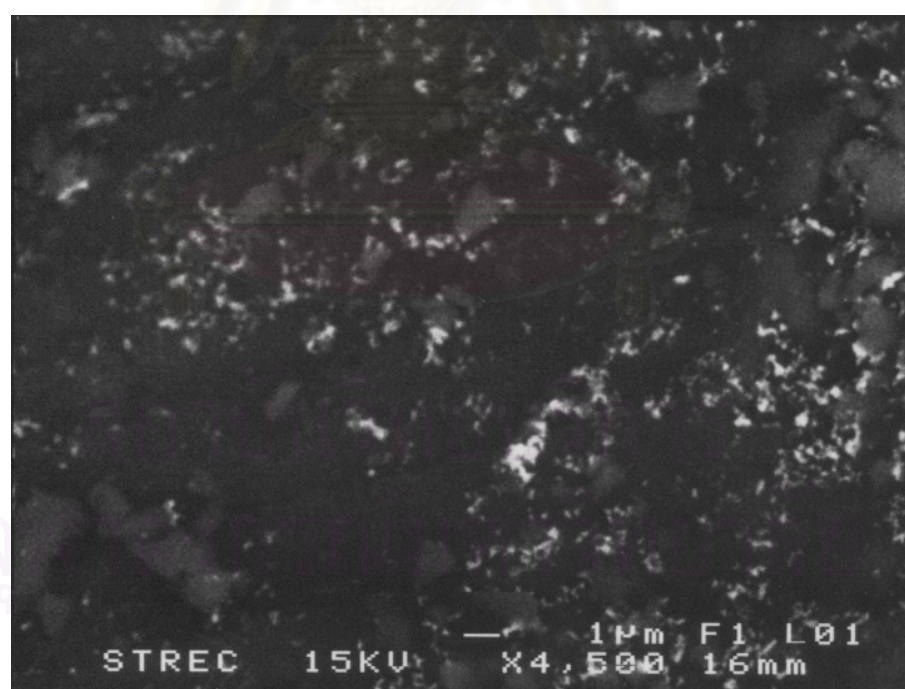
(b)

Figure 5.22 SEM Micrographs (BSE mode) of (a) fresh and (b) spent MCM-41-large
pore supported Pd catalyst

5.2.5 Atomic Absorption Spectroscopy

AAS (atomic absorption spectroscopy) is a very common technique for quantitative measurement of atomic composition based on photon absorption of a vaporized aqueous solution prepared from the starting material.

The actual amounts of palladium loading before and after reaction determined by atomic adsorption spectroscopy are given in Table 5.5. Before reaction, palladium loading on the catalyst samples was approximately 0.29-0.48 wt%. After one 4-hour batch hydrogenation reactions of 1-hexene, palladium loading had decreased to 0.15-0.32 wt%. This indicates that leaching of palladium occurred during reaction. The order of the percentages of the amount of palladium leaching was Pd/SiO_2-small pore > Pd/SiO_2-large pore > Pd/MCM-41-small pore >> Pd/MCM-41-large pore. Pd/MCM-41-large pore showed almost no leaching of palladium into the reaction media within experimental error. The problem of metal leaching were discussed in section 6.3.

Table 5.5 Results from Atomic Adsorption.

Catalyst	%Pd (wt %)		% Metal loss
	Fresh catalyst	Spent catalyst	
Pd/SiO_2-small pore	0.35	0.15	57
Pd/SiO_2-large pore	0.29	0.18	38
Pd/MCM-41-small pore	0.48	0.32	33
Pd/ MCM-41-small pore	0.33	0.31	6

5.2.6 CO-Pulse Chemisorption

Chemisorption is the relatively strong, selective adsorption of chemically reactive gases on available metal sites or metal oxide surfaces at relatively higher temperatures (i.e. 25-400°C); the adsorbate-adsorbent interaction involves formation of chemical bonds and heats of chemisorption in the order of 50-300 kJ mol^{-1}.

The amounts of CO chemisorption on the catalysts, the percentages of Pd dispersion, and the Pd metal particle sizes are given in Table 5.6-5.8. The pulse CO chemisorption technique was based on the assumption that one carbon monoxide molecule adsorbs on one palladium site (Mahata and Vishwanathan, 2000, Ali and Goodwin, 1998, Sales *et al.*, 1999, Sarkany et al., 1993, Vannice *et al.*, 1981, and Nag, 1994). Before reaction, it was found that Pd/MCM-41-large pore exhibited the highest amount of CO chemisorption, whereas the other catalysts showed similar amounts of CO chemisorption. This was probably due to the dispersion of palladium being better on the large pore MCM-41. The percentages of Pd dispersion before and after reaction were calculated to be in the range of 4.5-11.2% and 2.5-7.2%, respectively, in the descending order of Pd/MCM-41-large pore > Pd/SiO$_2$-large pore > Pd/SiO$_2$-small pore > Pd/MCM-41-small pore.

Average particle size for reduced Pd^0 was calculated to be in the range of 10-24.9 nm before reaction and 15.5-44.8 nm after reaction. These average Pd^{0}metal particle sizes calculated based on CO chemisorption are not identical of course to the calculated PdO particle sizes obtained by XRD and TEM. The MCM-41-large pore supported catalysts appeared to have smaller average Pd particle sizes than those on other catalysts, resulting in their relatively high Pd dispersion. Overestimation of Pd metal particle sizes by CO chemisorption for the catalysts with small pores (Pd/SiO$_2$-small pore and Pd/MCM-41-small pore) is possibly due to (a) partial blockage of CO adsorption as a result of pore blockage by agglomeration of metal particles (Verdonck *et al.*, 1980) and (b) localized destruction of the well-defined pore structure forming cracks and holes where larger metal particles could form and chemisorption would also be restricted (Gustafson and Lunsford, 1982), or (c) chemisorption suppression. After reaction, the amount of CO chemisorption and

%Pd dispersion decreased significantly for all catalyst samples by approximately 35-50% of that of the fresh catalysts.

Table 5.6 Results from Pulse CO Chemisorption

Catalyst	CO chemisorption[a] ($x10^{18}$ molecule CO/g cat)		%decrease
	Fresh catalyst	Spent Catalyst	
Pd/SiO$_2$-small pore	1.29	0.79	39
Pd/SiO$_2$-large pore	1.20	0.61	49
Pd/MCM-41-small pore	1.22	0.67	45
Pd/MCM-41-large pore	2.10	1.34	36

[a] Error of measurement was ± 5%.

Table 5.7 Results from Pulse CO Chemisorption.

Catalyst	Pd dispersion[b] (%)		%decrease
	Fresh catalyst	Spent Catalyst	
Pd/SiO$_2$-small pore	6.5	4.0	38
Pd/SiO$_2$-large pore	7.3	3.7	49
Pd/MCM-41-small pore	4.5	2.5	44
Pd/MCM-41-large pore	11.2	7.2	36

[b] Based on the total palladium loaded. An assumption of $CO/Pd^0_s=1$ was used where Pd^0_s is a reduced surface atom of Pd

Table 5.8 Results from Pulse CO Chemisorption.

Catalyst	Pd^0 particle size[c] (%)		%Increase
	Fresh catalyst	Spent Catalyst	
Pd/SiO$_2$-small pore	17.2	28.0	63
Pd/SiO$_2$-large pore	15.3	30.3	98
Pd/MCM-41-small pore	24.9	44.8	80
Pd/MCM-41-large pore	10.0	15.5	55

[c] Based on $d = (1.12/D)$ nm (Mahata and Vishwanathan, 2000), where D = fractional metal dispersion.

5.2.7 Temperature programmed reduction (TPR)

TPR (temperature-programmed reduction) is the measurement of the rate of reduction as a function of temperature (at a linear temperature ramp). This technique allows the study of the oxidation states of surface and bulk of solid.

The reducibility of the catalysts is important since the active phase for hydrogenation is the metallic Pd^0 phase. The H_2 consumption in TPR profile correspond to the complete reduction of $Pd^{2+} \longrightarrow Pd^0$, assuming that palladium is presented as Pd^{2+} ($H_2/Pd = 1$), which is the expected state for the preparation of the catalysts. TPR profiles of supported Pd catalysts are presented in Figure 5.19. In most cases, PdO particles reduced readily to PdH_2 at ambient temperature once H_2 was introduced to the system. A positive peak of H_2 consumption in TPR profile is attributed both reactions (1) for the reduction of PdO to PdH (palladium hydride). A significant negative peak at 75-80°C was observed for all the catalysts. This peak corresponds to the decomposition of palladium hydride (reaction 2). It is well known that Pd particles are able to absorb H_2 with their structure to form a β-PdH_x phase. For Pd/MCM-41-small pore, a small positive reduction peak at ca.48°C was observed. It is attributed to a portion of the PdO that could not be reduced at ambient temperature.

It has been reported by Koh et al. that about 70% of the PdO contained in MCM-41-supported catalysts can be reduced at sub-ambient temperature and the other 30% is reducible by 50°C. It has also previously been reported that there is a stronger metal-support interaction between metal and an MCM-41 support when the pore size of that support is very small (i.e., 3 nm) (Panpranot *et al.*, 2002). In the case of amorphous silica (SiO_2), there would appear to be no different in metal-support interaction (Pd-SiO_2) between the small and large pore supported Pd catalysts.

$$1.5\ H_2 \quad + PdO \longrightarrow Pd^sH\ +\ H_2O \tag{1}$$

$$Pd^bH_x \qquad \longrightarrow Pd^b\ +\ 0.5xH_2 \tag{2}$$
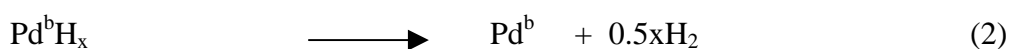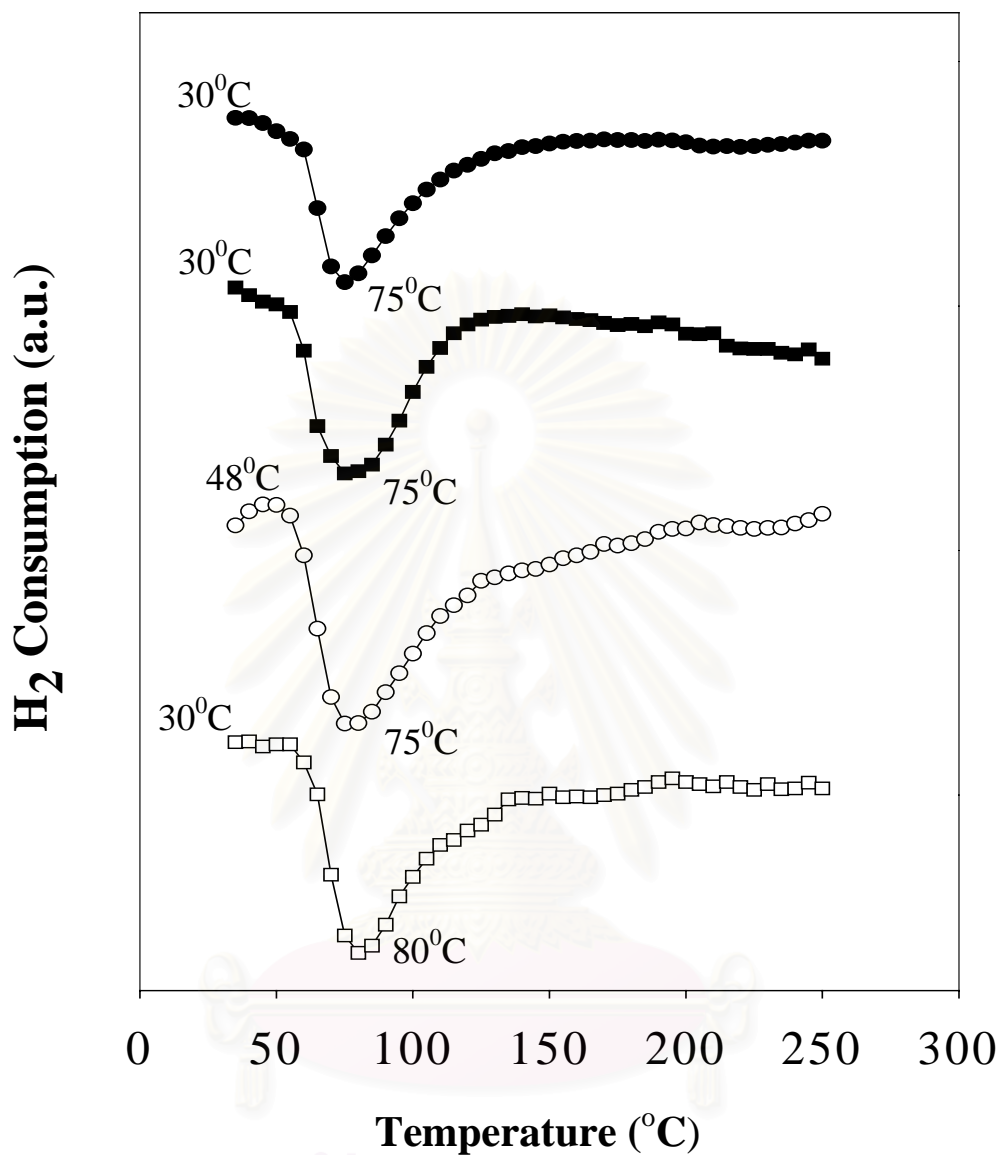
Figure 5.23 TPR profile for supported Pd catalysts :(●) Pd/SiO$_2$-small pore, (■) Pd/SiO$_2$-large pore, ($_\circ$) Pd/MCM-41-small pore, and ($_\square$) Pd/MCM-41-large pore

5.3 Catalyst Durability and Catalyst Deactivation

The durability of the catalysts under repeated catalytic cycles were tested on Pd/MCM-41-small pore catalyst since there appeared to be a difference in reducibility of the catalysts and it exhibited significant amount of metal loss during reaction. The experiment was carried out following reaction conditions in Table 5.1. 7.5 ml of 1-hexene was injected at 2 h. intervals. After different number of reaction cycles (1, 2, 3, or 4), the used catalyst was filtered out, dried at room temperature, and calcined in air at $500^{\circ}C$ for 2 h in order to remove any carbon deposited. Then CO chemisorption was performed on the used catalysts following the same procedure as for fresh the catalysts. Figure 5.24 shows the initial reaction rates and the number of palladium active sites as measured by CO chemisorption versus the number of reaction cycles undergone.

It was found that the reaction rate slowly decreased after the first cycle. This might be due to leaching of palladium metal from the supports and/or a decrease in the amounts of palladium active sites due to sintering of the palladium and/or coke deposition on the catalysts (Alber et al., 2001 and Besson and Gallezot, 2003). The amounts of carbon deposited on the catalysts after reaction are shown in Table 5.9. The quantities of carbon in the support and spent catalyst are shown in Table 5.10. It was found that MCM-41 (both small and large pore) had higher amount of % Carbon in the samples than in the SiO_2, this is due to MCM-41 was prepared with an organic templates as starting materials. The % carbon in the spent catalyst was still observed in small amount after re-calcination and was found to increased with the number of reaction cycles.

Table 5.9 The results from CO-pulse chemisorption, AA, and Carbon Analyzer of Pd/MCM-41-small pore catalyst

Number of reaction cycle	CO chemisorption $(x10^{18}$molecule CO/g cat)	Initial rate (mol/min.g) $x10^{-3}$	%Pd by AA (wt %)	%carbon in spent catalyst (wt %)
1	1.20	3.89	0.48	0.54
2	0.67	2.35	0.32	0.51
3	-	1.95	-	-
4	0.67	0.98	0.37	0.86

[a] Error of measurement was ± 5%

Table 5.10 The results from Carbon Analyzer of supports and spent catalysts.

	% carbon in sample (wt %)
Support	
SiO$_2$-small pore	0.10
SiO$_2$-large pore	0.09
MCM-41-small pore	0.54
MCM-41-large pore	0.40
Spent catalysts	
Pd/SiO$_2$-small pore	0.13
Pd/SiO$_2$-large pore	0.18
Pd/MCM-41-small pore	0.51
Pd/MCM-41-large pore	0.40

(a)

(b)
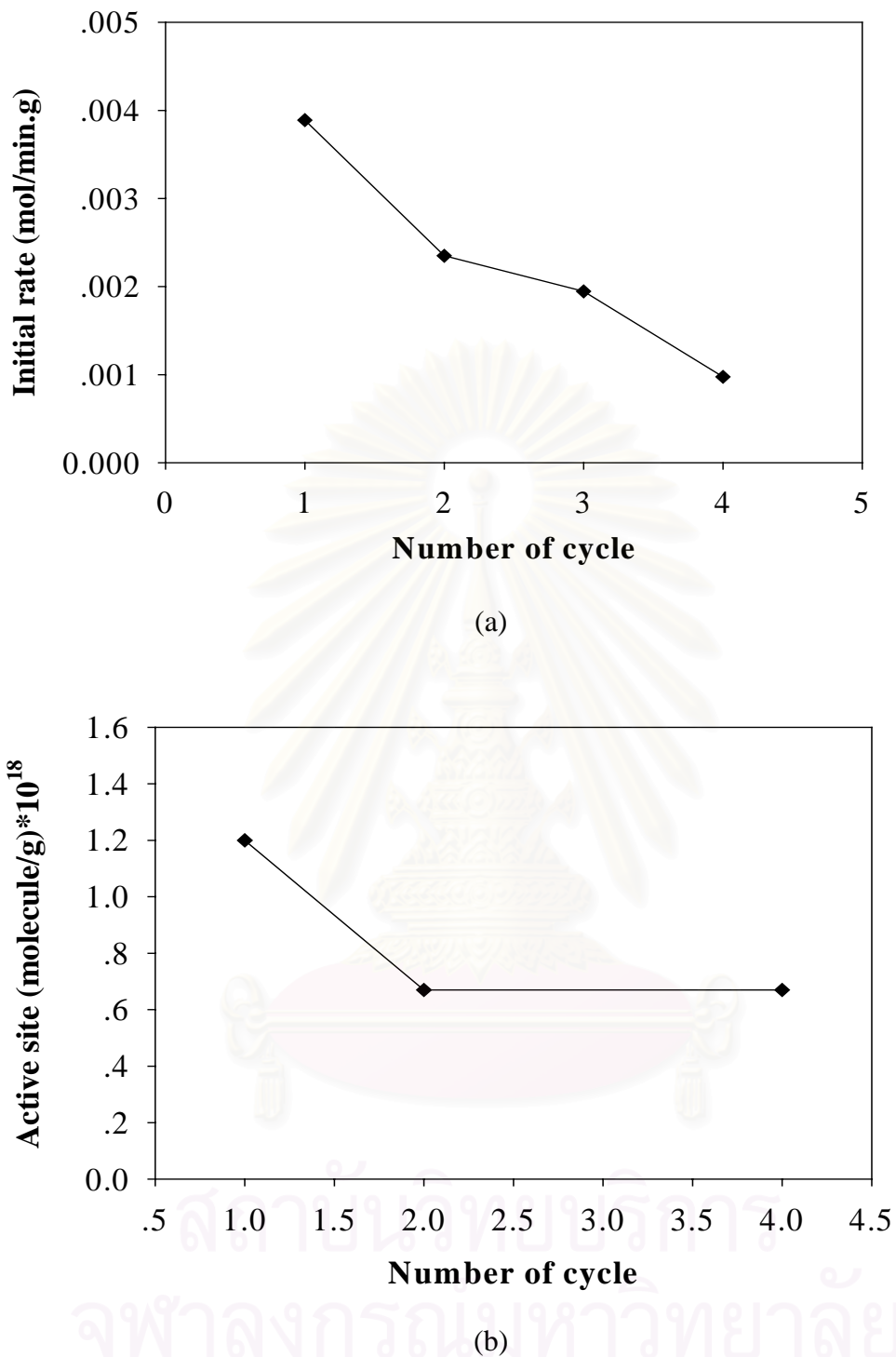
Figure 5.24 Stability of Pd/MCM-41-small catalyst as a Function of Number of
Reaction Cycles (reaction conditions: 30°C, 1 atm, and 1-hexene/ethanol
= 15/400 ml).

CHAPTER VI

DISCUSSION

In this chapter, the effects of silica type and silica pore structure on: (1) Pd dispersion and location on the supports, (2) liquid-phase hydrogenation activity, and (3) catalyst deactivation of were discussed in more details in section 6.1, 6.2, and 6.3, respectively.

6.1 Effect of Type of Silica and Silica Pore Structure on Pd Dispersion and Location on the Supports

For Pd/SiO$_2$-large pore, the XRD and TEM results for PdO and CO chemisorption on the reduce Pd^0 metal gave particle sizes small enough to exist within the large pores of the support. The pores were large enough that the metal particles did not block the pore structure resulting in little decrease in BET surface area and pore volume. This large pore SiO$_2$-supported catalyst had apparently little trouble in adsorbing the Pd precursor solution in its pore during the incipient wetness impregnation and in accommodating the Pd particles formed.

For Pd/MCM-41-large pore, the decrease in BET pore diameter upon loading with palladium suggests that the pores are somewhat blocked up. Based on XRD, and TEM of PdO and CO chemisorption on the reduced Pd^0 metal, the metal particle sizes were small enough such that, they could be significantly in the mesopores of this material.

In the case of Pd/SiO$_2$-small pore and Pd/MCM-41-small pore, PdO particles were found by XRD and TEM to be much larger than the average pore diameters. CO chemisorption results confirm the large metal particles existing on the reduced catalysts. Also, addition of Pd did not significantly affect average pore diameters for these two small-pore supports for these two small-pore supports. Therefore, it is likely that most of the Pd particles were on the outside support surfaces of these

catalysts and not in the micropores. However, CO chemisorption determined larger average particle sizes than XRD and TEM because of the less than 100% reduction for Pd/MCM-41-small pore as determined by TPR and possibly to some blockage of the metal surfaces of metal particle located inside the micropores.

6.2 Effect of Type of Silica and Silica Pore Structure on Liquid-Phase Hydrogenation Activity

In previous studies reported in the literature, the effect of different kinds of support materials such as Al_2O_3, SiO_2, TiO_2, and ZrO_2 on hydrogenation have been investigated. However, the effect of catalyst structure for similar support compositions has not been studied to much of a degree. In this study, the effect of pore size and pore structure of the same material (silica) in liquid phase hydrogenation was reported.

The activity of the catalysts were found to be in the order of Pd/MCM-41-large pore > Pd/MCM-41-small pore $\approx$ Pd/SiO$_2$-large pore > Pd/SiO$_2$-small pore. The reaction results are probably influenced simultaneously by 2 phenomena: (1) mass transport effects during reaction (for a given silica type, larger pore supported catalysts were more active than smaller pore supported ones) and (2) pore structure effects (Pd/MCM-41 catalysts were more active than Pd/SiO$_2$ for a similar pore size).

The effect of pore size on the liquid-phase diffusion resistance has also been reported in the literature for other catalyst systems (Huang and Sachtler, 1997 and Takahashi *et al.*, 2002). For example, Huang and Sachtler studied ruthenium supported on mesoporous sulfated zirconia for the liquid phase hydrogenation of stearonitrile and compared with Ru supported on either microporous sulfated zirconia or zeolite HY. They found that the mesoporous catalyst was significantly more active than the microporous catalyst. The zeolite supported catalyst was inactive under the same reaction conditions. In this study, we also found that this effect can be minimized by using large pore MCM-41-supported catalysts.

For a similar pore size, Pd/MCM-41-small pore had similar number of active sites as Pd/SiO$_2$-small pore. However, Pd/MCM-41-small pore exhibited higher activity than Pd/SiO$_2$-small pore suggesting that there is an effect of the different support structures on the catalytic properties of the active sites.

6.3 Effect of Type of Silica and Silica Pore Structure on Catalyst Deactivation.

The main causes of deactivation of metal catalyst in liquid phase reaction are particle sintering, metal and support leaching, deposition of inactive metal layer or carbon, and poisoning by strongly adsorbed species (Besson and Gallezot, 2003). The later cause (poisoning), however, was not included in this study because only high purity grade chemicals and gases were used in the reaction study.

6.3.1 Deposition of Carbon

The definition of carbon and coke are somewhat arbitrary and by convention related to their origin. Carbon is a product of CO disproportionate, whereas coke is produced by decomposition or condensation of hydrocarbons on catalyst surfaces and typically consists of polymerized heavy hydrocarbons. Nevertheless, coke forms may vary from high-molecular weight hydrocarbons to primarily carbons such as graphite, depending upon the conditions under which the coke was form and aged (Farrauto and Bartholomew, 1997). In this study the carbon deposits had to be avoid in order to obtain a good contrast of SEM and TEM images of the spent catalysts. It is well known that carbon deposits can be easily removed by combustion at high temperature. Therefore after reaction, the catalysts were re-calcined in air at 500°C for 2 hour before characterization. The Carbon analyzer results confirm removal of carbon deposited for all catalysts. However, since MCM-41 was prepared from an organic templates, % Carbon remained in the sample was higher than that of SiO$_2$. There is no effect of the pore size on % carbon remaining in the samples.

6.3.2 Crystallite Growth, Sintering, and Agglomeration

Morphological changes of palladium entities due to particle growth by different processes including sintering and agglomeration are a major cause for a decrease of activity down to uneconomic levels or even complete deactivation of palladium catalysts (Albers, *et al.*, 2001). Sintering of supported metal particles may occur close to room temperature because of atomic migration process. Sintering of metal particles resulting in loss of active surface area and is usually an irreversible catalyst deactivation. Sintering can be easily followed by XRD and TEM particle size measurements and by H_2 or CO chemisorption (Bergeret and Gallezot, 1997).

In this work, the catalysts before and after reaction were characterized using various analysis techniques in order to investigate sintering of the catalysts. The characterization results indicating that sintering of palladium may have occurred after reaction include:

(1) a decrease in BET surface areas of the catalysts after reaction which was probably due to pore blocking of metal sintering

(2) an increase in the PdO particle sizes of spent catalysts as determined by XRD and TEM

(3) a decrease of XRD characteristic peaks of MCM-41-small pore for Pd/MCM-41-small pore after reaction

(4) a decrease in the amount of Pd active sites as measure by CO chemisorption

Overall, Use of large pore SiO_2 support resulted in the greatest amount of Pd sintering. It should be noted that the lower the surface area, the higher probability of a metal particle to be closed to other ones and consequently higher sintering probability.

The sintering of palladium in liquid-phase hydrogenation has also been reported in the literature for other catalyst systems (Sermon, 1972, Schuurman *et al.*, 1992, Bakos *et al.*, 1997, Choudary *et al.*, 1999, and Dominguez-Quintero *et al.*, 2003). For example, Choudary *et al.* studied the hydrogenation of alkene and semi-

hydrogenation of alkyne of Pd catalysts supported on mesoporous materials, Pd/Si-K10 and Pd/MCM-41 and microporous Pd/Y-zeolite. A lower activity was found due to sintering of palladium. Dominguez-Quintero investigated palladium nanoparticle in the hydrogenation catalysis of different substrates (1-hexene, cyclohexene, benzene, 2-hexanone and benzonitrile). The catalysts from hydrogenation of 1-hexene were reused in four different batch reactions and no significant decrease in activity. However, after the fourth batch reaction, the TEM analysis of the material showed a 30% increase in size.

6.3.3 Palladium Leaching

Leaching of active metal is one of the main causes of catalyst deactivation in liquid phase hydrogenation reaction. As far as metal catalysis is concerned, leaching of metal atoms depends upon the reaction medium (pH, oxidation potential, chelating properties of molecules) and upon bulk and surface metal properties. In this study, the order of percentage of palladium leached was Pd/SiO_2-small pore > Pd/SiO_2-large pore > Pd/MCM-41-small pore > Pd/MCM-41-large pore where Pd/MCM-41-large pore showed almost no leaching of palladium into the reaction media within experimental error. It would appear that Pd/MCM-41-large pore is the only catalyst with Pd supported in relatively small pores. Thus, it is suggested that metal loss is affected primarily by whether the Pd particles are located on the external surface or in large pores (the greater loss) or in mesopores (less loss). This loss is probably related to the metal particle sizes.

The mechanism of metal leaching involves usually metal compounds that are formed that are soluble in the reaction mixture. Since it is unlikely that 1-hexene forms compound with Pd at room temperature, unless it is some hydride-organic complex. It is likely that Pd hydride formation is the cause of metal loss. It is well known that Pd particles are able to absorb H_2 within their crystal structure to form a Pd-β-hydride phase. A number of publications (Palzewska, 1975, Noronha, *et al.*, 1999, Neri *et al.*, 2001, and Shen *et al.*, 2001) have reported that formation of Pd hydride depends on the particle size of palladium; larger Pd particles were more easily to form Pd hydride whereas smaller Pd particle may be unable to form Pd-β-hydride

phase. This β-hydride phase which was formed at room temperature was unstable at T > 80°C and could be detected in the TPR pattern from desorption of H_2 at this temperature.

However, under certain conditions, Pd-β-hydride phase can appear as a soft material with higher mechanical abrasion (Alber et al., 2001). This may be a reason that larger Pd particles on the external surfaces of the catalyst granules form the Pd-β hydride phase that is lost (leached) from the catalysts. However, it should be noted that Pd/SiO$_2$-large pore also lost a significant amount of Pd during reaction, eventhough most of its Pd particles can be assumed to have been inside its large pores, and therefore, not susceptible to physical abrasion. Thus, it is more likely that a soluble Pd compound was formed on the larger Pd particles.

In addition, the results from the repeated catalytic cycles experiments showed that in most cases, a significant amount of Pd was leached during reaction as confirmed by AAS but the active sites as measured by CO chemisorption reached a limiting value. It did not further decrease with the number of catalytic cycles. This suggests that the Pd leaching during the first run was mostly non-catalytically active Pd.

CHAPTER VII

CONCLUSIONS AND RECOMMENDATIONS

7.1 Conclusions

The effects of silica type and silica pore structure in liquid phase hydrogenation over supported Pd catalysts were studied by several characterization techniques. The following conclusions can be drawn from the investigations:

1. Type of silica, pore size and pore structure of the silica supports used for Pd catalysts were found to affect both characteristics and catalytic properties of the catalysts for liquid-phase hydrogenation of 1-hexene. The larger pore MCM-41-supported Pd catalyst exhibited superior catalytic activity and the lowest amount of metal loss during reaction compared to small pore SiO_2, small pore MCM-41, or large pore SiO_2 supported ones.

2. In term of dispersion and metal location, the use of larger pore supports (SiO_2 or MCM-41), Pd particles were formed in the pores whereas use of smaller pore supports resulted in Pd particles primarily on the outside surface of the catalysts.

3. The reaction results are probably influenced simultaneously by 2 phenomena: (1) mass transport effects during reaction (for a given silica type, larger pore supported catalysts were more active than smaller pore supported ones) and (2) pore structure effects (Pd/MCM-41 catalysts were more active than Pd/SiO_2 for a similar pore size).

4. The catalyst activity seemed to be related to the difference in Pd dispersion, which was itself a function of the support pore structure (or pore tortuousity). The structure of MCM-41 may also affect the crystal structure of the supported Pd resulted in more active centers for Pd catalysts.

5. Particle sintering and palladium leaching caused catalyst deactivation. Use of large pore SiO_2 supports resulted in the greatest amount of Pd sintering while Pd/SiO_2-small pore resulted in the highest amount of Pd loss during reaction.

6. The leaching of the Pd seemed to be primarily a function of Pd particle size, with larger particles being more susceptible. This loss of Pd from the catalyst during reaction was most likely due to formation of Pd hydride, which is known to form more easily on larger particles.

7. When compared the same type of silica, larger pore supported Pd catalysts having smaller Pd particles than smaller pore supported ones, resulted in lower amount of palladium leaching. When compared silica with the same pore size, Pd/MCM-41-small pore showed lower amount of palladium leaching than Pd/SiO_2-small pore. As shown by TPR, Pd/MCM-41-small pore was found to be more difficult to reduce than Pd/SiO_2-small pore, consequently less palladium hydride was formed.

8. A large amount of metal leaching occurred for the non-catalytically active Pd as confirmed by atomic absorption and CO chemisorption results from repeated catalytic cycle experiments.

7.2 Recommendation

From the previous conclusion, recommendation for the future study can be:

1. In this work, smaller Pd particle resulted in higher activity and lower amount of metal loss so the palladium precursor should be varied to give smaller Pd particle.

2. The results suggest a marginal influence of the support in the reactivity of Pd, it would be interesting to further investigate similar aspect using more "reactive" supports, like ceria based materials.

3.   The causes of particle sintering after reaction should be investigated.

REFERENCES

Alber, P., Pietsch, J., and Parker, S.F. Poisoning and deactivation of palladium catalyst. J. Mol. Catal. A 173 (2001): 275-286.

Ali, S. H., and Goodwin, Jr., J. G., SSITKA Investidation of Palladium Precursor and Support Effects on CO Hydrogenation over Supported Pd Catalysts. J. Catal. 176 (1998): 3-13.

Aramendia, M.A., Borau, V., Jimenez, C., Marinas, J., Porras, A. and Urbano, F.J. Selective Liquid-Phase Hydrogenation of Citral over Supported Palladium. J.Catal. 172 (1997): 46-54.

Bakos, I., Mallat, T., and Baiker, A. Product-induced corrosion of Pt/graphite during catalytic oxidation of sorbose studied by in situ STM and cyclic voltammetry. Catal. Lett. 43 (1997): 201-207.

Beck, J.S., US Patent No. 5,057,296 (1992)

Beck, J.S., Vartuli, J.C., Roth, W.J., Leonowicz, M.E., Kresge, C.T., Schmitt, K.D., Chu, C.T., Oslon, D.H., Sheppard, E.W., McCullen, S.B., Higgins, J.B., and Schlemker, J.L. A New Family of Mesoporous Molecular Sieves Prepared with liquid Crystal Templates. J. Am. Chem. Soc. 114 (1992): 10834-xxxxx.

Besson, Michele, and Gallezot, Pierre Deactivation of metal catalysts in liquid phase organic reactions Catal. Today 81 (2003): 547-559.

Blaser, Hans-Ulrich, Indolese, Adriano, Schnyder, Anita, Steiner, Heinz and Studer, Martin. Supported palladium catalysts for fine chemicals synthesis. J. Mol. Catal. 173 (2001): 3-18.

Choudary, B.M., Kantam, M. Lakshmi, Reddy, N. Mahender, Rao, K. Koteswara, Haritha, Y., Bhaskar, V., Figueras, F. and Tuel, A. Hydrogenation of acetylenics by Pd-exchanged mesoporous caterials. Appl. Catal. A. 181 (1999): 139-144.

Cho, D.H., Chang, T.S., Ryu, S.K., and Lee, Y.K. Characterization and catalytic activities of MoMCM-41. Catal. Lett. 64 (2000): 227-232.

Corma, A. From Microporous to Mesoporous Molecular Sieve Materials and Their Use in Catalysis. Chem. Rev. 97 (1997): 2373-2419.

Dalal, Mahesh K., and Ram, R. N. Hydrogenation of 1-hexene using polymer supported Pd (II) complex catalyst Eur. Polym. J. 33 (1997): 1495-1498.

Dalal, Mahesh K., and Ram, R. N. Catalytic activity of polymer-bound Ru(III)-EDTA complex. Bull. Mater. Sci. 24,2 (2001) : 237-241.

Dobrovolna, Zuzana, Kacer, Petr and Cerveny, Libor. Competitive hydrogenation in alkene-alkyne-diene systems with palladium and platinum catalysts. J.Mol.Catal. 130 (1998), 279-284.

Dobson, N A, Eglinton, G, Krishnamurti, M, Raphael, R A and Willis, R G, Selective catalytic hydrogenation of acetylenes. Tetrahedron 16 (1961): 16-24.

Dominguez-Quintero, Olgioly, Martinez, Susana, Henrequez, Yurgenis, D'Ornelas, Lindora, Krentzien, Heinz and Osuna, Julio. Silica-supported paladium nanoparticles show remarkable hydrogenation catalytic activity Jol.Mol.Catal. 197 (2003): 185-191

Drelinkiewicz, Alicja, Stejskal, Jaroslac, Waksmundzka, Anna, and Sobczak, Janusz W. Physicochemical and catalytic properties of palladium deposited on polyaniline-coated silica gel. Synthetic Metals (2003)

Duca, Dario, Liotta, Leonarda F. and Deganello, Giulio. Liquid phase hydrogenation of phenylacetylene on pumice supported palladium catalysts. J.Catal. 154 (1995): 69-79.

Duca, D., Liotta, L.F., and Deganello, G. Liquid phase hydrogenation of phenylacetylene on pumice supported palladium catalysts. Catal. Today 24 (1995): 15-21.

Farrauto, R.J and Bartholomew,C.H. Fundamentals of Industrial Catalytic Processes. London: Blackie Academic and Professional, 1997

Giorgi, Javier B., Schroeder, Thomas, Baumer, Marcus, and Freund, Hans-Joachim. Study of CO adsorption on crystalline-silica-supported palladium particles Surf. Sci. 498 (2002): L71-L77.

Gruttadauria, Michelangelo, Liotta, Leonarda F., Noto, Renato and Deganello, Giulio. Palladium on pumice: new catalysts for the stereoselective semihydrogenation of alkynes to (z)-alkenes. Tetrahedron 42 (2001): 2015-2017.

Heidenreich, Roland G., Krauter, Jurgen G.E., Pietsch, Jorg, and Kohler Klaus. Control of Pd leaching in Heck reactions of bromoarenes catalyzed by Pd supported on activated carbon Jol. Mol. Catal. A 182-183 (2002): 499-509.

Huang, Y. Y., and Sachtler, W.M.H. The effect of catalyst pore structure on liquid phase catalysis: Hydrogenation of stearonitrile over ruthenium supported on mesoporous sulfated zirconia. App. Catal. A 163 (1997): 245-254.

Jackson, S. David and Shaw, Lindsay A. The liquid phase hydrogenation of phenyl acetylene and styrene on a palladium/carbon catalyst. Appl.Catal.A 134 (1996): 91-99.

Jackson, S. David, Kelly, Gordon J., Watson, Simon R., and Gulickx, R. Cycloalkene hydrogenation over palladium catalysts. Appl. Catal. A 187 (1999): 161-168.

Johnstone, Robert A.W., Liu, Jun-Yao, Lu, Ling and Whittaker, David. Hydrogenation of alkenes over palladium and platinum metals supported on a variety of metal (IV) phosphates. J. Mol. Catal. 191 (2002): 289-294.

Kacer, Petr and Cerveny, Libor. Structure effects in hydrogenation reactions on noble metal catalysts. Appl.Catal.A. 229 (2003): 193-216.

Klug, H.P., and Alexander, E. X-Ray Diffraction Procedures For Polycrystalline Amorphous Materials. 2nd ed. New York: Wiley, 1974.

Koh, C.A., Nooney, R. and Tahir, S. Characterisation and catalytic properties of MCM-41 and Pd/MCM-41 materials. Catal.Lett. 47 (1997): 199-203.

Kresge, C.T., Leonowicz, M.E., Roth, W.J., and Vartuli, J.C., US Patent No. 5,098,689 (1992)

Krishnankutty, N, Li, J., and Vannice MA. The effect of Pd precursor and pretreatment on the adsorption and absorption behavior of supported Pd catalysts. Appl. Catal. A 173 (1998): 137-144.

Lashdaf, M., Krause, A.O.I., Lindblad, M., Titta, M., and Venalainen, T. Behaviour of palladium and ruthenium catalysts on alumina and silica prepared by gas and liquid phase deposition in cinnamaldehyde hydrogenation. Appl. Catal. A241(2003): 65-75.

Li, Hexing, and Xu, Yeping. Liquid phase benzene hydrogenation to cyclohexane over modified Ni-P amorphous catalysts. Materials Letters 51 (2001): 101-107

Mahata, N., and Vishwanathan, V. Influence of palladium precursors on structural properties and phenol hydrogenation characteristics of supported palladium catalysts. J. Catal. 196 (1996): 262-270.

Marler, B., Oberhagemann, U., Vartmann, S., and Gies, H. Influence of the sorbate type on the XRD peak intensities of loaded MCM-41. Microporous Mater. 6 (1996): 375-383.

Mastalir, A., Kiraly, Z., Szollosi, Gy. and Bartok, M. Preparation of Organophilic Pd-Montmorillonite, An Efficient Catalyst in Alkyne Semihydrogenation. J. Catal. 194 (2000): 146-152.

Mastalir, Agnes, Kiraly, Zoltan, Szollosi, Gyorgy and Bartok, Mihaly. Steroselective hydrogenation of 1-phenyl-1-pentyne over low-loaded Pd-montmorillonite catalysts. Appl. Catal. A 213 (2001): 133-140.

Michalska, Zofia M., Ostaszewski, Bogdan, Zientarska, Jolanta and Sobczak, Janusz W. Catalytic hydrogenation of alkadienes and alkynes by palladium catalysts supported on heterocyclic polyamides. J. Mol. Catal. 129(1998): 207-218.

Musolino, M.G., Cutrupi, C.M.S., Donato, A., Pietropaolo, D., and Pietropaolo, R. Liquid phase hydrogenation of 2-butyne-1,4-diol and 2-butene-1,4-diol isomers over Pd catalysts: roles of solvent, support and proton on activity and products distribution. J. Mol. Catal. A 195 (2003): 147-157.

Nag, N. K. A study on the dispersion and catalytic activity of gamma alumina-supported palladium catalysts. Catal. Lett. 24 (1994): 37-46.

Neri, G., Musolino, M.G., Pietropaolo, D., and Galvagno, S. Particle size effect in the catalytic hydrogenation of 2,4-dinitrotoluene over Pd/C catalysts Appl. Catal. A 208(2001): 307-316.

Nijhuis, T.A., Koten, G. van., and Moulijn, J.A. Optimized palladium catalyst systems for the selective liquid-phase hydrogenation of functionalized alkynes. Appl. Catal. A238(2003): 259-271.

Nishimura, Shigeo. Handbook of Heterogeneous Catalytic Hydrogenation for Organic Synthesis. USA: John Wiley & Sons, 2001.

Noronha, F.B., Baldanza, M.A.S., and Schmal, M. CO and NO Adsorption on Alumina-Pd-Mo Catalysts: Effect of the Precursor Salts J. Catal. 188 (1999): 270-280.

Nozoe, Tatsuhiro, Tanimoto, Kohei, Takemitsu, Takatomo, Kitamura, Toshiyuki, Harada, Tadao, Osawa, Tsutomu and Takayasu, Osamu. Non-solvent hydrogenation of solid alkenes and alkynes with supported palladium catalyst. Solid State Ionics, 141 (2001): 695-700

Olah, George A. and Molnar, Arpad. Hydrocarbon Chemistry. USA: John Wiley & Sons, 1995.

Palinko, Istvan Effects of surface modifiers on the liquid-phase hydrogenation of alkenes over silica-supported platinum, palladium and rhodium Appl.Catal.A 126 (1995), 39-49

Panpranot, J., Goodwin, Jr., J.G., and Sayari, A. Synthesis and characteristics of MCM-41 supported CoRu catalysts. Catal. Today 77 (2002): 269-284.

Pasqua, L., Testa, F., Aiello, R., Renzo, F. Di, and Fajula, F. Influence of pH and nature of the anion on the synthesis of pure and iron-containing mesoporous silica. Microporous and Mesoporous Mater. 44-45 (2001): 111-117.

Perez-Zurita, M. Josefina, Cifarelli, Michell, Cubeiro, M. Luisa, Alcarez, Juan, Goldwasser, Mireya, Pietri, Egle, Garcia, Luis, Aboukais, Antoine, and Lamonier, Jean-Francois. Palladium-based catalysts for the synthesis of alcohols. J. Mol. Catal. A 206 (203): 339-351.

Rylander, P.N. Hydrogenation Methods. Great Britain: Academic Press Limited, 1985.

Sandoval, VH., and Gigola, CE. Characterization of Pd and Pd-Pb/alpha-Al2O3 catalysts. A TPR-TPD study. Appl. Catal. A 148 (1996): 81-96

Sarkany, A., Zsoldos, Z., Furlong, B., Hightower, J. W., and Guczi, L. Hydrogenation of 1-Butene and 1,3-Butadiene Mixtures over Pd/ZnO Catalysts. J. Catal. 141 (1993): 566-582.

Schneider, M., Wildberger, M., Maciejewski, M., Duff, D.G., Mallat, T. and Baiker, A. Preparation, Structural Properties, and Hydrogenation Activity of Highly Porous Palladium-Titania Aerogels. J.Catal. 148 (1994): 625-638.

Sheldon, R.A. and Bekkum, H. Van. Fine Chemicals through Heterogeneous Catalysis. Federal Republic Germany: WIEY-VCH, 2001.

Shen, W.J., Ichihashi, Y., Ando, H., Okumura, M., Haruta, M., and Matsumura, Y. Influence of palladium precursors on methanol synthesis from CO hydrogenation over Pd/CeO$_2$ catalysts prepared by deposition-precipitation method. Appl. Catal. A 217 (2001): 165-172

Shimazu, Shogo, Baba, Noriyuki, Ichiku, Nobuyuki and Uematsu, Takayoshi. Regioselective hydrogenation of dienes catalyzed by palladium-aminosilane complexes grafted on MCM-41. J. Mol.Cal 182 (2002): 343-350.

Shuurman, Y., Kuster, B.F.M., Van der Wiele, K., and Martin, G.B. Selective oxidation of methyl α-D-glucoside on carbon supported platinum: III. Catalyst deactivation. Appl. Catal. A 89 (1992): 47-68.

Singh, Utpal K. and Vannice, M. Albert. Liquid-Phase Citral Hydrogenation over SiO_2-Supported Group VIII Metals J.Catal. 199 (2001): 73-84.

Singh, Utpal K. and Vannice, M. Albert. Influence of metal-support interactions on the kinetics of liquid-phase hydrogenation. Jol. Mol. Catal. A163(2000): 233-250

Tanaka, S., Mizukami, F., Niwa, S., Toba, M., Maeda, K., Shimada, H. and Kunimori, K. Preparation of highly dispersed silica-supported palladium catalysts by a complexing agent-assisted sol-gel method and their characteristics. Appl.Catal.A 229(2002): 165-174.

Wang, Chen-Bin., Lin, Hung-Kuan, and Ho, Chi-Man. Effects of the addition of titania on the thermal characterization of alumina-supported palladium. Jol. Mol. Catal. A 180 (2002): 285-291

Zhao, Fengyu, Murakami, Kenji, Shiraai, Masayuki, and Arai, Masahiko. Recyclable Homogeneous/Heterogeneous Ctalytic Systems for Heck Reaction trough Reversible Transfer of Palladium Species between Solvent and Support J. Catal. 194 (2000): 479-483.

Zhao, Xiu S., Lu, G.Q. (Max), and Millar, Graeme J. Advance in Mesoporous Molecular Sieve MCM-41. Ind. Eng. Chem. Res. 35 (7) (1996): 2075-2090.

APPENDICES

APPENDIX A

CALCULATION FOR CATALYST PREPARATION

Preparation of 0.5%Pd/MCM-41 and 0.5%Pd/SiO$_2$ catalysts by the incipient wetness impregnation method are shown as follows:

Reagent: - Palladium (II) nitrate dehydrate [Pd (NO$_3$)$_2$ · 2H$_2$O]

Molecular weight = 266.42 g

- Support: - MCM-41 and SiO$_2$

Example Calculation for the preparation of 0.5% Pd/MCM-41 catalyst

Based on 100 g of catalyst used, the composition of the catalyst will be as follows:

Palladium = 0.5 g

MCM-41 = 100-0.5 = 99.5 g

For 1 g of catalyst

Palladium required = 1×(0.5/100) = 0.005 g

Palladium 0.005 g was prepared from Pd (NO$_3$)$_2$ · 2H$_2$O and molecular weight of Pd is 106.42

the Pd (NO$_3$)$_2$ · 2H$_2$O content = $\dfrac{\text{MW of Pd (NO}_3)_2 \cdot 2\text{H}_2\text{O} \times \text{Palladium required}}{\text{MW of Pd}}$

= (266.42/106.42)×0.005 = 0.0125 g

Since the pore volume of the pure silica support is 1.8 ml/g and 0.78 ml/g for MCM-41 and SiO$_2$, respectively. Thus, the total volume of impregnation solution which must be used is 1.62 ml for MCM-41 and 0.7 ml for SiO$_2$ by the requirement of incipient wetness impregnation method, the de-ionised water is added until equal pore volume for dissolve Palladium (II) nitrate dehydrate.

APPENDIX B

CALCULATION OF THE CRYSTALLITE SIZE

Calculation of the crystallite size by Debye-Scherrer equation

The crystallite size was calculated from the half-height width of the diffraction peak of XRD pattern using the Debye-Scherrer equation.

From Scherrer equation:

$$D = \frac{K\lambda}{\beta \cos\theta} \qquad (B.1)$$

where D = Crystallite size, Å

K = Crystallite-shape factor = 0.9

λ =   X-ray wavelength, 1.5418 Å for CuKα

θ =   Observed peak angle, degree

β =   X-ray diffraction broadening, radian

The X-ray diffraction broadening (β) is the pure width of a powder diffraction free from all broadening due to the experimental equipment. α-Alumina is used as a standard sample to observe the instrumental broadening since its crystallite size is larger than 2000 Å. The X-ray diffraction broadening (β) can be obtained by using Warren's formula.

From Warren's formula:

$$\beta = \sqrt{B_M^2 - B_S^2} \qquad (B.2)$$

Where B_M =   The measured peak width in radians at half peak height.

B_S =   The corresponding width of the standard material.

Example: Calculation of the crystallite size of Pd/MCM-41-large pore

The half-height width of 111 diffraction peak $\quad=\quad 0.95^{o}$ (from the figure B.1)

$$= \quad (0.95 \times \pi)/180$$

$$= \quad 0.0165 \text{ radian}$$

The corresponding half-height width of peak of α-alumina (from the Bs value at the 2θ of 34.08^{o} in figure B.2) $\quad=\quad 0.00422$ radian

The pure width, $\beta \quad=\quad \sqrt{B_M^2 - B_S^2}$

$$= \quad \sqrt{0.0165^2 - 0.00438^2}$$

$$= \quad 0.016 \text{ radian}$$

B $\quad=\quad$ 0.016 radian

$2\theta \quad=\quad 34.08^{o}$

$\theta \quad=\quad 17.04^{o}$

$\lambda \quad=\quad 1.5418$ Å

The crystallite size $\quad=\quad \dfrac{0.9 x 1.5418}{0.016 \cos 17.04} \quad=\quad 90.07$ Å
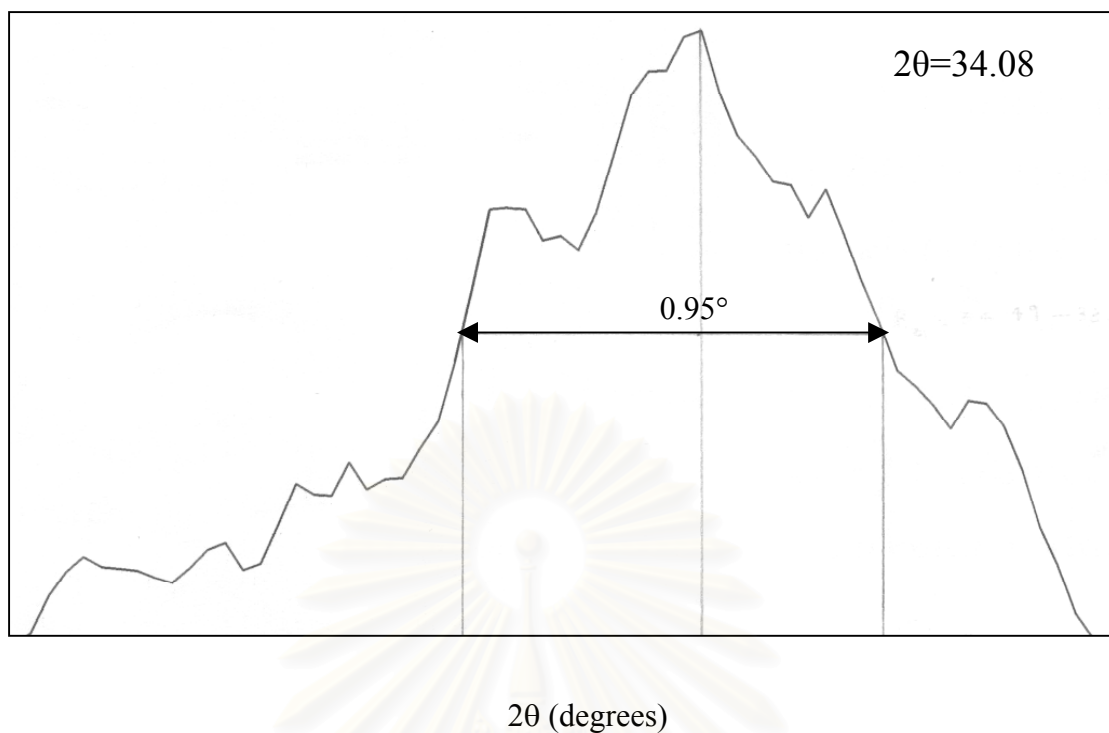
$$= \quad 9.1 \text{ nm}$$

Figure B.1 The 111 diffraction peak of Pd/MCM-41-large pore for calculation of the
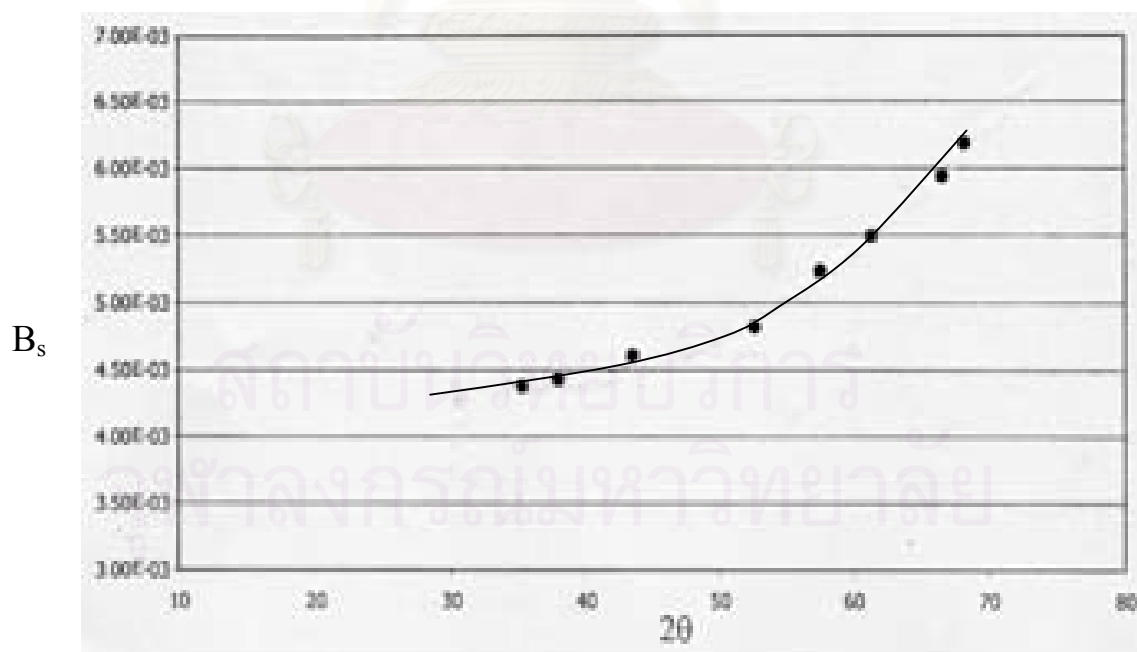
crystallite size

Figure B.2 The plot indicating the value of line broadening due to the equipment.

The data were obtained by using α-alumina as a standard

APPENDIX C

CALCULATION FOR METAL ACTIVE SITES AND DISPERSION

Calculation of the metal active sites and metal dispersion of the catalyst measured by CO adsorption is as follows:

Let the weight of catalyst used	= W	g
Integral area of CO peak after adsorption	= A	unit
Integral area of 40 µl of standard CO peak	= B	unit
Amounts of CO adsorbed on catalyst	= B-A	unit
Volume of CO adsorbed on catalyst	= 40×[(B-A)/B]	µl
Volume of 1 mole of CO at 30°C	= 24.86×10^6	µl

Mole of CO adsorbed on catalyst $= [(B-A)/B]×[40/24.86×10^6]$ mole

Molecule of CO adsorbed on catalyst $= [1.61×10^{-6}]× [6.02×10^{23}]×[(B-A)/B]$ molecules

Metal active sites $= 9.68×10^{17}×[(B-A)/B]×[1/W]$ molecules of CO/g of catalyst

Molecules of Pd loaded $= [\%wt \text{ of Pd}] ×[6.02×10^{23}]/ [MW \text{ of Pd}]$ molecules/g of catalyst

Metal dispersion (%) $= 100×[\text{molecules of Pd from CO adsorption/molecules of Pd loaded}]$

APPENDIX D

SAMPLE OF CALCULATION

D1 Calculation of Hydrogen consumed

The calculation of hydrogen consumed are as follow:

Let   P   =   hydrogen consumed, psi

      T   =   temperature during operation, K

      V   =   volume of hydrogen stored tank, 3.6 L

      R   =   0.0821 L atm/mol K

      n   =   mole of hydrogen

From ideal-gas equation

$$PV = nRT$$

$$n = PV/RT$$

$$n = \frac{P \text{ psi}}{} \left| \frac{1 \text{ atm}}{14.7 \text{ psi}} \right| \frac{3.6 \text{ L}}{0.0821 \text{ L. atm}} \left| \frac{\text{mol.K}}{T \text{ K}} \right.$$

$$n = 2.9829P/T \quad \text{mol}$$

The molar volume of an ideal gas is 22.4 L at STP (0°C and 1 atm)

Hydrogen consumed   = $2.9829P \times 22.4/T$ L

                           $2.9829P \times 22,400/T$ cm^3

D2 Calculation of Initial rate

At t = 10 min

Weight of catalysts = 1 g.cat

      Initial rate   = $d \text{ mole } [H_2]/dt$

                    = $\dfrac{(2.9829P/T) \text{ [mole]}}{10 \text{ [min.] [g.cat.]}}$

D3   Calculation of Turnover frequencies (TOF)

Metal active site   =   y   molecule

$$\text{TOF} = \frac{\text{Initial rate}}{\text{(numbers of active site)}}$$

$$= \frac{(0.29829P/T) \text{ mole } H_2}{[\text{g cat.}][\text{min}]} \left| \frac{[\text{g cat.}]}{y [\text{active site}]} \right| \frac{[\text{min}]}{[\text{s}]}$$

$$= (0.29829P/yT) \quad [\text{s}^{-1}]$$

D4   Determination of the Activation Energy

From Arrhenius Equation:

$$k = A \exp(-E_{act}/RT)$$

In the logarithmic form:

$$\log k = \log A - E_{act}/RT$$

Where

k = the overall rate constant, min^{-1}

A = the frequency factor, min^{-1}

E_{act} = the activation energy, kJ/mole

R = the gas constant, 8.314 J/mol K

T = absolute temperature, K

From figure 5.4:

The slope of the curve   =   -2.1583   K

$$\frac{-E_{act}}{2.303R} = -2.1583 \times 10^3 \quad \text{K}$$

$$E_{act} = 2.1583 \times 2.303 \times 8.314 \times 10^3 \quad \text{J/mol}$$

$$= 41 \quad \text{kJ/mol}$$

APPENDIX E

LIST OF PUBLICATIONS

1. Joongjai panpranot, Kanda pattamakomsan, Jame G. Goodwin, Jr. and Piyasarn Praserthdam, " A Comparative Study of Pd/SiO_2 and Pd/MCM-41 Catalysts in Liquid-Phase Hydrogenation", Proceeding of The 3rd Asia-Pacific Congress on Catalysis, APCAT-3, Dalian, China, Oct. 12-15, 2003, 182.

The 3rd Asia-Pacific Congress on Catalysis, APCAT-3

October 12-15, 2003, Dalian, China

State Key Laboratory of Catalysis
Dalian Institute of Chemical Physics
Chinese Academy of Sciences
457 Zhongshan Road
Dalian 116023, China

Tel: +86-411-4379085, 4379070
Fax:+86-411-4694447
http://www.apcat3.dicp.ac.cn
E-mail:apcat@dicp.ac.cn
shen98@dicp.ac.cn
canli@dicp.ac.cn

June 16, 2003

Dear Dr Kanda Pattamakomsan,

Title of abstract: A COMPARATIVE STUDY OF Pd/SiO2 AND Pd/MCM-41 CATALYSTS IN LIQUID-PHASE HYDROGENATION
Reference Code: O-37

We are pleased to inform you that the above abstract has been accepted as **Oral presentation** at the 3rd Asia-Pacific Congress on Catalysis (APCAT-3), to be held in October 12-15, 2003, Dalian, China.

All oral presentations should be timed for 20 min followed by 5 min of questions from the audiences. Overhead transparency projection as well as a PC for PowerPoint presentations will be available. Poster presentations will be exhibited for enough period of time (1-2 days) so as to have extensive discussion. The maximum space available for each poster will be 0.90m (width) × 1.6m(height) and mounting materials will be provided.

Since a significant progress has been achieved on prevention and control of SARS in China, the Organization Committee of APCAT-3 recently made the decision that the conference will be held as scheduled in October 12-15,2003, Dalian, China. Your understanding and active participation in APCAT-3 are greatly anticipated and highly appreciated.

Information on conference registration and accommodation are available online at http://apcat3.dicp.ac.cn and the technological program will also be available soon. If you have any questions concerning the conference including visa application, please do not hesitate to contact the organizing committee.

We are looking forward to meeting you in Dalian.

Sincerely yours,

Can Li
Professor
Chairman of the APCAT-3

A Comparative Study of Pd/SiO₂ And Pd/MCM-41 Catalysts in Liquid-Phase Hydrogenation

Kanda Pattamakomsan, Joongjai Panpranot and Piyasan Praserthdam
Center of Excellence on Catalysis and Catalytic Reaction Engineering
Department of Chemical Engineering, Chulalongkorn University, Bangkok 10330,
Thailand

Introduction

Liquid-Phase hydrogenation is one of the most useful, versatile, and environmentally acceptable reaction routes available for organic synthesis. [1] Such reaction is usually catalyzed by supported noble metal such as Pt, Pd, Rh and Ru. Various supports have been used such as activated carbon, silica, alumina and polymers. However, for such fast and exothermic reaction the large pore supports are usually preferred. [2]

In this study, we compared the characteristics and the catalytic properties of MCM-41-supported Pd catalysts to those of high surface area amorphous silica (SiO₂) supported ones. Mesoporous silicate MCM-41 with different pore diameters of 3 nm (M1) and 7 nm (M2) were synthesized and used to support Pd catalysts. Our investigation focused on determining the influence of textural properties of the silica supports on Pd dispersion, reduction behavior and catalytic properties for liquid-phase hydrogenation.

Experimental

Supported Pd catalysts were prepared by the incipient wetness impregnation of the supports with an aqueous solution containing the desired amount of Pd nitrate dihydrate to give final loading of 0.5%Pd. The catalysts were dried overnight at 383K and were calcined in air at 773 for 2 h.

Pd contents were determined by atomic adsorption spectroscopy. The catalysts were characterized using different characterization techniques such as BET, X-ray diffraction (XRD), CO chemisorptions, scanning electron microscopy (SEM) and thermogravimetric analysis (TGA)

Liquid-phase hydrogenation of 1-hexene was carried out at 298 K and 1 atm in autoclave. Approximately 1 gram of supported Pd catalyst was placed into the autoclave. The Pd catalyst was reduced with hydrogen at ambient temperature for 2 hour. The reaction mixture was composed of 15 ml of 1-hexene and 400 ethanol and was first kept in 600 ml feed column then the mixture was flushed with nitrogen to start the reaction. Experiments were carried out at stirring velocities in the range 1400 rpm. The content of hydrogen consumption was monitored every ten minute by noting the change in pressure of hydrogen. The products were determined by Gas Chromatograph. (GC)

Results and Discussion

BET surface areas of Pd supported catalysts were 869, 726, 675 m²/g for Pd/M1, Pd/M2 and Pd/SiO₂ respectively. (BET surface area of the original supports of M1=1223, M2= 901, SiO₂= 716 m²/g) XRD results showed that crystallite size of PdO was larger on SiO₂ support than on MCM-41. SEM also showed catalyst granule size in the order of Pd/SiO₂> Pd/M2>Pd/M1.

Liquid-phase hydrogenation of 1-hexene was carried out in order to compare the activity of the different silica supported Pd catalysts. The kinetics of hydrogenation can be followed by measuring the rate of consumption of hydrogen and were reported in Fig.1 The activity was found to be in the order of Pd/M2> Pd/M1>Pd/SiO$_2$.

As expected the high surface area of MCM-41-supported Pd catalysts resulted in higher hydrogenation activity than the SiO$_2$-supported ones. However, the diffusion resistance in the small pore of M1 may also have an impact on the catalyst activity, as seen on Pd/M1.
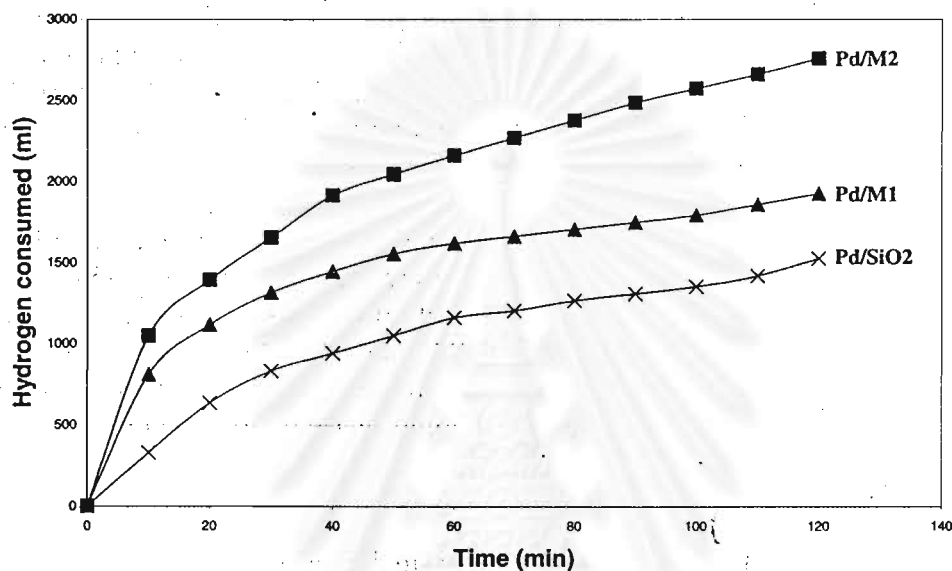

Figure 1. Consumption of hydrogen as a function of time for the hydrogenation of 1-hexene on silica supported Pd catalysts.

References

[1] R.J. Farrauto and C.H. Bartholomew, Fundamentals of Industrial Catalytic Process, Blackie Academic and Professional, London, 1997
[2] B.M. Chouary, M. L. Kantam, N.M. Reddy, K.K. Rao, Y. Haritha,, V. Bhaskar, F. Figueras, and A. Tuel, Appl. Catal. A. 181 (1999) 139

VITA

Miss Kanda Pattamakomsan was born in September 25th, 1981 in Bangkok, Thailand. She finished high school from Satriwittaya2 School, Bangkok in 1998, and received bachelor's degree in Chemical Engineering from the department of Chemical Engineering, Faculty of Engineering, Kasetsart University, Bangkok, Thailand in 2002.